Changes in lipidomic profile induced by lipopolysaccharide and skin sensitizer in dendritic cells and keratinocytes

Setembro, 2011

Alterações no perfil lipidómico induzidas por lipopolissacarídeo e sensibilizador cutâneo em células dendríticas e queratinócitos

DISSERTAÇÃO DE MESTRADO EM INVESTIGAÇÃO BIOMÉDICA

Deolinda da Conceição Ribafeita Santinha,

Dissertação de Mestrado apresentada à Faculdade de Medicina da Universidade de Coimbra para a obtenção do grau de mestre em Investigação Biomédica, desenvolvida sob a orientação da Professora Doutora Maria Teresa de Teixeira Cruz e co-orientação da Professora Doutora Maria do Rosário Gonçalves dos Reis Marques Domingues e do Professor Doutor Paulo Carvalho Pereira.

Agradecimentos

A realização deste trabalho só foi possível, com a carinhosa colaboração de todas as pessoas que me acompanharam ao longo deste percurso. Obrigada a todos pelo apoio na sua execução e pelo enriquecimento dos meus conhecimentos.

Dirijo um especial agradecimento:

Às minhas orientadoras, Professora Teresa Cruz e Professora Rosário Domingues, pela excelente orientação científica, motivação que sempre me transmitiram, pela disponibilidade e apoio ao longo deste ano, e em especial na revisão crítica deste manuscrito. Obrigada pelos ensinamentos, pela confiança que depositaram em mim e pela amabilidade com que o fizeram.

Ao excelente grupo de investigação em Imunobiologia Celular do CNC, em especial à Susana e ao Bruno pela disponibilidade e trabalho incansável com as culturas celulares, pelos ensinamentos e pela boa vontade que sempre demonstraram. Ao João pela importante ajuda, e aos restantes colegas de grupo por todo apoio e carinho com que me receberam. A todos o meu especial agradecimento!

Ao importante grupo de Espectrometria de Massa da UA, que tão carinhosamente me receberam, em particular, à Cristina, à Beta e à Cláudia pela indispensável disponibilidade e ajuda, pelos conselhos e pelo trabalho constante. E às alunas de mestrado, Luísa, Tânia, Gabriela e Raquel, pela preciosa inter-ajuda, permanente apoio, amizade e compreensão.

À Doutora Bárbara Macedo do IBMC, pela sua importante colaboração neste trabalho, pelos seus conhecimentos, e pela incansável disponibilidade.

Ao pessoal da Residência da UA, pela amizade e companheirismo, pelas jantaradas, noites de farra, de crepes, gelados e afins… Obrigada pela indispensável e animada companhia.

Ao pessoal do Mestrado, pelo companheirismo e apoio mútuo ao longo deste percurso, em particular à João, à Sandra, à Beta, e à Ana, pela amizade, disponibilidade e especial companheirismo.

A todos os meus amigos e família, em especial à Patricia, à Daniela, à Marta, à Lili e ao Luís e aos meus primos, Marco, Pedro e Catarina, pelos bons momentos de descontracção, pelas palavras de motivação, apoio incondicional e importante amizade.

Aos meus pais e ao meu irmão que são para mim fonte de motivação, coragem e entusiasmo, pelo seu exemplo de firmeza e perseverança. Obrigada pela força, pelo carinho, pelo apoio inestimável e confiança que depositam em mim.

Dedico este trabalho

À minha Mãe

Ao meu Pai

Ao meu Irmão

E à minha Madrinha

“Onde não falta vontade existe sempre um caminho”

John Ronald Tolkien

Resumo

A Dermatite de Contacto Alérgica, uma das doenças ocupacionais mais comuns, é a patologia resultante de uma resposta imune alérgica após a exposição cutânea a um grande subconjunto de químicos. Actualmente, o potencial sensibilizador cutâneo de químicos é apenas avaliado através de testes *in vivo* que utilizam animais. Contudo, face à legislação europeia em vigor, que impõe a adopção de novas abordagens, é imperativo desenvolver testes *in vitro* alternativos e eficazes para a avaliação da sensibilização cutânea. O objectivo deste estudo foi identificar o perfil lipídico de células dendríticas (DCs) e queratinócitos (KCs) e avaliar as alterações que ocorrem no seu perfil após a exposição ao potente estímulo pró-inflamatório, o lipopolissacarídeo (LPS), e ao forte sensibilizador cutâneo (DNFB), a fim de demonstrar o papel dos lípidos e as alterações lipídicas que ocorrem durante a maturação das DCs e identificar bons biomarcadores para posteriormente usar numa abordagem *in vitro* alternativa. O perfil lipídico foi avaliado por espectrometria de massa, usando uma abordagem lipidómica, que combina TLC e posterior análise por ESI-MS e ESI-MS/MS. Os resultados obtidos neste estudo permitem observar que durante a maturação DC e após exposição ao alergénio ocorrem alterações no conteúdo total de ceramidas e no seu perfil, ocorrendo um aumento das ceramidas C16, C24:1 e C24:0. A identificação e caracterização das alterações lipídicas desencadeadas pelo LPS e sensibilizador cutâneo nos KCs revelam modificações importantes no conteúdo total de fosfatidilserinas e alterações no seu perfil, promovendo uma drástica redução numa das mais abundantes fosfatidilserinas presentes nos queratinócitos, PS(16:0/18:1 ou 16:1/18:0).

O padrão de alteração destes lípidos fornece uma fonte extremamente rica de informação para avaliar a modulação de espécies específicas de lípidos induzida pela exposição das DCs e KCs a um sensibilizador cutâneo e ao LPS, que pode ser integrado numa estratégia com vista à redução do uso de animais para avaliar o potencial de sensibilização cutânea.

Palavras-chave: Dermatite de Contacto Alérgica; Células Dendríticas; Queratinócitos; Lipidómica; Fosfolípidos; Esfingolípidos; Lipopolissacarídeo; Sensibilizador Cutâneo; Espectrometria de Massa.

Abstract

Allergic contact dermatitis (ACD), one of the commonest occupational diseases, is the clinical condition that can result from an allergic immune response following skin exposure to a large subset of chemicals. There are currently no validated non-animal approaches for the prediction of skin sensitization potential of contact allergens. However, existing and forthcoming European legislation imposes the adoption of new alternative approaches; thus, it is imperative to develop an effective alternative *in vitro* approach for skin sensitization evaluation. The aim of this study was to identify the lipidomic profile of dendritic cells (DCs) and keratinocytes (KCs), and evaluate the changes that occur in their profile after exposure to the potent pro-inflammatory stimulus, lipopolysaccharide (LPS) and to the strong skin sensitizer (DNFB), in order to demonstrate the lipid role and even lipid changes that occur during DC maturation and disclose good biomarkers for further use in an alternative *in vitro* approach. The lipid profile was evaluated by mass spectrometry, using a lipidomic approach, that combine TLC and further analysis by ESI-MS and ESI-MS/MS. The results obtained in this study allow observing that during DC maturation and after allergen exposure occur significant changes in the cellular levels of both signalling and structural lipids, mainly in total content of ceramides and in their profile, increasing the C16, C24:1 and C24:0 ceramides. The identification and characterization of lipidic changes triggered by LPS and skin sensitizer in KCs reveal major changes in total levels of phosphatidylserine and their profile, promoting a drastic reduction in one of the most abundant PS presents in KCs, PS(16:0/18:1 or 16:1/18:0).

The pattern of change of these lipids give an extremely rich source of data for evaluating modulation of specific lipid species triggered during DCs and KCs exposure to a skin sensitizer and LPS, which could be used in an integrative test strategy towards the reduction of animals use for skin sensitization prediction.

Key-Words: Allergic contact dermatitis; Dendritic Cells; Keratinocytes; Lipidomic; Phospholipids; Sphingolipids; Lipopolysaccharide; Skin sensitizer; Mass Spectrometry.

Abbreviations

ACD	Allergic Contact Dermatitis
APCs	Antigen Presenting Cells
BC	Benzalkonium Chloride
C1P	Cer-1-Phosphatase
CCR	Chemokine Receptors
Cer	Ceramide
CID	Collision-Induced Dissociation
CL	Cardiolipin
cysLTs	Cysteinyl Leukotrienes
DCs	Dendritic cells
DNFB	2,4 - Dinitrofluorbenzene
EPCA	Epithelial Cell Adhesion Molecule
ESI	Electrospray Ionization
FAs	Fatty Acids
FSDC	Fetal Skin-derived Dendritic Cell line
GC	Gas Chromatography
GM-CSF	Granulocyte–Macrophage Colony Stimulating Factor
H	Hydrogen
H^+	Proton
H_2O	Water
HaCat	Human keratinocyte cell line
HPLC	High Performance Liquid Chromatography
iDCs	immature Dendritic Cells
IFN	Interferon
IL	Interleukin
KCs	Keratinocytes
LC	Liquid chromatography
LCs	Langerhans cells
LPS	Lipopolysaccharide
µg	Microgram
µl	MicroLiter
m/z	Mass/charge
MAPKs	Mitogen-Activated Protein Kinases
mDCs	mature Dendritic Cells
mg	Miligram
MHC	Major Histocompatibility Complex
min	Minute
ml	MiliLiter
MMPs	Matrix metalloproteinases
MS	Mass Spectrometry
MS/MS	Tandem mass spectrometry
Na^+	Sodium ion
PAMPs	Pathogen-Associated Molecular Patterns
PC	Phosphatidylcholines
PE	Phosphatidylethanolamines

PG	Phosphatidylglycerol
PGE2	Prostaglandin E2
PI	Phosphatidylinositol
PLs	Phospholipids
PS	Phosphatidylserine
SLs	Sphingolipids
SM	Sphingomyelin
TGF	Transforming Growth Factor
TLC	Thin Layer Chromatography
TLRs	Toll-Like Receptors
TNF	Tumor Necrosis Factor
TOF	Time-Of-Flight
UV	Ultra-violet
v	Volume
λ	Wavelength

Index

Introduction **3**

1. Allergic Contact Dermatitis 3

1.1 Dendritic Cells 7

1.2 DC Migration and Maturation 9

1.3 Keratinocytes 13

2. Lipids 15

2.1 Definition and classification 16

2.2 Structure and function 17

Fatty acids 17

Glycerophospholipids 18

Sphingolipids 20

3. Lipidomics 22

3.1 Lipid Isolation 25

3.2 Lipids Analysis 26

Lipid Separation 26

Mass Spectrometry 28

Tandem mass spectrometry 34

4. Mass spectrometry in phospholipids and sphingolipids analysis 36

5. Aims 45

Material and Methods **49**

1. Material 49

2. Methods 49

2.1Cell Culture 49

2.2 Lipid Extraction 50

2.3 Lipid Separation 51

2.4 Silica Extraction 52

2.5 Determination of phospholipid content 52

2.6 Determination of ceramide content 53

2.7 Determination of protein content 54

2.8 Conditions of Electrospray Mass spectrometry 54

2.9 Statistics 55

Results and Discussion **59**

I. Changes in lipidomic profile triggered during dendritic cells maturation 59

II. Changes in lipidomic profile induced by skin sensitizer in dendritic cells 60

Separation of Phospholipid Classes by TLC 60

Phosphorus assay of major phospholipid classes 61

Analysis of lipid classes by mass spectrometry 64

III. Changes in lipidomic profile triggered by lipopolysaccharide and skin sensitizer in keratinocytes 72

Separation of Phospholipid Classes by TLC 72

Phosphorus assay of major phospholipid classes 73

Analysis of lipid classes by mass spectrometry 75

Conclusion **97**

Paper **101**

References **133**

Figure Index

Figure 1. Cellular and molecular events triggered during the development of Allergic contact dermatitis 4

Figure 2. Skin anatomy and cellular effectors 6

Figure 3. Cellular and molecular events triggered during migration of dendritic cells. 11

Figure 4. Keratinocytes are central skin sentinels 15

Figure 5. Schematic representation of phospholipid structure. 18

Figure 6. The subclasses of glycerophospholipids 19

Figure 7. Schematic representation of Cardiolipin Structure 20

Figure 8. Schematic representation of sphingolipids structure and of the main sphingolipids: Ceramides and Sphingomyelin 21

Figure 9. Scheme of SL metabolism 22

Figure 10. Lipidomics – system level scale analysis of lipids and their interactions. 23

Figure 11. Representative Scheme of several steps of a lipidomic approach 25

Figure 12. Scheme of the main components of a mass spectrometer. 29

Figure 13. Schematic representation of a Electrospray ionization interface 30

Figure 14. Mass spectrometers. (A) Micromass® Q-ToF 2 mass spectrometer; (B) LXQ Linear Ion Trap Mass Spectrometer 34

Figure 15. Schematic representation of the different MS/MS experiments. 36

Figure 16. ESI–MS/MS spectrum of the $[MH]^+$ at *m/z* 760 (below) and of $[MNa]^+$ at *m/z* 782.6 (above), corresponding to PC (16:0/18:1) 38

Figure 17. ESI–MS/MS spectrum of the $[MH]^+$ at *m/z* 746.8 (below) and of $[MNa]^+$ at *m/z* 768.5 (above), corresponding to PE (18:0/18:1) 40

Figure 18. ESI–MS/MS spectrum of the $[M-H]^-$ at *m/z* 760.4 corresponding to PS (16:0/18:1) 41

Figure 19. ESI–MS/MS spectrum of the $[M-H]^-$ at *m/z* 837.6 corresponding to PI (16:0/18:0) 43

Figure 20. ESI–MS/MS spectrum of the $[M-H]^-$ at *m/z* 536 corresponding to Cer (d18:1/16:0). 44

Figure 21. Effect of skin sensitizer and irritant on the phospholipid content in dendritic cells. (A) Typical TLC of total lipids extracted from DCs before and after treatment of cells by DNFB (skin sensitizer) and BC (irritant); (B) PL content, % from total lipids refers to the relative percentage of phospholipid phosphorus recovered from the respective spot in TLC..... 63

Figure 22. Phosphatidylcholine (PC) and Sphingomyelin (SM) MS spectra 65

Figure 23. Phosphatidylinositol (PI), Phosphatidylserine (PS) and Phosphatidyl-ethanolamine (PE) MS spectra. 68

Figure 24. Ceramide MS spectra..... 69

Figure 25. Effect of LPS, DNFB and BC on the phospholipid content in keratinocytes. (A) Typical TLC of total lipids extracted from KCs before and after treatment of cells by LPS, DNFB and BC; (B) PL content, % from total lipids refers to the relative percentage of phospholipid phosphorus recovered from the respective spot in TLC..... 74

Figure 26. Phosphatidylcholine (PC) spectra..... 77

Figure 27. Sphingomyelin (SM) spectra 79

Figure 28. Phosphatidylethanolamine (PE) spectra..... 81

Figure 29. Phosphatidylinositol (PI) spectra..... 85

Figure 30. Phosphatidylserine (PE) spectra..... 87

Figure 31. Cardiolipin (CL) spectra 89

Figure 32. Ceramide (Cer) spectra 91

Table Index

Table 1. Lipid classification as suggested by Fahy et al (46). 17

Table 2. Identification of $[M+H]^+$ ions observed in the MS spectra of PC. 66

Table 3. Identification of $[M+H]^+$ ions observed in the MS spectra of SM 67

Table 4. Identification of $[M-H]^-$ ions observed in the MS spectra of PE, PI, PS and Cer 70

Table 5. Identification of $[M+H]^+$ ions observed in the MS spectra of PC, SM and PE. 82

Table 6. Identification of $[M-H]^-$ ions observed in the MS spectra of PI, PS, CL and Cer..... 92

CHAPTER I

Introduction

I. Introduction

1. Allergic Contact Dermatitis

Skin sensitization is the induction of an allergic immune response following skin exposure to a large subset of small reactive chemicals (haptens) that can be found in the environment and in many household products. Allergic contact dermatitis (ACD) is a result of a hapten-specific T-cell-mediated inflammatory reaction occurring in sensitized individuals upon allergen challenge (Figure 1).

In normal skin reside epidermal dendritic cells (DCs), also known as Langerhans cells (LCs), in a functional resting state, characterized by high antigen-processing capacity. Briefly, in the sensitization phase, allergens that have penetrated into the skin are internalized by skin DCs, which subsequently migrate to the draining lymph nodes, via afferent lymphatics. In the T-cell-rich paracortical area of the lymph node, DCs encounter naïve T cells and activate these through interaction between major histocompatibility complex (MHC)–peptide complex and T-cell receptor. Allergen-specific T cells expand and generate effector and memory cells, being subsequently recruited, from the circulation, into the skin. Following subsequent re-exposure of the sensitized subject to the same chemical allergen, an accelerated and more aggressive secondary immune response will be elicited and thereby the clinical manifestation of the disease occurs. As a consequence of the local release of proinflammatory cytokines and chemokines, circulating allergen-specific T cells and antigen presenting cells (APCs) meet at the site of allergen challenge. At this stage, non-dedicated APCs, such as Keratinocytes (KCs), also present the allergen to T cells. This results in the release of proinflammatory cytokines and chemokines by epidermal cells that will recruit more allergen-specific T cells. Infiltrating T cells release inflammatory cytokines, interferon (IFN)-γ, and interleukin (IL)-4, which stimulate KCs to produce chemokines, amplifying cellular infiltration. These infiltrating cells migrate into dermal and epidermal compartments. Finally, the skin site clinically develops an eczematous reaction. After a period comprising days or weeks, allergen removal and down-regulatory factors are locally released, resulting in clinically healed skin (1, 2).

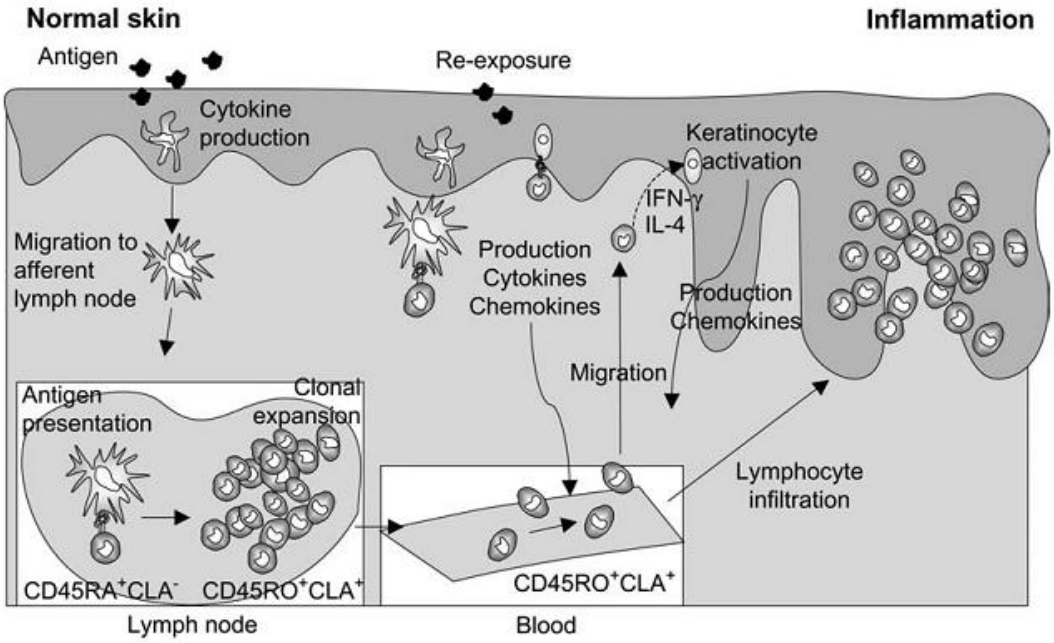

Figure 1. Cellular and molecular events triggered during the development of Allergic contact dermatitis (2).

ACD is one of the most common occupational diseases in developed countries and 19.5% of the general population is sensitive to at least one allergen (3).

The origin and nature of the compounds able to induce ACD are very diverse, but they share some common features: contact allergens are low molecular weight chemicals named haptens, that are not immunogenic by themselves and need to bind to epidermal proteins. These then act as carrier proteins to form the hapten-carrier complex that finally acts as the antigen (4). Several *in vivo* models have been demonstrated accurate in predicting chemicals that possess skin sensitizing properties, such as the local lymph node assay (5). However, for the prediction of skin sensitization potential of contact allergy provoking substances, there is currently no validated non-animal alternative approaches, thus it is imperative to develop an effective alternative *in vitro* approach for skin sensitization evaluation (6). The main goal of this work was to identify lipid changes selectively modulated by a strong skin sensitizer, contributing for the development of an alternative *in vitro* approach for skin sensitization evaluation.

As the primary interface between the body and the environment, the skin provides a first line of defense against microbial pathogens and physical and chemical insults. Immunosurveillance of such a large and exposed organ presents unique challenges for immune sentinels and effector cells. Human skin has two main compartments: the epidermis and the dermis (Figure 2).

The **epidermis** is the outer compartment and contains several layers. The bottom layer contain just one line of undifferentiated epidermal cells, known as basal KCs, which divide frequently and move to the next layer, begin a maturation process. This maturation process is characterized by increasing production of keratin proteins and lipids until they reach the outermost layer that it is largely responsible for the barrier function of the skin, which excludes many toxic agents and prevents dehydration. Specialized cells of the epidermis include melanocytes, which produce the pigment melanin, and LCs which are the main skin-resident immune cell.

The epidermis has a simple histology, but the underlying **dermis** is anatomically more complicated, with greater cell diversity. It contains many specialized immune cells, including dermal DCs, $CD4^+$ T helper (TH) cells, γδ T cells and natural killer T (NKT) cells. Moreover, macrophages, mast cells, fibroblasts and nerve-related cell types are also present (Figure 2). The dermis is drained by lymphatic and vascular vessels, through which migrating cells can traffic (7).

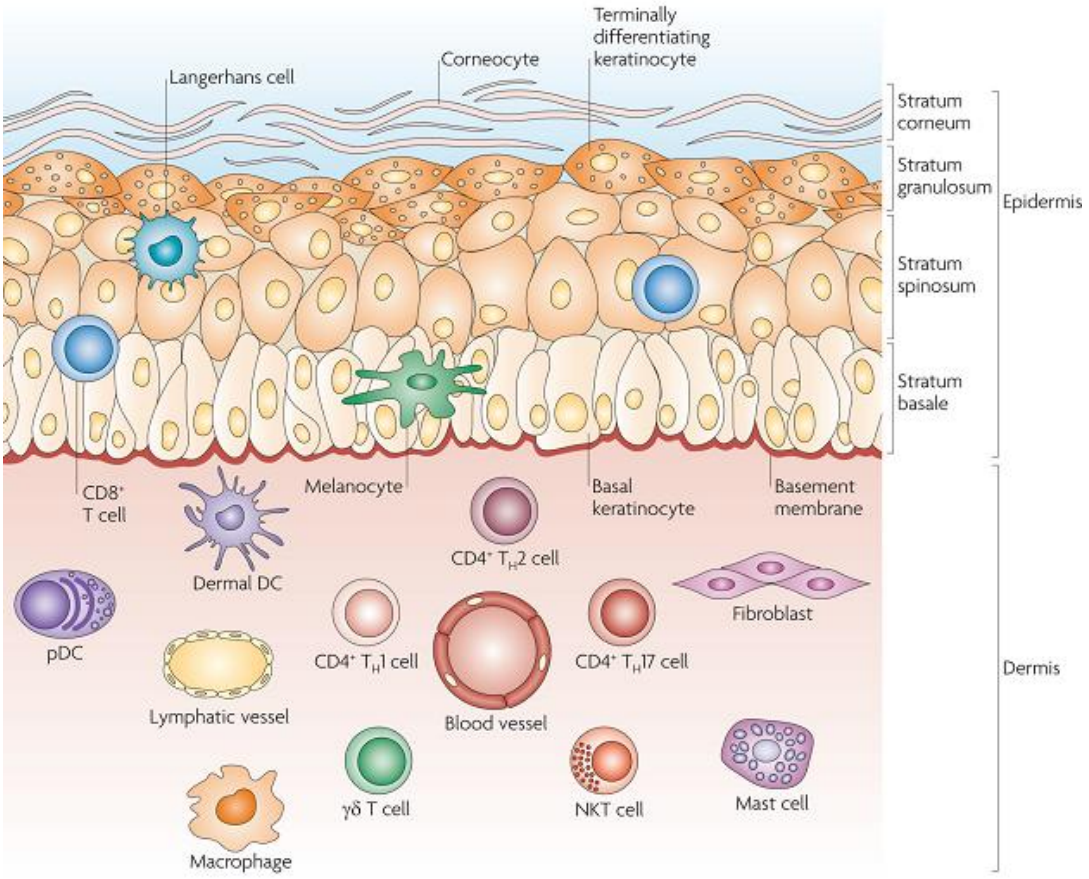

Figure 2. Skin anatomy and cellular effectors (7). The structure of the skin reflects the complexity of its functions as a protective barrier, in maintaining the body temperature, in gathering sensory information from the environment and in having an active role in the immune system.

Due to their anatomical location and their significant role in the development of ACD, the use of KCs and DCs to evaluate sensitizing potency *in vitro* is amply justifiable. Accordingly, assessment of potency of allergenic activity of low molecular weight compounds, based on IL-1α and IL-18 production by KCs, was previously demonstrated (8). As, exposure of DCs cultures to different skin sensitizers has shown that DCs suffer phenotypical and functional modifications, acquiring markers of mature DCs, as occurs after DCs contact with lipopolysaccharide (LPS), pro-inflammatory cytokines or CD40 ligand. In contrast, chemical irritants do not trigger DC maturation. This specific activation elicited by skin allergens form the basis for a raft of DCs-based predictive assays (9). Therefore, in this work, we analyzed the lipid profile of a fetal skin-derived dendritic cell line (FSDC), that is a skin dendritic cell precursor with antigen-presenting

capacity (10) and of a human keratinocyte cell line (HaCat) that has the characteristics of basal epidermal KCs (11). These cell lines were exposed to the potent pro-inflammatory stimulus, lipopolysaccharide (LPS), a known stimulus of DC maturation, to the strong skin sensitizer 2,4-dinitrofluorbenzene (DNFB) and to the contact irritant benzalkonium chloride (BC).

1.1 Dendritic Cells

Dendritic cells (DCs), are immune cells and represent an heterogeneous cell population residing in most peripheral tissues, particularly at sites of interphase with the environment, e.g. skin and mucosa. In the epidermis, they represent 1–3% of the cells and dynamically influence the induction and modulation of innate and adaptive immunity (2). As described above, DCs have a crucial role in ACD, by virtue of their specialized ability to acquire, process, and present antigens to T cells. Some other cell types, such as macrophages or activated parenchymal cells, may, under certain circumstances, serve as antigen-presenting cells that drive the activation and proliferation of memory T cells. However, DCs appear to be the only class of antigen-presenting cells that have the capacity to stimulate the expansion of naïve T cells and thereby initiate primary immune response (12).

Naïve T cells accumulate in paracortical regions of lymph nodes and the spleen, migrating to these locations directly from the vasculature. Immature DCs (iDCs) also circulate in the blood, but are more abundant within epithelial and connective tissues, where they are ideally positioned to acquire antigens, such as allergens and microorganism antigens, that typically initially establish infection in the periphery. Because naïve T cells do not, for the most part, enter peripheral tissues, their interaction with and activation by DCs results from the migration of DCs into lymph nodes.

During migration, DCs lose their capacity to internalize further antigens and acquire the capacity to present antigens to naïve T cells, in a well coordinated succession of events referred to as maturation (2, 7, 13, 14). Antigens are presented in such a way that antigen-specific naïve T cells become activated and start to proliferate

(T-cell priming). Moreover, when DCs initiate a T-cell-mediated adaptive immune response, they also play an important role in polarization of T-cell reactivity towards type-1, or type-2, or type-17, or also Treg responses (2, 15).

According to their localization in distinct anatomical compartments of the skin, there are two main populations of DC present in normal human skin: Langerhans cells (LCs) are the main DCs subset in the epidermis, where they constitutively reside in the supra-basal layers and are regularly spaced among KCs, whereas dermal DCs reside in the dermis (Figure 2). In addition to their different anatomical locations, different DC types in the skin might have specific functional properties, such as secretion of pro-inflammatory mediators (inflammatory DCs), production of type I IFNs (plasmacytoid DCs (pDCs)), or cross-presentation (CD103 (also known as integrin $\alpha e)^+$ skin DCs) (7).

LCs represent approximately 1-3% of epidermal cells and form a constituent part of the skin immune system. They are typically characterized by the expression of the type II transmembrane Ca^{2+}-dependent lectin, langerin/CD207, in mice and CD1α in humans, and a special type of intracytoplasmic organelle known as the Birbeck granule(2). In addition, LCs has been distinguished from other cells by the expression of epithelial cell adhesion molecule (EPCAM), which is not expressed by langerin$^+$ dermal DCs (16). LCs originate from bone-marrow-derived progenitors, as indicated by their CD45 expression. However, the process of LC differentiation and their migration into the epidermis is not clearly understood. Several studies suggest that skin-resident LC precursors exist in the dermis under normal non-inflammatory conditions. These LC precursors co-express Langerin and CD14, and their final migration into the supra-basal layer of the epidermis is most likely controlled by KC-derived CXCL14 (17). Additionally, it is also suggested that an arrangement of transforming growth factor (TGF)-β 1 and CCL20 is required for the recruitment of human LC precursors through the dermal–epidermal barrier (18). Thus, the final differentiation of LC precursors depends on the cytokine environment of the epidermis. It has been described that the cutaneous cytokines granulocyte–macrophage colony-stimulating factor (GM-CSF), IL-15, and TGF-β_1 contribute to the establishment of immature LC in the epidermis (2). Because of their specialized location, LCs constitute the first immunological barrier to pathogens. *In vitro* studies have shown that LCs take up and process lipid antigens and

microbial fragments for presentation to effector T cells (19). In addition, human LCs have been shown to preferentially induce the differentiation of Th2 cells, being able to prime and cross-prime naive $CD8^+$ T cells (20).

Dermal DCs were identified more than 120 years after LCs were discovered (21).They are located at the level of the capillaries and in the higher part of the reticular human dermis, migrating rapidly to lymph nodes in order to colonize micro-anatomical areas in the paracortex of lymph nodes (22). Recent data obtained from a model of ACD showed that dermal DCs, and not LCs, isolated from draining lymph nodes induced T cell proliferation (23). There is no exclusive marker for dermal DCs comparable to langerin/CD207, making dDCs difficult to track *in vivo*, often being overlooked in studies of skin immunity.

1.2 DC Migration and Maturation

In the peripheral tissues, immature DCs capture and process antigens, such as allergens and microorganism antigens, thereafter, they migrate towards T-cell-rich areas of the secondary lymphoid organs where they present antigens to naïve T cells. Thus, the migration of DCs from the skin is one of the first steps in the initiation phase of an immune response. Skin contact with antigens is known to stimulate various epidermal cytokines, e.g. IL-6, tumor necrosis factor (TNF)-α, GM-CSF, and CXCL2/CXCL3 (macrophage inflammatory protein-2, MIP-2), among which IL-1β and TNF-α are essential in DCs migration (Figure 3). The signalling events triggered by these cytokines result in altered expression of adhesion molecules that mediate interactions with the extracellular matrix, epidermal, and dermal cells and facilitate DCs migration out of the epidermis. One of the most important events is the reduced expression of CD324 (E-cadherin), which allows DCs to dissociate from surrounding KCs caused by TNF-α, IL-1β, or IL-1α production (24, 25). Another adhesion molecule, junctional adhesion molecule 1 (JAM-1), is expressed by DCs and therefore affects DCs migration (26).

Simultaneously, production of epidermal basement membrane degrading enzymes, such as matrix metalloproteinases (MMPs), is upregulated in activated LCs.

The MMP-2, MMP-3, and MMP-9 have been described to facilitate the passage of LCs across the basement membrane, being also essential for migration of LCs and dermal DCs through the dermal tissue matrix, by cleavage of type IV collagen. Several studies have demonstrated that inhibitors of MMPs prevented the emigration of LCs from the epidermis and thus, DC accumulation in the afferent lymph node, in response to the epicutaneous application of sensitizers, such as nickel, oxazolone (OXA), and dinitrochlorobenzene (DNCB) (27).

DC migration is also associated with the expression of chemokine receptors on the surface of these cells. Immature DCs (iDCs) express chemokine receptors, and these can guide them to inflammatory sites where antigen sampling occurs, promoting their differentiation into a mature phenotype. This maturation process is associated with a switch in chemokine receptor profile. Skin-homing chemokine receptors are downregulated (CCR1, CCR2, CCR5, and CCR6), whereas receptors involved in homing to the local lymph node are upregulated (CCR4, CXCR4, and CCR7). CCR7 is the most important chemokine receptor for the mobilization of DCs from the periphery to the afferent lymph nodes (28). Both lymphatic and high endothelial venules produce CCL21, a major CCR7 ligand. In addition, residing DCs in the paracortical areas of the lymph nodes produce CCL19, a second ligand of CCR7. This orchestrates the encounter of DCs and naïve T cells in the paracortical lymph node areas, an imperative event for the DC maturation as it will be described below.

Furthermore, lipid mediators are also required for DC migration, such as cysteinyl leukotrienes (cysLTs) and prostaglandin E2 (PGE2) produced at the sites of inflammation and synthesized in the cell from the essential fatty acids of diacylglycerol or other phospholipids. These lipid mediators promote the upregulation of CCR7, optimal DC chemotaxis to the chemokine CCL19 but not to CCL21, and the expression of others proteins necessary for DC entry into afferent lymphatics.

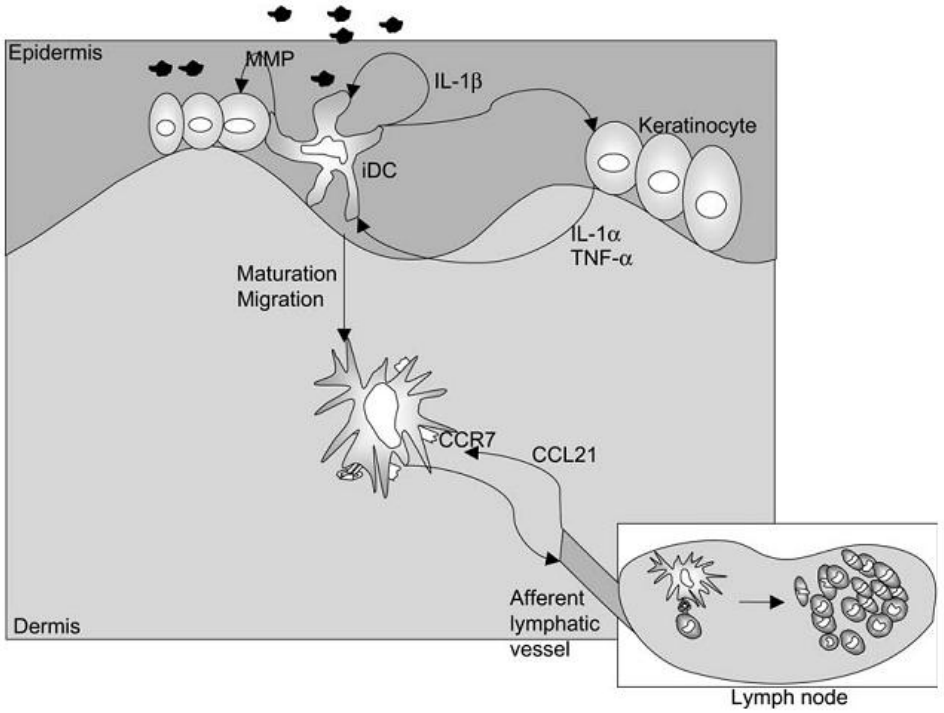

Figure 3. Cellular and molecular events triggered during migration of dendritic cells (2). Skin contact with a hapten triggers migration of DCs. Production of cytokines – particularly TNF-α, IL-1 α, and IL-1β – facilitates migration of LCs out of the epidermis. At later stage, CCR7–CCL21 interaction plays a pivotal role in the migration of LCs into the T-cell areas of lymph nodes.

Tissue injury, microbial, and other changes of homeostasis provide danger signals, which activate DCs and trigger their exchange from immature antigen-capturing cells (iDC) to mature antigen-presenting DC (mDC), in a well coordinated succession of events referred to as maturation process.

The first step of DC maturation is the contact with antigens, in which DCs used a broad range of pathways to facilitate antigen uptake. Many of these pathways, e.g. through $\alpha_v\beta_5$-integrins or CD36, may also be used for uptake of self antigens (29). Following antigen uptake, maturation of iDCs is associated with several coordinated events: loss of endocytic/phagocytic receptors, upregulation of co-stimulatory molecules (e.g. CD80 and CD86), change in morphology, and upregulation of class II MHC molecules (2). Functionally matured DCs (mDCs) are accumulated in T-cell-rich areas of lymphoid tissues. Within the paracortical areas, the conditions are optimal for antigen-bearing mDCs to encounter naïve T cells that specifically recognize the

antigen–MHC molecule complexes. The dendritic morphology of these antigen-presenting cells powerfully facilitates multiple cell contacts, allowing the binding and activation of antigen-specific T cells. Antigen-specific T cells expand abundantly and generate effector and memory T cells, which are released by the efferent lymphatics into the circulation.

DC maturation can be initiated *in vitro* by inflammatory stimuli, such as proinflammatory cytokines (e.g. TNF-α and IL-1β), LPS, CD40 ligation and contact allergens (30, 31). Immature DCs express a large array of receptors that can recognize specific motifs of pathogens, denominated pathogen-associated molecular patterns (PAMPs), which are ligands for Toll-like receptors (TLRs) on APCs. Basically, bacterial components can be recognized by DCs through TLR1, TLR2, TLR4, TLR5, and TLR6 and viral RNA through TLR3, TLR7 and TLR8 (32). In addition, iDC express C-type lectins, like CD209 that recognizes carbohydrate structures on pathogens.

In this study we used as maturation stimulus of DCs a bacterial PAMP, LPS that is a TLR4 ligand and a potent inducer of DC maturation, discussed later. The skin sensitizers may also activate the innate immune system in a similar way to PAMPs. Like PAMPs, contact sensitizers can trigger signaling cascades and induce DC activation, with subsequent upregulation of costimulatory molecules, and cytokine production (33, 34). These maturation stimuli induce phosphorylation of mitogen-activated protein kinases (MAPKs), such as extracellular signal-regulated kinases (ERKs), c-Jun N-terminal kinases (JNKs), and p38 MAPK, with distinct roles in the maturation process. For instance contact sensitizers trigger p38 MAPK activation, which is a critical player in the initiation of contact hypersensitivity. In addition, DC maturation elicited by contact sensitizers is also characterized by the expression of surface molecules, such as CD40, CD80, CD83, CD86, and MHCII and the upregulation of inflammatory cytokines. In contrast, these events are not triggered by irritants (2, 6).

Once DCs enter the regional lymph node, T cells that possess TCRs complementary to the MHC molecule–antigen complex on the surface of the LCs become activated. The polarization of naïve T-cells into various effectors lineages is dependent on a set of three distinct signals. The “antigen-specific” signal is provided by interaction between the peptide-bearing MHC molecule on the DC and the TCR on the naive T cell. The potent “costimulatory” signal is triggered upon contact-dependent interactions,

namely between the costimulatory molecules CD80 or CD86 expressed on DCs with CD28 expressed on T cells. The combination of these two signals results in antigen-specific activation and proliferation of naïve T cells with the development of effector and memory T cells. Additional factors (the last signal) are needed for polarization of T cells towards type-1, type-2, type-17 or Treg cells (for $CD4^+$ T cells) and type-1 or type-2 cytotoxic T cells (for $CD8^+$ T cells) (2).

Briefly, a variety of "danger" signals induce DC maturation, ultimately resulting in the generation of antigen-specific T cells, which in turn facilitates immunity.

1.3 Keratinocytes

Similar to DCs, keratinocytes (KCs) can sense pathogens and mediate immune responses able to discriminate between harmless commensal organisms and harmful pathogens. As DCs, epidermal KCs express several TLRs (Figure 4), located either on the cell surface (TLR1, 2, 4, 5 and TLR6) or in endosomes (TLR3, 7, 8 and TLR9) that recognize various evolutionarily conserved PAMPs, which include LPS, used in this work. TLR expression by KCs is crucial for promoting skin immune responses, activation of these receptors on human KCs leads to a predominant Th1-type immune response with production of type I IFNs (35).

A recently discovered class of proteins that are encoded by the nucleotide-binding domain leucine-rich repeat-containing (NLR) gene family can also recognize PAMPs and endogenous danger-associated molecular patterns (DAMPs), such as irritants and toxins. Activation of these receptors results in the elicitation of pro-inflammatory signalling pathways, through the inflammasome - a large multiprotein complex formed by an NLR, the adaptor protein ASC (apoptosis- associated speck-like protein containing a caspase recruitment domain) and pro-caspase 1. The assembly of the inflammasome leads to the activation of caspase 1, which cleaves pro-interleukin-1β (pro-IL-1β) and pro-IL-18 to generate the active pro-inflammatory cytokines (36). It has recently been established that contact sensitizers, such as haptens, applied to the skin induce inflammasome-dependent IL-1β and IL-18 processing and secretion and thus allergic contact dermatitis reactions (37). Therefore, KCs exposure to PAMPs, like LPS,

contact sensitizers or irritants, such as DNFB and BC, respectively, triggers the activation of intracellular sensors contained in the inflammasome complex of KCs, leading to the activation of caspase 1 and to the processing and secretion of key pro-inflammatory cytokines. This in turn results in the activation of tissue-resident immune cells that induce and perpetuate an inflammatory response.

In the skin, KCs constitutively secrete or are induced to release, numerous cytokines, including IL-1, IL-6, IL-10, IL-18 and TNF-α. Of particular interest with regard to the skin is the production of IL-1 by KCs. IL-1 is a pleiotropic cytokine with a broad range of biological effects, including the activation of T helper cells and DCs and the promotion of B cell maturation and clonal expansion (38). In healthy skin, KCs constitutively synthesize both pro-IL-1α and pro-IL-1β but cannot process them or secrete them in their active forms. Following exposure to stimuli, KCs process and release IL-1β through activation of the inflammasome. However, the regulation of IL-1α secretion in keratinocytes is still unclear.

As to DCs, KCs are also an important source of chemokines and express chemokine receptors, modulating the immune response, through the attraction of different cell types into the skin. Thus, the expression of CC-chemokine ligand 20 (CCL20) by activated keratinocytes regulates the trafficking of LCs precursors to the epithelium, an important point de interaction between KCs and DCs. Furthermore, by expressing CXC-chemokine ligand 9 (CXCL9), CXCL10 and CXCL11 activated keratinocytes attract effector T cells to the skin during diseases and can also recruit neutrophils to the inflamed epidermis by producing CXCL1 and CXCL8 (7).

As a result, KCs are pro-inflammatory effector cells that are strategically positioned at the outermost layer of the body to react in a timely fashion to harmful insults by the coordinated production of pro-inflammatory cytokines and chemokines.

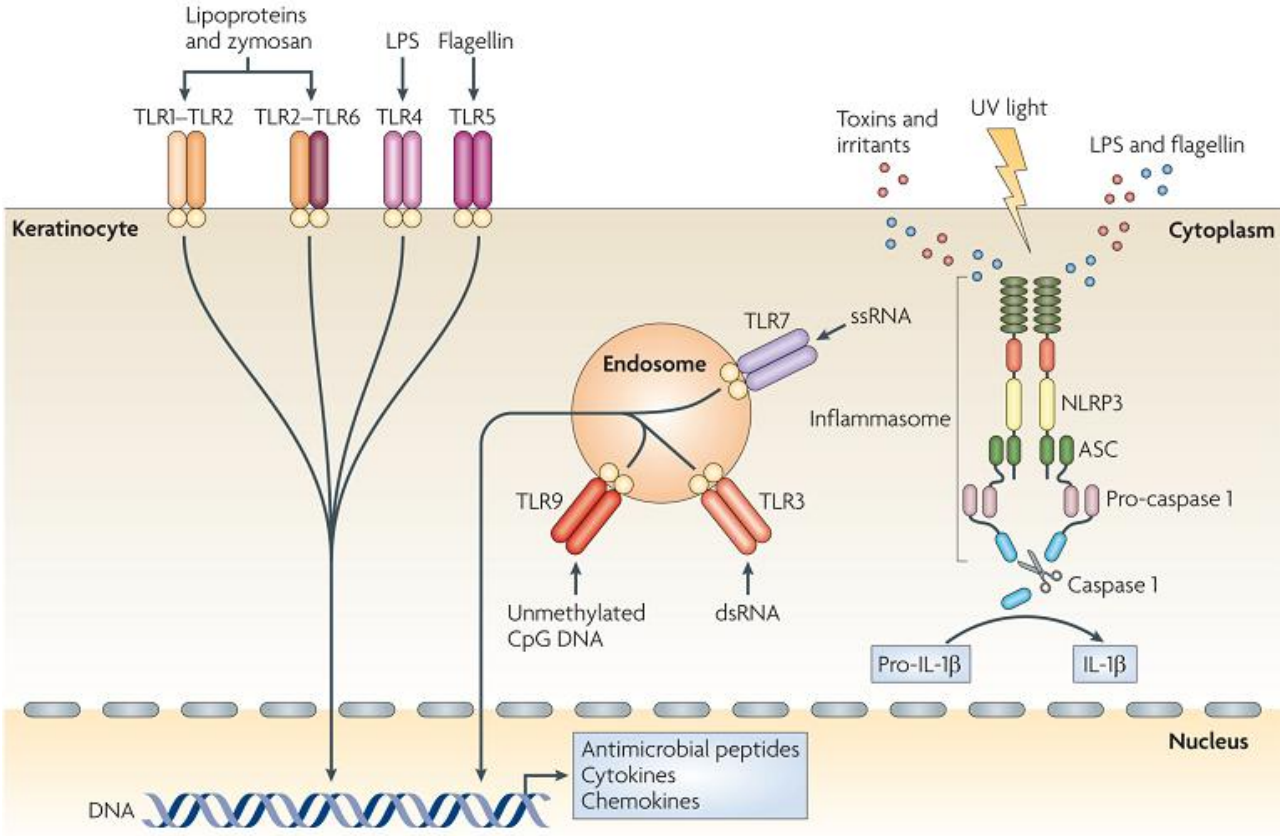

Figure 4. Keratinocytes are central skin sentinels (7). Keratinocytes can recognize foreign and dangerous agents, for example pathogen-associated molecular patterns (PAMPs) of microbial origin and danger-associated molecular pattern (DAMPs), such as irritants and toxins, through Toll-like receptors (TLRs) and the inflammasome machinery.

2. Lipids

Once considered passive bystanders, with the only functions as providers of energy and a basic structure of membranes, lipids are now considered as cellular constituents that have multiple roles in cell functions, regulating several important biological processes. The majority of cellular lipids composed the membrane bilayer, whose integrity and physical characteristics are fundamental in biological systems. Lipids can also promote appropriate hydrophobic medium for the functional implementation of membrane proteins and their interactions. The chemical and physical properties of membranes are largely dependent on the lipid composition (39, 40). Thus, as major structural elements of cellular membranes, the membrane fluidity depends on the lipids and proteins contents, as well as their mutual interactions.

Consequently, membrane fluidity controls, at least in part, the cellular events that occur at the cell membrane interphase, such as ligand–receptor interactions, endocytosis and antigen presentation (41, 42). In addition, membrane lipid metabolism is regulated by distinct types of extracellular receptor-regulated pathways in a variety of ways, including modifications associated with membrane fusion, secretion, trafficking, and plasma membrane shape changes. Also, changes in bilayer structure seem to regulate the activities of enzymes, channels, and transport proteins. Furthermore, a variety of lipids play a very important role in the regulation of various cellular functions by acting as signaling molecules (phosphatidylinositol (PI) and Ceramide (Cer)), or as precursors for second messengers (e.g. inositol trisphosphates (IP3)/DAG) (43, 44). Besides these important characteristics, the increasing attention from lipid researchers but also for clinical chemistry and pharmaceutical industry, is essential since alterations in lipid metabolism is involved in the pathogenesis of several common diseases such as cancer, diabetes, atherosclerosis as well as neurodegenerative and inflammatory diseases (45).

2.1 Definition and classification

Traditionally, “lipids” can be defined as apolar compounds that are insoluble in water and may be enriched by the treatment/extraction with organic solvents such as chloroform or hexane (46). Even though this is true in most cases, there are substances that we now see as lipids (saccharolipids for example) that are more soluble in water than in chloroform and, and besides, several peptides and very hydrophobic proteins are actually soluble in chloroform (47). There are other definitions that use a more biological approach. William Christie defined lipids, for the first time in 1987, as “fatty acids and their derivates and substances related biosynthetically or functionally to these compounds” (48). In order to reach a consensus, several of the world leading lipid researchers recently proposed a lipid classification system and by these authors, lipids are defines as “hydrophobic or amphipathic small molecules that may originate entirely or in part by carbanion-based condensations of thioesters (fatty acids, polyketides, etc.) and/or isoprene units (prenols, sterols, etc.)” (46). Their lipid

classification system proposed an organization of lipids into 8 groups based on chemical and structural features (Table 1) and put forward schemes for nomenclature. This effort, which is made with the intention of facilitating the systematization and cataloging of lipids, will be very useful when creating lipid databases for the use in lipidomics and system biology. Below it is presented a short description of the lipid classes relevant for the work included in this thesis.

Category	Abbreviation	Example
Fatty acyls	FA	Dodecanoic acid
Glycerolipids	GL	Triacylglycerol
Glycerophospholipids	GP	Phosphatidylcholine
Sphingolipids	SP	Ceramide, Sphingomyelin
Sterol lipids	ST	Cholesterol, Cholesterol ester
Prenol lipids	PR	Retinol
Saccharolipids	SL	Lipid X
Polyketides	PK	Tetracycline

Table 1. Lipid classification as suggested by Fahy et al. (46)

2.2 Structure and function

Fatty acids

Fatty acids (FAs), as the simplest and one of the most important lipid classes, are a basic element of all lipids. Structurally, natural FAs are synthesized in a fashion that leads to ethylene (C_2H_4)-spaced products of different chain lengths and their aliphatic tail (chain) is either saturated or unsaturated. Unsaturated fatty acids have one or more double bonds, that are included at various positions and at various stages in the biosynthetic and metabolic processes, resulting in a vast amount of different molecules (49). FAs are used as building blocks of more structurally complex lipids and also are important precursors of a variety of bioactive lipid molecules. For example, arachidonic acid is the precursor of eicosanoids, which function as signaling molecules through specific receptors and play important roles in inflammatory processes (50).

Glycerophospholipids

As the major group of lipids, **Glycerophospholipids**, also referred to as **Phospholipids (PLs)**, are ubiquitous in nature and are the major components of biological membranes (46). The principal feature of PLs is the presence of a functional polar head group attached to the end of the glycerol backbone via a phosphodiester bond. Thus, PLs can be subdivided into distinct classes according on the polar head group attached to the *sn-3* position on the glycerol backbone (Figure 5).

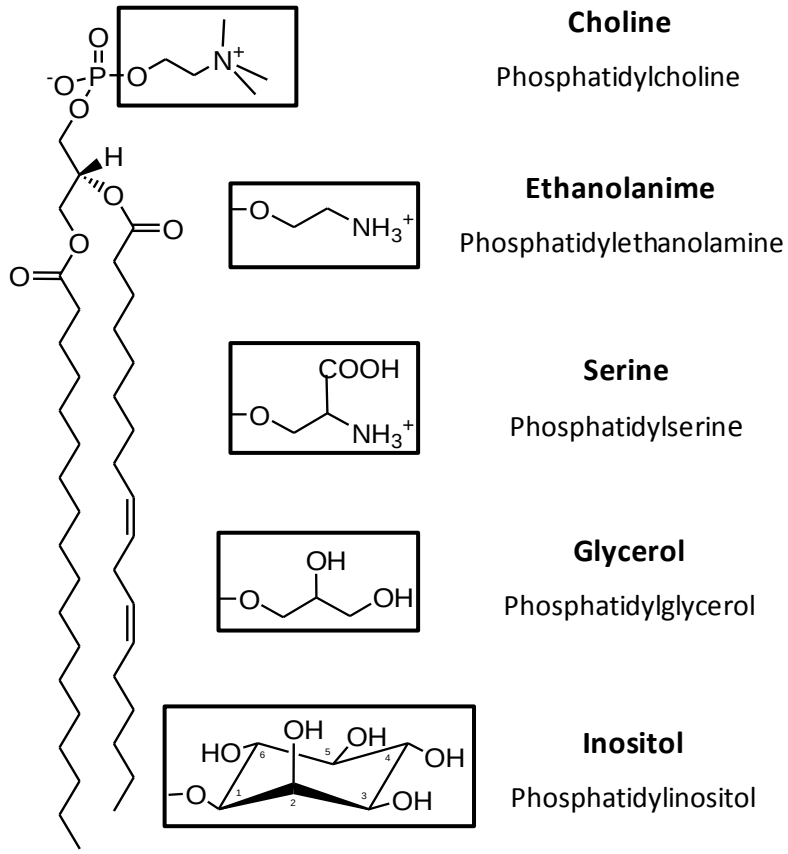

Figure 5. Schematic representation of phospholipid structure. Structure of a phospholipid with the indication of the structure of the polar head groups characteristic of the principal classes of phospholipids: phosphatidylcholine, phosphatidylethanolamine, phosphatidylserine, phosphatidylinositol and phosphatidylglycerol.

Based on the different polar head groups, PLs can be divided into phosphatidylcholine (PC) and phosphatidylethanolamine (PE) that are the most common sub-classes and may constitute as much as 55 and 35 %, respectively, of the

total lipids in certain tissues (51). Other sub-classes include phosphatidylserine (PS), phosphatidylglycerol (PG) and phosphatidylinositol (PI).

Various FAs are linked to the glycerol backbone at *sn*-1 and *sn*-2 positions. The "typical" phospholipids consist of fatty acid chains joined to the glycerol backbone by ester linkage. By contrast, ether-linked phospholipids contain either an alkyl ether or vinyl ether bond at the *sn-1* position. Due to the different chemical bonds of the aliphatic chains at the *sn*-1 position of glycerol backbone, each class is further divided into three subclasses (Figure 6), i.e., phosphatidyl (1,2-dialcyl), plasmanyl (1-alkyl, 2-acyl) and plasmenyl (1Z-alkenyl, 2-acyl), corresponding to the ester, alkyl ether and vinyl ether linkages, respectively (52). In mammalian cells, ether-linked lipids are mostly species of PC or PE.

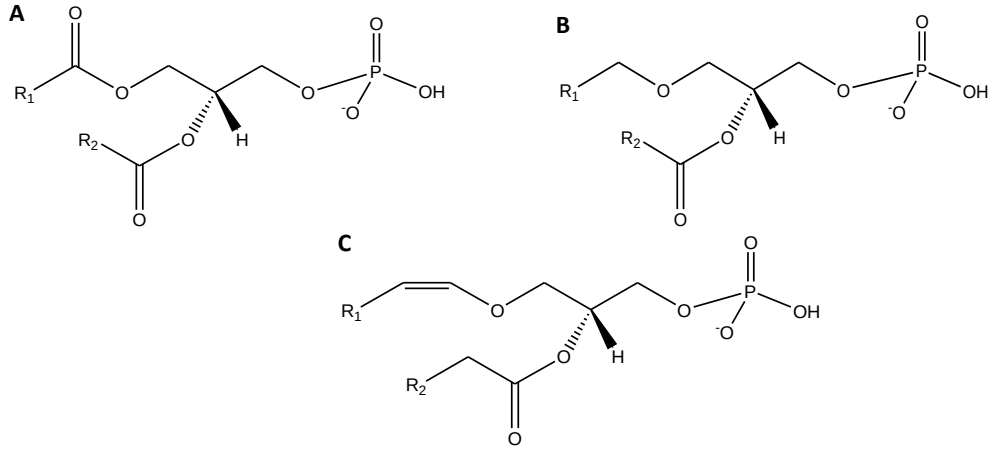

Figure 6. The subclasses of glycerophospholipids. (A) phosphatidyl, (B) plasmanyl and (C) plasmenyl.

PLs participate in various biological activities involving metabolic pathways, cell signalling by acting as second messengers themselves or as precursors for the generation of second messengers, membrane anchoring and substrate transport. In addition, some lipid molecular species such as PEs, PCs and PIs have been found as potential biomarkers involved in several diseases such as obesity and cancer as well as neurodegenerative and inflammatory diseases (45).

Cardiolipin (CL, 1,3-bis(sn-3-phosphatidyl)-sn-glycerol) is a phospholipid different from previous ones, and even considered as a separate class. CL is a dimeric phospholipid, since it has two phosphatidic acids linked in a central glycerol group. It has three molecules of glycerol in its structure, and has four fatty acyl chains. The relationship between the three glycerol molecules creates a unique environment for each ester linkage (Figure 7). The fact that the headgroup alcohol is shared by two phosphate moieties is a feature with important implications regarding the overall physical properties of CL within the context of a lipid bilayer, namely in their mobility and conformational flexibility (53). This lipid is almost exclusively located in mithocondria membrane. Figure 7 represents the general structure of cardiolipin.

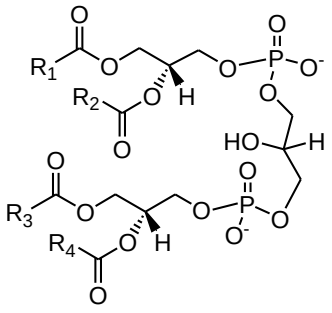

Figure 7. Schematic representation of Cardiolipin Structure.

Sphingolipids

The second major category of polar lipids are sphingolipids (SLs) that contain as a common structural feature the **sphingoid base** backbone composed of a hydrophobic moiety and a hydrophilic head group (Figure 8).

The sphingoid base is synthesized from a serine and a long-chain fatty acyl-CoA and further metabolism leads to the generation of several other sub-groups of SLs, with Ceramide (Cer) [and dihydroceramide (dhCer)] as the center of SL biosynthesis, catabolism, and as precursors of complex SLs. Cer can be produced in at least two distinct ways. First, it can be synthesized through the *de novo* pathway through formation of sphingoid base catalyzed by serine palmitoyl transferase to generate 3-keto-dihydrosphingosine. Subsequently, 3-keto-dihydrosphingosine is reduced to form dihydrosphingosine (sphinganine) which is then acylated by (dh) Cer synthases to

produce dhCer or Cer. Second pathway of Cer production is through the hydrolysis of complex lipids, especially sphingomyelin (SM). In this hydrolytic pathway, SM is cleaved by one of several sphingomyelinases (SMases), releasing phosphocholine and Cer. Another important source of Cer is provided by the breakdown of glycosphingolipids (glucosylceramide) (54).

In the SL biosynthetic reactions, Cer is primarily used for the synthesis of SM by transferring a phosphocholine headgroup from PC through the action of SM synthases, thereby also generating diacyl-glycerol (DAG). Cer can also be phosphorylated by Cer kinase, which in turn can be recycled by a Cer-1-phosphatase (C1P) or glycosylated by glucosyl or galactosyl Cer synthases. Finally, Cer can be metabolized by ceramidases (CDases), removing the amide-linked FA to form Sphingosine (Sph). On the other hand, Sph is available for recycling into SL pathways or for phosphorylation by Sph kinases, to form Sph-1-phosphate (S1P) (Figure 9) (54).

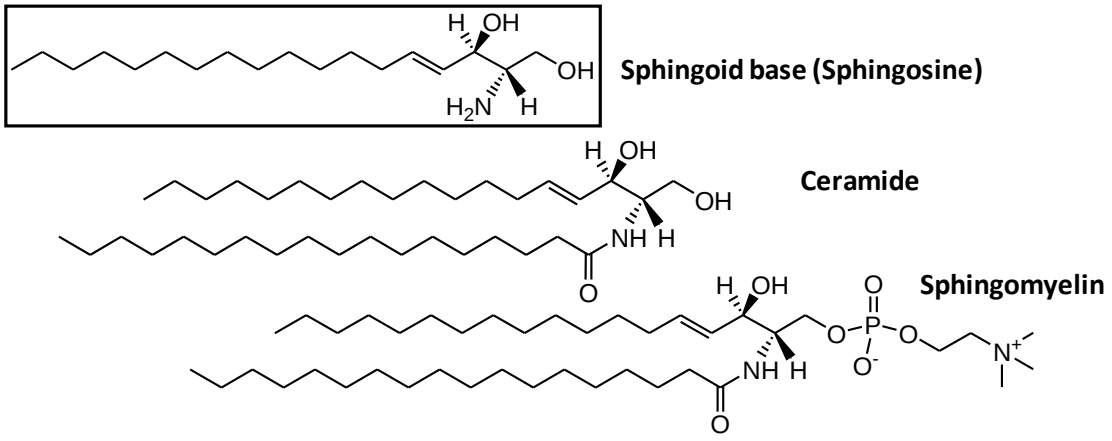

Figure 8. Schematic representation of sphingolipids structure and of the main sphingolipids: Ceramides and Sphingomyelin.

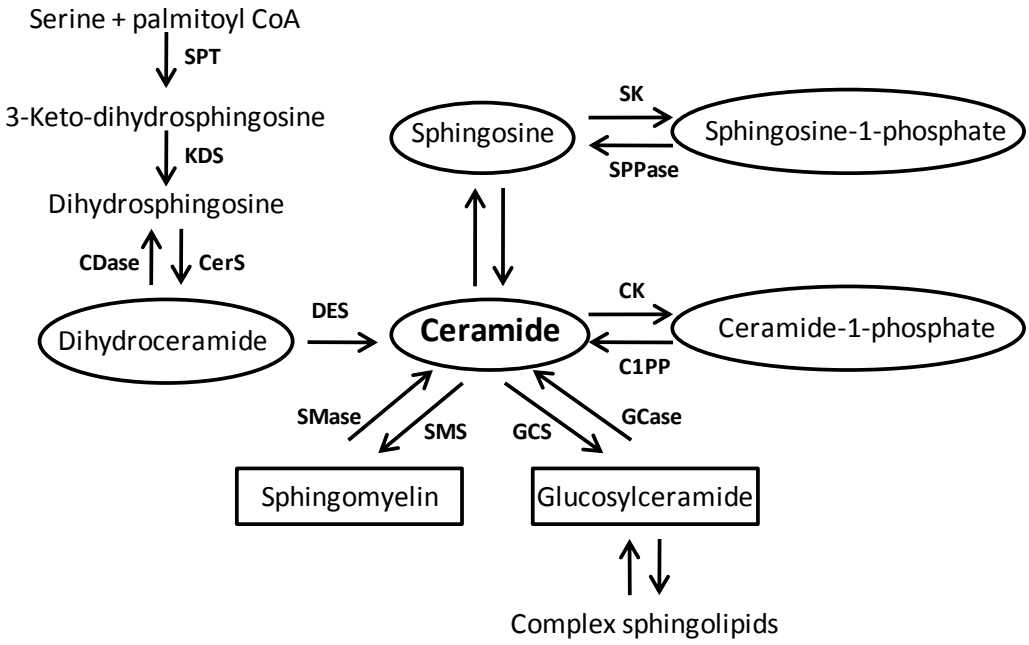

Figure 9. Scheme of SL metabolism. Pathways are shown as described in the text. SPT, serine palmitoyl transferase; KDS, 3-keto-dihydrosphingosine reductase; DES, dihydroceramide desaturase; SPPase, Sph phosphate phosphatase; CK, Cer kinase; C1P P, C1P phosphatase; SMS, SM synthase; GCS, glucosylceramide synthase; GCase, glucosyl ceramidase.

Sphingolipids are found in many living organisms (from yeast, plants, to humans) and in virtually all cell types, comprise more than 300 species. Besides playing structural roles in cellular membranes, sphingolipid metabolites act as bioactive signaling molecules involved in the regulation of cell growth, differentiation, senescence, apoptosis, migration and adhesion (54, 55). Bioactive sphingolipids are induced by several agonists, and, in turn, they regulate several downstream targets that mediate their various effects on cell function (54). The relevant sphingolipids for this study are ceramides and sphingomyelins.

3. Lipidomics

The crucial role of lipids in cell, tissue and organ physiology is demonstrated by a large number of genetic studies and by many human diseases that involve the disruption of lipid metabolic enzymes and pathways. So far, the explosion of

information in the fields of genomics and proteomics has not been matched by a corresponding advancement of knowledge in the field of lipids, which is largely due to the complexity and diversity of lipids and the lack of powerful tools for their analysis. However, those genomic and proteomic innovations revealed the need to explore metabolic processes at the system level and lead inevitably to the development of lipidomics.

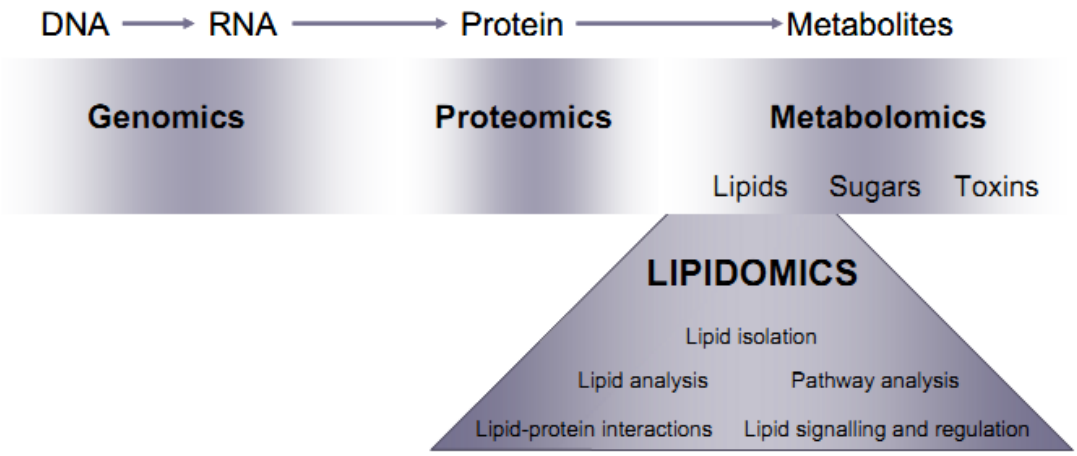

Figure 10. Lipidomics – system level scale analysis of lipids and their interactions. Genes encode proteins that collectively together with environmental factors, lead to the metabolite inventory of a cell, tissue or body fluid. Novel approaches now allow for qualitative and quantitative measurements at each level on global scales (genomics, proteomics and metabolomics). Lipidomics, the systems-level scale analysis of lipids and their interacting partners, can be viewed as a sub-discipline of "metabolomics" (49).

Lipidomics is categorized as subgroup of metabolomics (Figure 10), and has been defined as "the systems-level analysis of lipids and their interacting moieties" (49). Other definitions imply that lipidomics is more than just the characterization of lipids and involves also the comprehensive understanding of the influence of all lipids on a biological system (56). This new discipline, which was first mentioned in a peer-reviewed scientific paper in 2003 (57), is a relatively young field of biomedical research but this field is a promising area, with a variety of applications, in biomarkers development and its importance is now widely recognized. This was reflected because researchers realized the importance of lipids into different inter-related areas. First,

the importance of lipids as a part of the etiology of diseases such as atherosclerosis, obesity and Alzheimer's disease has been approved. Other, researchers have perceived that the study of specific pathways requires the analysis of multiple lipids, namely, the metabolism of several molecular lipids and lipid classes are interwoven. Finally, and perhaps most importantly, this field of research has expanded because of important developments in the arsenal of analytical tools available. Of major importance is mass spectrometry (MS), which allows even low abundant lipids to be analyzed in a high-throughput manner. Thus, lipidomics is a rapidly growing field that provides insight as to how specific lipids play roles in normal physiological and disease states.

The lipidomic study includes several steps that they are represented in Figure 11, the first correspond to **lipid isolation** from tissues or cells by specific methods that take advantage of the high solubility of the hydrocarbon chains of lipids in organic solvents, as will be described below. The following step is the **analysis of lipids** extracted, either directly by MS or after their separation, usually by chromatography. Subsequently, the identification and quantification of each molecular species using phosphorous assay that measures the inorganic phosphate present in the sample of PLs, and/or additional analysis by MS allows a more detailed analysis. These steps deliver a "lipid profile", which is a biochemical snapshot of the lipid inventory of the cell or tissue under investigation. Different functional states of the cells or tissue, as in this work were induced by different stimuli applied, can produce differences in such profiles, therefore, the careful assessment of such differences may allow the formulation of a hypothesis of metabolic pathways that might be affected. This step is identified as corresponding to **pathway analysis**.

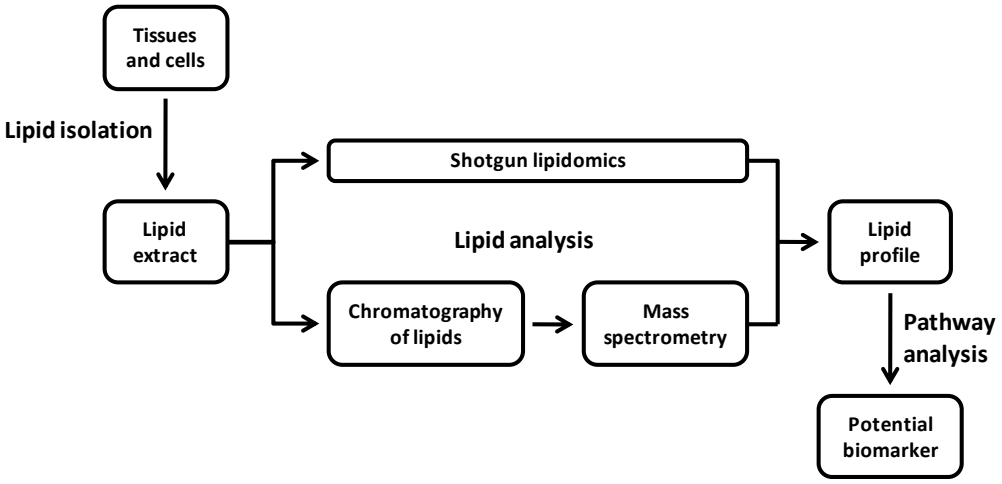

Figure 11. Representative scheme of several steps of a lipidomic approach.

3.1 Lipid Isolation

The first step in the lipid analysis is the extraction of the lipids and removal of non-lipid components from the tissue, cells or biofluid of interest. Lipids are typically extracted with organic solvents from the sample. A number of different organic solvents can be used, and the extractions can be adapted for high recoveries of specific lipid classes, such as PLs or SLs, for example (58). For the isolation of broad spectrum of lipid classes, including PLs, there are two common methods used in this approach, one described by Folch, Lees and Sloane (59), and other described by Bligh and Dyer (60). The basic principle of these methods is that initially a mixture of chloroform and methanol is added to the sample creating a mono-phase system that extracts the lipids from the sample matrix. Then, an amount of water is added to produce a biphasic system, the chloroform layer (bottom phase) of which should contain lipids and the methanol-water layer (upper phase) the non-lipid components. Thus, the chloroform dissolves fat, methanol have a function of breaks down the lipid-protein bonds and inactivates the lipase, while the water wash the non-lipid compounds. To minimize the risk of fatty acid oxidation or the lipids hydrolysis during the isolation process it is recommended that all extractions be made at low temperature (4ºC), as fast as possible after the lipids removal from the tissue or cell culture. The difference between the two methods is that the Folch method uses a mixture of chloroform methanol in

the proportion of 2:1, while the method of Bligh and Dyer use a mixture of chloroform methanol in the proportion of 1:2.

In the work included in this thesis, all the total lipidic extract was extracted according to Bligh and Dyer method, a process where extraction and separation are simultaneous, in which the precipitated proteins are isolated between the two liquid phases. In addition, this method is particularly suitable for lipid extraction of incubation medium, tissue homogenates or cell suspensions.

3.2 Lipid Analysis

Lipid Separation

After lipid extraction from biological samples, the lipid extract contain several molecular lipidic species of distinct lipid classes study in detail, that can be separated by different chromatography methods to proceed with further identification and quantification of each molecular species. In all chromatographic methods the closely related analytes of a complex mixture are transported in a mobile phase that can be a gas or liquid. The mobile phase is forced through a stationary phase that is fixed inside a column or on a plate. The components of mixture are separated based on their physical and chemical characteristics, and according to the different affinity for the two phases. Due to the differences in distribution of the each molecular species between the two phases, they will be separated from each other.

The most popular techniques of chromatography are: thin-layer chromatography (TLC), gas chromatography (GC), liquid chromatography (LC) and high-performance liquid chromatography (HPLC) (61). These techniques can also function as a pre-separation when coupled with MS, facilitating further analysis and identification of lipids, already divided by their families. The techniques more used for lipid analysis are TLC and HPLC, in this study both techniques were used.

TLC was the first chromatography used for analysis of phospholipids, nevertheless, even nowadays is indispensable tool of modern analytical chemistry. There are two

very important reasons why planar chromatography is still alive in modern biochemistry: The increasing commercial availability of pre-coated TLC plates has significantly improved the reproducibility of separation that was quite limited in the past when home-made TLC plates were primarily used. Additionally, the availability of many different absorbent materials including high-performing silica, bonded phases and impregnated layers have increased the versatility of TLC for numerous and quick separations particularly in the lipid field (62, 63).

In addition, although there are several potential concerns against the application of TLC (e.g. the lower chromatographic resolution in comparison to HPLC and the potential oxidation of the analyte caused by exposition to atmospheric oxy-gen), there are many advantages that make TLC clearly competitive method. For example, TLC is a suitable, simple and relatively inexpensive method, where in single TLC plate may be simultaneously applied many different samples, allowing the separation of different lipid classes from total lipid extracts, and also achieves separation even within the PL classes and particularly, TLC allows that remaining contributions of a previous run are completely excluded (61, 62).

In fact, TLC is the simplest method for lipids separation, which the stationary phase is a solid phase and the mobile phase is a liquid phase. The stationary phase is normally of silica gel, that due to the presence of hydroxyl groups, render the surface of silica gel highly polar and thus the mobile phase usually used in the separation of lipids is quite apolar (i.e. the used solvent system contains significant amounts of solvents such as hexane or chloroform). Thus, TLC is a solid-liquid adsorption technique in which the solvent molecules compete with the molecules of the sample for binding sites on the stationary phase. In other words, the lipid separation happens according to the different polarity of the head groups of the PL of interest. As the mobile phase travels along the surface of the stationary phase, via capillary action, it transports the analyte particles along the silica gel surface. Thus, the fraction of time necessary for the analyte bind at the silica gel surface relative to the time it spends in solution determines the retention factor (RF) of the analyte. The ability of an analyte to bind to the surface of the silica gel in the presence of a particular solvent or mixture of solvents can be viewed as a the sum of two competitive interactions. First, polar groups in the solvent can compete with the analyte for binding sites on the

surface of the silica gel, as mentioned above. Therefore, if a highly polar solvent is used, it will interact strongly with the surface of the silica gel and will leave few sites on the stationary phase free to bind with the analyte. The analyte will, therefore, move quickly past the stationary phase. Similarly, polar groups in the solvent can interact strongly with polar functionality of the analyte and prevent interaction of the analyte with the surface of the silica gel. This effect also leads to rapid movement of the analyte past the stationary phase. There are also several chemical modifications that can be made to the silica gel to improve separation of PLs classes, as coating the plate with boric acid (61).

Chromatographic techniques only provide rough information about lipid composition. Usualy this information is complemented with analysis using other methodology, namely mass spectromertry (MS).

Mass spectrometry

In the past, MS was already considered to play an important role in lipid research. In 1960 the pioneers in lipid MS studies, Ragnar Ryhage and Einar Stenhagen stated that "…its wide applicability and power are not as yet fully appreciated" (64). In the following decades MS of lipid, and especially MS coupled to gas-chromatography (GC/MS), played a important role within the field. However, as lipids are mostly non-volatile compounds, much effort was made in the early days to get the lipids to be analysed by MS in other ways. Thus, the advent of new ionization techniques, especially electrospray ionization (ESI), the situation has now profoundly changed so that it is now possible to directly, without any tedious derivatization steps, produce gas-phase molecular ions for most lipids and thus allowing their easy analysis by MS (65).

MS is a powerful analytical tool that can supply both qualitative and quantitative data. It is based on the detection of ions (charged molecules) after their separation according to both their total atomic mass (m) and electrical charge (z) by electric and magnetic fields. Thus, the data generated by the mass spectrometer is represented by the ration of mass of the ion and it charge (as *m/z*) versus their relative abundance (as a relative intensity) (58). Therefore, MS has the capability to provide information about the molecular weight, elemental composition and also structural composition, which

can be precious when analyzing unknown analytes. For known analytes, it is mainly used as a selective mass filter, which means that it can sort out the mass of the analyte from interfering substances and therefore provide extremely selective data.

The mass spectrometer consists of three major componds: the **ion source**, in which is produced in a beam of ions in gas phase resulting from ionization of analyte molecules from the sample, the **mass analyzer**, where the ions are selected and separated according to the ratio mass/charge (*m/z*) and the **detector**, in which the separated ions are collected and characterized by producing a signal whose intensity is related to the number of detected ions. These detectors are coupled to a computer that allows to integrate the information received and transformed it into a mass spectra, according to the relative abundance in function of the *m/z* of each ion (58). These different components are represented in Figure 12 and will be described in detail below.

For obtained the mass of small molecules the mass spectrometers have an important feature, these instruments need a high vacuum (10^{-5}-10^{-7} Torr) (58) that allows the unperturbed transmission and detection of the gas phase ions without simultaneous reactions.

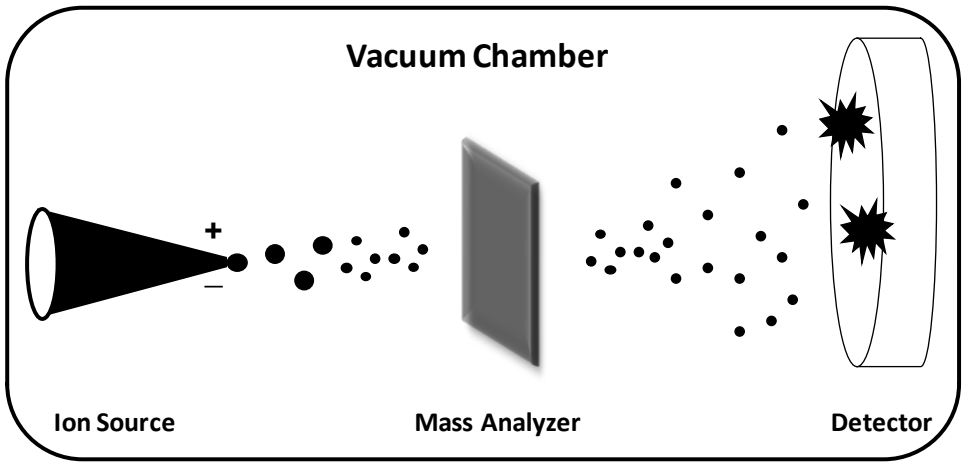

Figure 12. Scheme of the main components of a mass spectrometer.

1. Ion Source

Since the mass spectrometer utilizes electric and magnetic fields to move and manipulate the analytes, one requirement is that the analytes become ionized before entering the mass analyzer. The second condition is that the ions are in gas phase.

Both of these ocurred in the ion source. There are a number of different ion sources available and the choice depends heavily on the application. MS investigations of various classes of lipids have been performed utilizing a variety of ionization techniques, including chemical ionization (CI), fast atom bombardment (FAB), electrospray ionization (ESI), secondary ion mass spectrometry (SIMS), and matrix-assisted laser desorption/ionization (MALDI). Actually, the soft ionization techniques such as ESI and MALDI are the two ionization methods commonly used in lipidomic studies (66, 67). These ionization techniques allows the analysis of biomolecules of high molecular weight, nonvolatile and thermolabile, without excessive degradation and with a high probability of detection of the molecular ion, and the study of intact lipid molecular species from very small amounts of samples, with minimal sample preparation (without derivatization) (42). Thus, due the excellent sensitivity and ease of continuous sample introduction with ESI coupled with tandem mass spectrometry provide opportunities to explore the structure and fragmentation process of complex lipids in greater detail (42, 68). In addition, the ions generated by ESI have also minimized some of the problems, such as the complication of spectra with matrix ions associated with FAB-MS (69).

ESI, initially developed by Fenn et al. (1989), has been extensively used in many applications for the analysis of a broad range of compounds (70). The principles of the ESI process can be schematically represented as shown in Figure 13.

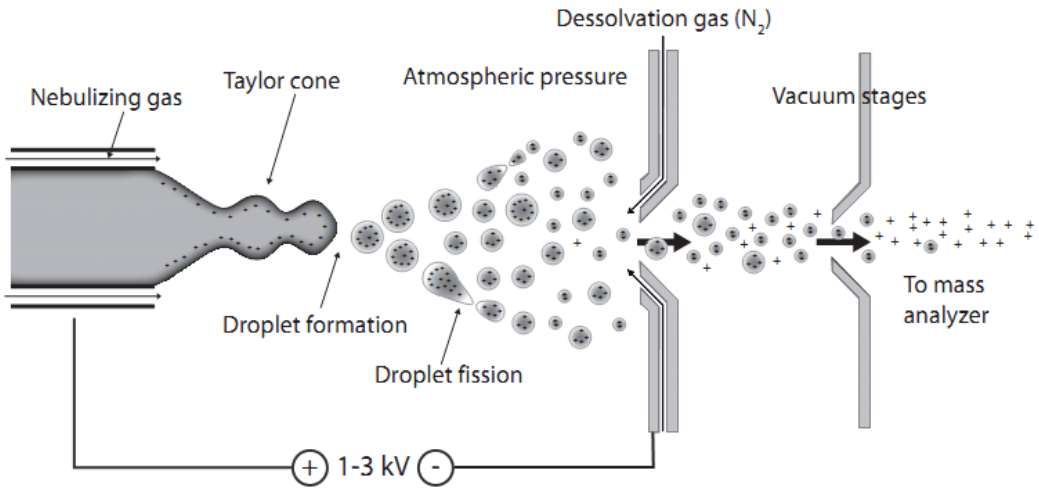

Figure 13. Schematic representation of a Electrospray ionization interface.

Initially, a solution containing the analytes of interest is introduced continuously into the ESI ion source through a metallic needle using a continuous flow, by using a syringe pump or as the eluent flow from liquid chromatography. The analyte solution flow passes through the electrospray needle that is subjected a strong electric field under atmospheric pressure. (57). Thus, the high voltage will charge the molecules of the solvent, in which the sample is mixed, as well as the sample molecules, producing ions primarily via protonation (if is applied a positive electric potential in the end of needle) such as $[M+H]^+$ or deprotonation (if is applied a negative electric potential in the end of needle) as $[M-H]^-$, either applied a or via formation of cations adduct (e.g. Na^+) or anions adduct (e.g. Cl^-), depending on the chemical properties of the molecules.

Once they are charged, with the same charge, the molecules will repel one another forcing the liquid to exit trough the tip, initially forming a cone of liquid, known as Taylor cone, after which the droplets form the final spray. These droplets then pass either through a curtain of heated inert gases (most often nitrogen) or through a heated capillary, or both, leading a subsequent evaporation of solvent from each droplet, decreasing its size as it drifts toward the end wall of the ionization chamber. Consequently, the charge density on its surface increases until it reaches the point that the surface tension can no longer sustain the charge (the Rayleigh limit) at which the Coulomb repulsion becomes of the same order as the surface tension. When the ions become close enough together their electric charges will make them repel each other, because of the Coloumb force. The resulting instability, sometimes called "Coulombic explosion" the droplets explode to form smaller droplets until each droplet corresponds to a single charged molecule and the solvent is completely evaporated (57, 70). Although many physicochemical features of the ionization and fragmentation process are still unclear, droplet surface tension and the spatial proximity of surface charges on sprayed droplets are critical determinants of the ionization process.

2. Mass analyzers

From the ion source the ions are transported through an intermediate vacuum region and further on into the high vaccum of the mass analyzer. In the mass analyzer, the ions are separated according to their mass to charge ratio (*m/z*). If the analytes are

all singly charged (z=1), which is almost always the case for lipids, this means that the separation will only depend on their mass.

There are several types of mass analyzers available but for lipids analysis by MS, and the three main types that are commonly used are: **quadrupole** (Q), **time of flight** (TOF) and **ion trap** analyzer. These analyzers can be used individually in mass spectrometers, or can be combined into complex instruments, the most commonly used Q-TOF, Q-Trap, and triple quadrupoles (QqQ). Since they all have their advantages and limitations, there are several features of the mass analyzer that have to be considered. The mass range might be important if the analyte of the interest have a high *m/z*. The resolution or resolving power is the ability of the mass analyzer to acquire distinct signals for two ions with a small mass difference. The speed of the instrument can be important for simultaneous elution of multiple analytes during an HPLC run. In addition, if the analyte has low abundance, which often is the case for bioactive lipids, the sensitivity of mass analyzer will be indispensable.

A **Quadrupole** consists of four circular parallel rods, that opposite rods are electrically connected and applied with a combination of direct-current and a radiofrequency potential. The ions will travel axially through the center of the four rods where they will be affected by electrical forces. The force will depend on the combination of the DC and RF potential. This means that for a certain *m/z* only a specific combination of these potentials will enable the ion to maintain a stable trajectory through the quadrupole and reach the detector. In quadrupole mass analyzer, a spectrum is generated by stepwise scanning through the *m/z* range of interest while recording the amount of ions reaching the detector. These mass analyzer are relatively inexpensive, small size, easy to use and maintain, and able to provide good accuracy in the measured mass values. However, the resolution is limited, have limited capacity in terms of range and resolving power, and have limited suitability for analysis of tandem mass spectrometry.

In a **time-of-flight (TOF)** mass analyzer the ions are accelerated by a potential often perpendicular to the ion path generated in the ion source. Since this will give the same kinetic energy to all ions (ideally), the difference in mass between different ions

will give them different velocities, i.e. with equal energy and will travel at speeds inversely proportional to the square roots of their masses. The ions are then allowed to drift in a field-free vacuum region towards the detector. The time-of-flight is the difference in time between the acceleration and the pulse generated from when the ions hit the detector. These instruments are simple, relatively inexpensive, with high sensitivity and accuracy, and the unlimited range masses analyzable.

A **linear ion trap** analyzer consists of a multi-pole where the ions are confined (trapped) radially by a two-dimensional (2D) radio frequency (RF) field, and axially by stopping potentials applied to end electrodes (71). For this analyzer there is a stability diagram, where the ions whose coordinates are within the diagram, and whose kinetic energy does not exceed the potential of the trap, are enclosed in the field until they are removed by collision. To make them leave, a radio frequency of small amplitude voltage is applied. This amplitude is then scanned in an ascending way and increasing mass ions are sequentially ejected from the trap and detected by a detector to produce a mass spectrum.

As the ions are trapped and accumulate over the time and can be combined with other mass analyzers and used to isolate ions of selected mass to charge ratios, to perform tandem mass spectrometry experiments, and to study ion molecule chemistry (71).

3. Detectors

After passing the mass analyzer, the ion beam is detected and transformed into a usable signal by the detector. Several types of detectors currently exist and they vary according to the design of the mass spectrometer and the application requirements. For all of them however, characteristics such as high sensitivity and linearity are highly desired. At present, the most commonly utilized detector is the electron multiplier (EM). This detector comes in a number of different variants but all work by the same principle. Ions exiting the mass analyzer reach a conversion dynode (depending on their charge) and strike the initial amplification dynode surface producing an emission of secondary electrons which are then attracted either to the second dynode, or into the continuous dynode where more secondary electrons are generated in a repeating

process ultimately resulting in a cascade of electrons. Typical amplification is of the order of one million to one. A multichannel plate (MCP) is an example of an EM detector that is frequently found in TOF instruments. The design of this detector allows very rapid readout and response, which is required when using a TOF mass analyzer.

In this study, lipid analysis was carried out by MS using ESI ionization and three distinct mass spectrometers: Q-ToF2 and Linear Ion Trap, Figure 14, and QqQ.

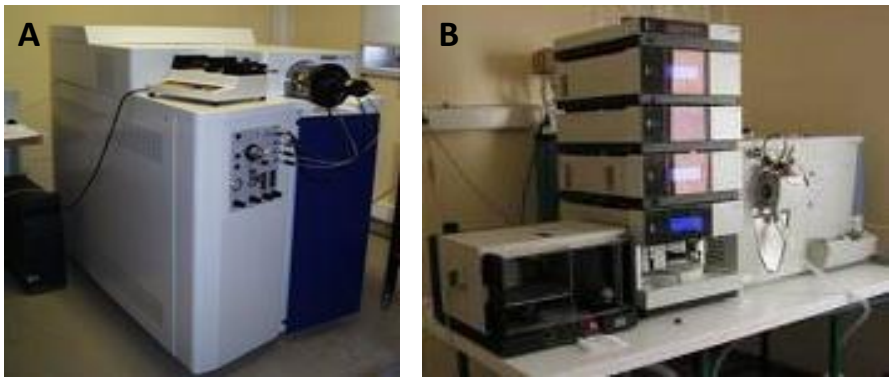

Figure 14. Mass spectrometers. (A) Micromass® Q-ToF 2 mass spectrometer; **(B)** LXQ Linear Ion Trap Mass Spectrometer.

Tandem mass spectrometry

Tandem mass spectrometry (MS/MS) employs two stages of mass analysis in order to examine selectively the fragmentation of a particular ions selected from a mixture of ions . The simplest form of MS/MS analysis combines two mass analysers, where the first one is used to select a single (precursor) mass that is characteristic of a given analyte in a mixture. The mass-selected ions pass through a region where they are activated in some way, usually by colision with a gas (in the collision cell), that causes them to fall apart to produce fragment (product) ions. This is usually done by colliding the ions with a neutral gas in a process called collisional activation (CA) or collision-induced dissociation (CID). The second mass spectrometer is used to separate the product ions according to *m/z* values. The resulting MS/MS spectrum consists only of product ions from the selected precursor ion. Using this technology we can draw several conclusions about the structure of the analyzed molecules and the spectra obtained gives us not only the most frequent molecular fragmentation but also as the most favorable, it is identified as MS/MS or MS^2, however, the number of steps can

increase in order to perform MS^n (n represents the number of generations of ions to be analyzed).

Usually several analyzers are coupled in series (tandem), separated by a collision cell, however, in some instruments, like the linear ion trap, only one analyzer is able to perform multiple mass spectrometry becoming efficient instruments in structural identification of molecules as phospholipids (68).

There are several kinds of MS/MS experiments that can be performed. The Figure 15 shows a schematic representation of three common types of MS/MS experiment. The most common and well-known MS/MS experiment is called **product ion scan**. In this way the precursor ion is focussed in MS1 and transferred into collision cell where it interacts with a collision gas and fragments. The product ions are then separated and measured according their *m/z* value by scanning MS2. Analyzing the product ions and knowing the mass of the precursor ion, structural information of lipid can be deduced (72). Using this type of MS/MS experiment we analysed, in the work of this thesis, the most classes of lipids allowing the identification and characterization of molecular lipids.

Another MS/MS experiment is a **precursor ion scan,** which is useful when it is known that a particular product ion is characteristic of a particular class of compounds. Therefore, in this case, all ionic species are separated in MS1 and will be sequentially transmitted to the cell collisions and the occurrence of a particular fragment ion with a single *m/z* value is measured by MS2. The computer analysis will show the precursors of the specific ion formed in the MS2.

In the cases where CID generates a neutral characteristic fragment, the two mass analyzers (MS1 and MS2) are scanned at a constant mass difference corresponding to the mass of the lost, neutral fragment. This is called **neutral loss scan**, that the MS2 separates the ions coming out of MS2 by the m/z value equal to the neutral loss mass (73).

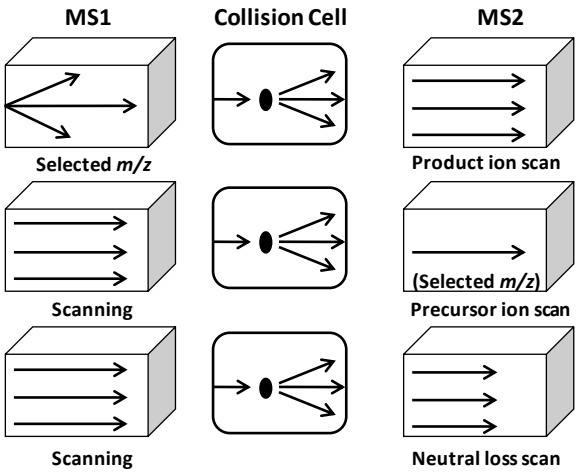

Figure 15. Schematic representation of the different MS/MS experiments.

4. Mass spectrometry in phospholipids and sphingolipids analysis

The most powerful contemporary analytical approach in lipidomics is Mass Spectrometry, due the combination of sensitivity, specificity, selectivity and speed this methodology. Thus, MS has been used to identify, quantify and characterize the each lipid component, in providing information about the molecular identity, composition and oxidative state, helping the elucidation of relations between structure-activity of different membrane lipids. In addition, tandem mass spectrometry (MS/MS) provides exhaustive information necessary for the structural characterization of new lipid, and the selectivity required to determine the lipid species present in complex mixtures (67). Although the MS/MS experiments, as product ion scan and neutral loss of polar head groups or fatty acids are widely used in the detection and identification of lipids, the knowledge of the fragmentation patterns is essential (72).

Nearly all PLs and SLs are readily ionizable, when subjected to ESI. However, the formation of the molecular species is governed by the polar head groups that distinguish the various classes. ESI analyses demonstrated that PC, PS, and PE class of PLs and SM which is a sphingolipid analogous to PC containing the same polar head attached to a ceramide, can be successfully analyzed as protonated ($[M+H]^+$) and alkali metal ($[M+Alk]^+$) adducts in the positive-ion mode, depending on the concentration of alkali metal or H^+ ion present in the sample (Alk = Li, Na, K) (58, 66).

The classes PI, PS and PE of PLs all yield prominent $[M-H]^-$ ions (74). Other PL species, such as cardiolipin, which bear multiple phosphoric acid charge sites, can form $[M-H]^-$,$[M+Na-2H]^-$ and $[M-2H]^{2-}$ ions in the negative-ion mode (66). The Ceramides, can be detected in negative mode, forming ions $[M-H]^-$ or as chloride adducts ($[M+Cl]^-$) in the negative-ion mode (75) or can also be detected in positive mode. The fragmentation patterns of these species give structural information of the lipids. In each case is shown the fragmentation of the polar head and the fatty acids, helping in the lipid identification process (68).

Phosphatidylcholines (PCs) are some of the most abundant species of neutral phospholipids in eukaryotic cells, and are characterized by the presence of a quaternary nitrogen atom situated in the choline headgroup, which positive charge is neutralized by the negative charge of the phosphate group. The quaternary nitrogen atom readily forms abundant $[MH]^+$ protonated ions by ESI because the phosphate anion can be protonated (66, 68). Furthermore, when various alkali metal ions such as Na^+ are present in the electrospray solvent, abundant sodiated species, $[M+Na]^+$, are observed in positive-ion electrospray.

Collision-induced decomposition (CID) of the positive protonated ion ($[MH]^+$) yields an abundant phosphocholine ion at *m/z* 184.1, which is typical of all phosphocholine-containing lipids, as SMs. Both PCs and SMs generates by fragmentation of their protonated ions ($[MH]^+$) an abundant ion with a *m/z* value of 184.1, characteristic of the choline polar head ($[H_2PO_4(CH_2)_2N(CH_3)_3]^+$). The fragmentation of the $[M+Na]^+$ show a typical loss of a neutral of 183 Da (due to loss of the polar head group) as well as a neutral loss of 59 Da, corresponding to the neutral loss of trimethylamine ($(CH_3)_3N$) (Figure 16). Therefore these lipid classes present in the middle of the sample were profiled together in positive mode using precursor ion scan of *m/z* 184.1. However, PCs and SMs can be easily discriminated, since protonated molecules of SMs exhibit odd *m/z* values due to the presence of an additional nitrogen atom.

Several studies revealed that the α-hydrogen of the fatty acyl at *sn-2* is more labile than that at *sn-1*, resulting in the more favorable formation of the

$[M+H-R`_2CH=CO]^+$ ion than the $[M+H-R_1CH=CO]^+$ ion, arising from losses of the fatty acyl substituents at *sn-2* and at *sn-1* as ketenes, respectively, while the formation of R_1COOH is more favorable than R_2COOH, arising from losses of the fatty acyl substituents at *sn*-1 and *sn*-2 as acids. Therefore, the position of the fatty acyl moieties on the glycerol backbone can be assigned (69).

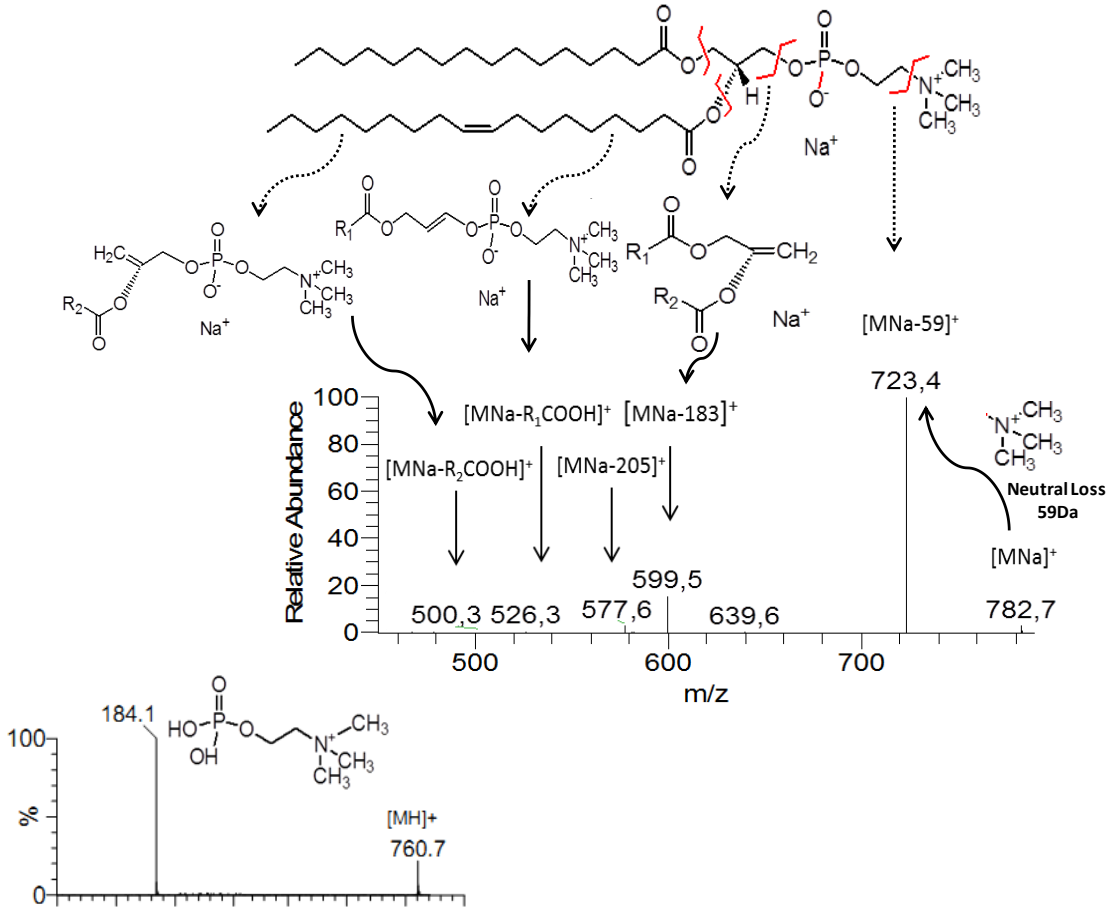

Figure 16. ESI–MS/MS spectrum of the $[MH]^+$ at *m/z* 760.6 (below) and of $[MNa]^+$ at *m/z* 782.6 (above), corresponding to PC(16:0/18:1). The scheme represents the MS/MS pattern of PC, showing the main points of fragmentation and their products, which correspond to product ions observed in the MS/MS spectrum of $[M+Na]^+$ ion. Fragmentation of $[MH]^+$ ions originated the characteristic ion of *m/z* 184.1 corresponding to the head group of PCs, and additional ions from $[M+Na]^+$ providing more structural information.

Phosphatydilethanolamine (PE) lipids constitute one of the major classes of lipids that are present in cell membranes. This type of lipid ionizes either in positive or negative mode. The product ion spectra (MS/MS) of the $[M+H]^+$ of PE are dominated by the ion $[M+H-141]^+$, arising from elimination of the phosphoethanolamine moiety ($HPO_4(CH_2)_2NH_3$) via the same bond cleavage as that of PC as described above (68, 69). Ionization of PE also produced cationized molecules, such as $[M+Na]^+$. The product ion spectrum of the $[M+Na]^+$ ion of PE(18:0/18:1)at *m/z* 768 (Figure 17) is dominated by the *m/z* 627 ($[M+Na-141]^+$) ion, and show also the ions at *m/z* 484 ($[M+Na-R_1COOH]^+$) and 486 ($[M+Na-R_2COOH]^+$), through which we can identify the faty acyl composition of these phospholipids. Apart from loss of 141 Da, the fragmentation pathway of these ions include also the loss of aziridine (-43 Da, CH_2CH_2NH)(76).

Collisional activation of PE $[M-H]^-$ ions yielded the characteristic carboxylate anions of *sn*-1 (R_1COO^-) and *sn*-2 (R_2COO^-) acyl residues. The relative abundance of R_2COO^- is usually higher than the R_1COO^- anion. The gas-phase $[M-H]^-$ ion of PE undergoes preferential losses of fatty acyl substituents as ketenes ($[M-H-RCH=C=O]^-$) over as acids ($[M-H-RCO_2H]^-$) (66). Other product ions corresponding to neutral loss of *sn*-1 and *sn*-2 fatty acyl residues (RCOOH and $RCH_2CH=C=O$) are also detected (77). The loss of fatty acyl as ketene/acid at *sn*-2 position is more favorable. The product ion produced by loss of 141 Da is absent.

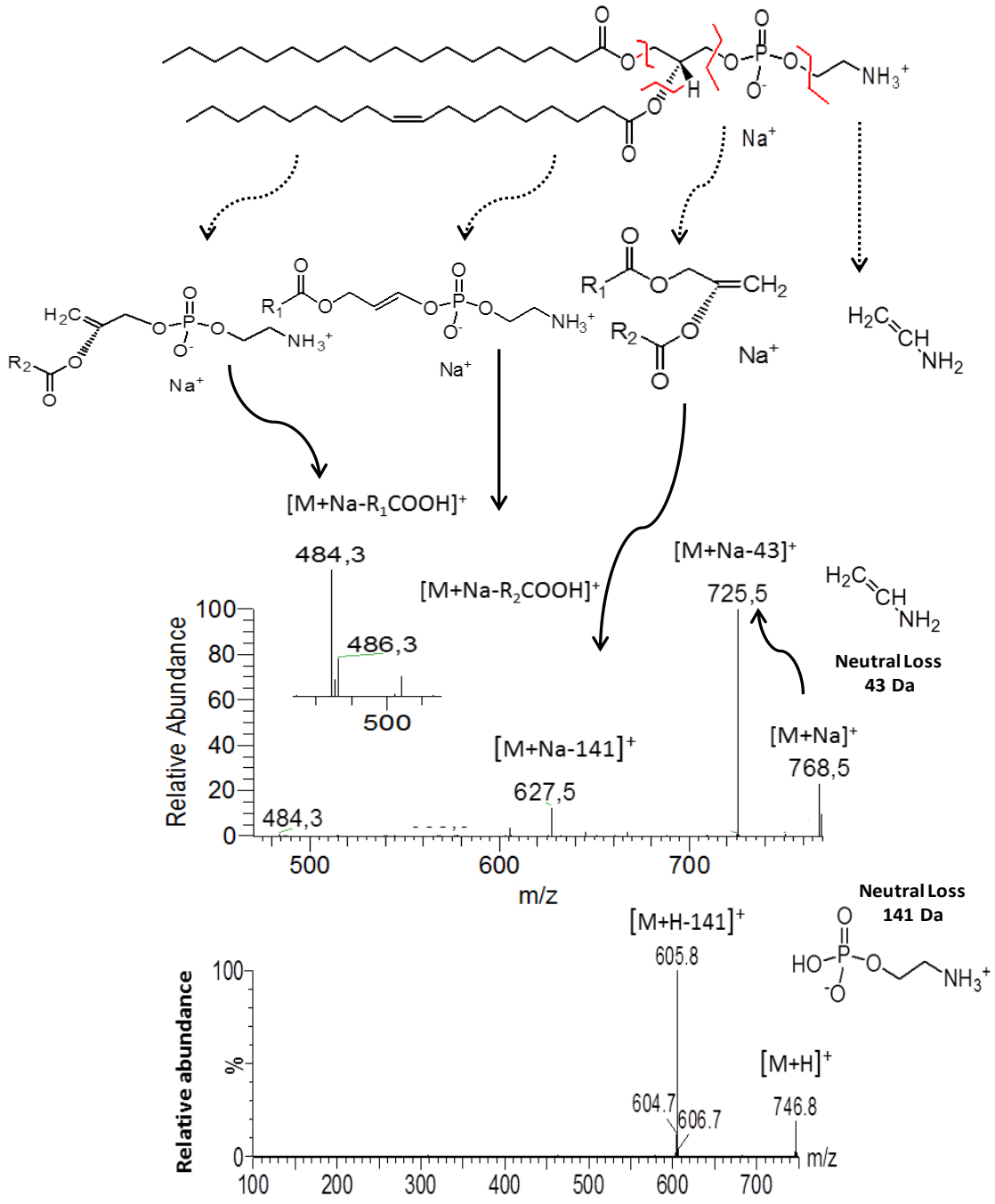

Figure 17. ESI–MS/MS spectrum of the $[MH]^+$ at *m/z* 746.8 (below) and of $[MNa]^+$ at *m/z* 768.5 (above), corresponding to PE(18:0/18:1). The scheme represents the MS/MS pattern of PE, showing the main points of fragmentation and their products, which correspond to product ions observed in the MS/MS spectrum of $[MNa]^+$ ion. Fragmentation of $[MH]^+$ ions originated the typical ion due to neutral loss of 141 Da that corresponds to the head group of PEs and additional ions from $[M+Na]^+$ providing more structural information.

Phosphatidylserine (PS) is an important phospholipid class that is predominantly found in the inner leaflet of the cell membranes (78). The presence of this phospholipid on the outer leaflet of a lipid bilayer initiates many biological events, including platelet aggregation, cell adhesion, and an indication of cellular apoptosis. The PS ionization results in the formation of positive and negative ions, however, PS ionize preferentially in the negative mode.

The MS/MS spectra of $[M-H]^-$ ions of PS typically shows major loss of serine group (neutral loss of 87 Da) that corresponds to product ion at *m/z* 673.3 observed in Figure 18. Apart from loss of 87 Da, the fragmentation pathway of these ions include also the formation of carboxylate anions (R_1COO^- and R_2COO^-) that allows discovering structural features of PS. The *sn*-1 carboxylate anion is typically more abundant than the *sn*-2. FA chains may also be lost as ketene ($[R_xCH_2CH=C=O]^-$) or as acid ($[M-H-R_xCO_2H]^-$), loss of FA at *sn*-2 position is more favorable (68, 69).

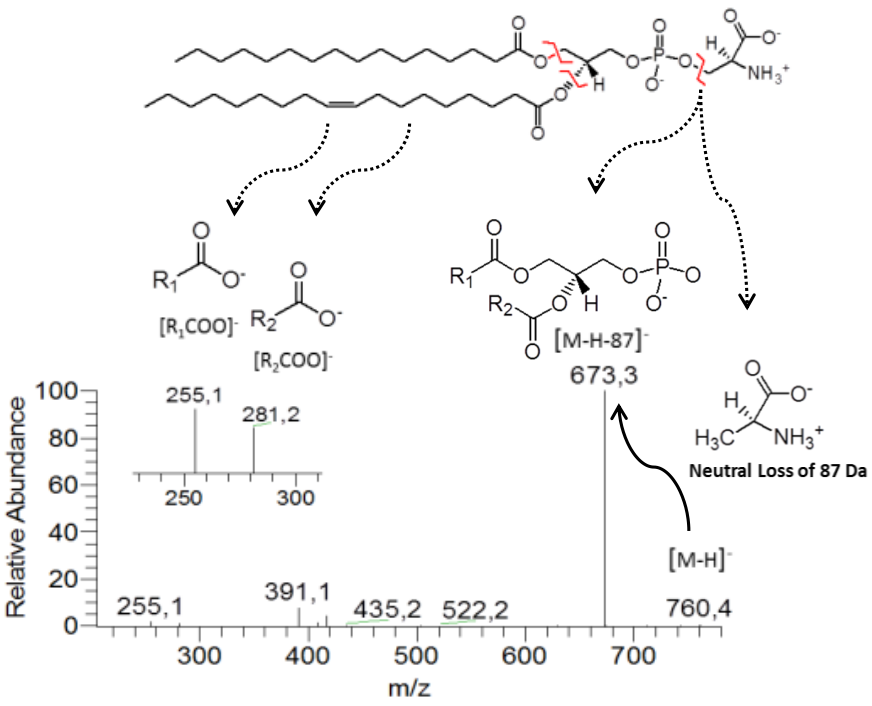

Figure 18. ESI–MS/MS spectrum of the $[M-H]^-$ at *m/z* 760.4 corresponding to PS(16:0/18:1). The scheme represents the MS/MS pattern of PS, showing the main points of fragmentation and their products, which correspond to product ions observed in the MS/MS spectrum. Fragmentation of $[M-H]^-$ ions gave the typical neutral loss of 87 Da, characteristic of its serine head group, and ions corresponding to the fatty acyls chains carboxylate anions ($[R_2COO]^-$ and $[R_1COO]^-$).

PLs that contain a phosphodiester of the six-carbon sugar inositol as a polar head group are found in all cells. In addition, there are several alternative forms that have one or two additional phosphate moieties, resulting in phosphatidylinositol-4-phosphate (PI-4-P) and phosphatidylinositol-4,5-bisphosphate (PI-4,5-2P). This PL class is quite important in signalling processes, since that the enzyme phospholipase C (PLC) hydrolyzes the polar head group to form inositol triphosphate (IP3), a signalling molecule that stimulates intercellular calcium release and as other product of the PLC reaction is the signalling molecule diacylglycerol known to induce an increase in protein kinase C (PKC) activity (79).

Phosphatidylinositol (PI) class also ionize preferentially in negative mode (68), with formation of $[M-H]^-$ ions and their the major fragmentation pathways under MS/MS analysis arise from neutral loss of free fatty acid substituents ($[M-H-R_xCO_2H]^-$) and neutral loss of the corresponding ketenes ($[M-H-R_xCH=C=O]^-$), followed by consecutive loss of the inositol head group, forming the ions $[M-H-R_xCO_2H-162$ (inositol) or $[M-H-R_xCH=C=O-162$ (inositol)] Figure 19 (80). The intensities of the ions arising from neutral loss of the *sn-2* substituent as a free fatty acid ($[M-H-R_2CO_2H]^-$) or as a ketene ($[M-H-R_2CH=C=O]^-$) are greater than those of ions reflecting corresponding losses of the *sn-1* substituent, reflecting those losses arise from charge-driven processes that occur preferentially at the *sn-2* position. These features permit assignment of the position of the fatty acid substituents on the glycerol backbone (69, 80).

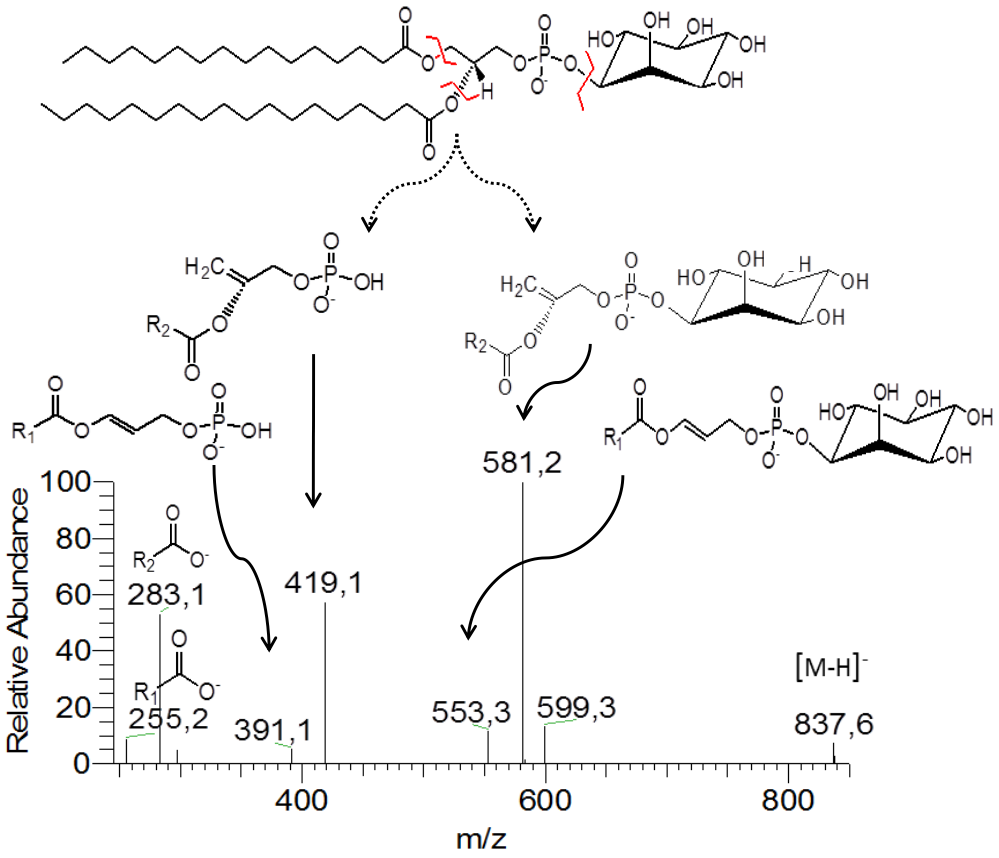

Figure 19. ESI–MS/MS spectrum of the $[M-H]^-$ at *m/z* 837.6 corresponding to PI(16:0/18:0). The scheme represents the MS/MS pattern of PI, showing the main points of fragmentation and their products, which correspond to product ions observed in the MS/MS spectrum. Fragmentation of $[M-H]^-$ ions gave the typical ions of neutral loss of fatty acyls with the inositol ($[M-H-R_xCOOH-162]^-$, loss of fatty acyls chains ($[M-H-R_xCOOH]^-$ and ions corresponding to the fatty acyls chains carboxylate anions ($[R_2COO]^- > [R_1COO]^-$).

Ceramides can ionize in both positive and negative mode, as $[M+H]^+$ and $[M+X]^+$ (X= Na, Li, K) species or $[M-H]^-$ and [M+X]- (X= Cl^-, $CH_3CO_2^-$, $CF_3CO_2^-$) species, respectively. Ceramide fragmentation results in the formation of two interesting ions corresponding to loss of 30 and 32 Da, which corresponds to loss of CH_2O and CH_3OH, respectively. The loss of fatty acyl moiety may be in the form of ketene as $RCH_2CH=C=O$, amide as $RCONH_2$ or carboxylate anion (RCO_2^-). Several others ion corresponding to loss or cleavage of sphingosine backbone may be also present in both positive and negative modes, such as the typical product ions resulting from neutral loss of 256 Da and product ions resulting from neutral loss of 240 Da (Figure 20) (81, 82).

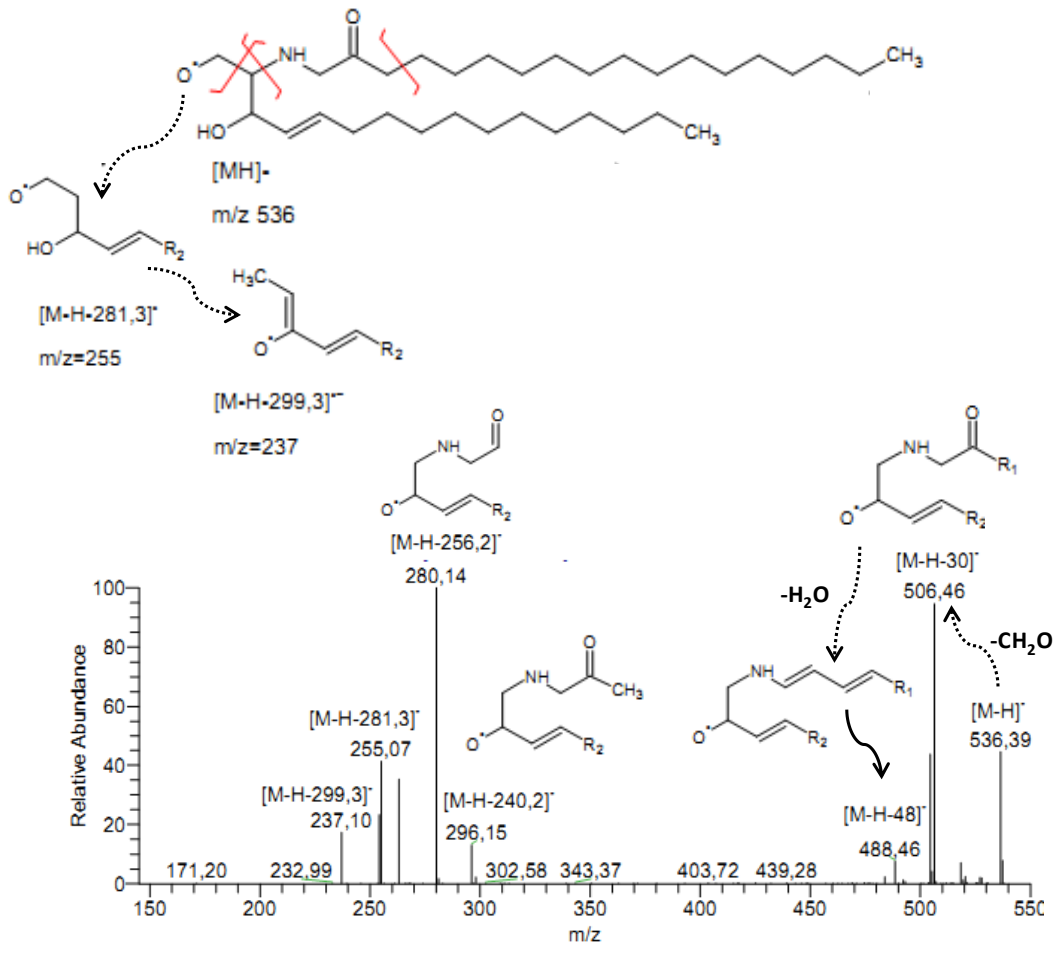

Figure 20. ESI–MS/MS spectrum of the $[M-H]^-$ at *m/z* 536 corresponding to Cer(d18:1/16:0). The scheme represents the MS/MS pattern of Ceramides, showing the main points of fragmentation and their products, which correspond to product ions observed in the MS/MS spectrum. Fragmentation of $[M-H]^-$ ions gave the typical ions of neutral loss of 30 and 48 Da and neutral loss of 256 Da and 240 Da.

5. Aims

The development of non-animal test methods for assessment of skin sensitization potential is an urgent challenge within the framework of existing and forthcoming legislation. Efforts have been made to replace the current animal tests, however it is widely recognized that this cannot be accomplished with a single approach, but rather with the integration of results achieved from different *in vitro* and *in silico* assays. Currently there are already some biomarkers known to be selectively modulated by skin sensitizers, such as CD40, CD86, IL-1, CXCR4 chemokine receptor and p38MAPK activation (83-85). However, the role of lipids, as phospholipids and sphingolipids, in allergic immune response, as well as its role in the process of dendritic cells maturation and keratinocytes activation triggered by LPS and skin sensitizers, has been overlooked.

Therefore, the overall aim of this work was to identify, through a lipidomics approach, alterations in the lipid profile of phospholipids and sphingolipids triggered by LPS and a skin sensitizer, contributing for the identification of potential lipid biomarkers for further use in an integrative test strategy towards the reduction of animals use for skin sensitization prediction.

The specific aims of this work were:

I. To study changes in the pattern of major phospholipids and sphingolipids triggered during dendritic cells maturation

II. To explore changes in major phospholipids and sphingolipids induced by the skin sensitizer 2,4-dinitrofluorobenzene in dendritic cells

III. To investigate the phospholipid and sphingolipid profiles modulated by LPS and skin sensitizer in keratinocytes.

CHAPTER II

Material and Methods

II. Material and Methods

1. Material

Lipopolysaccharide (LPS) from *Escherichia coli* (serotype 026:B6), 2,4-dinitrofluorobenzene (DNFB), contact irritant sodium benzalkonium chloride (BC), trypsin, chloroform, methanol, primuline, Iscove's Modified Dulbecco's Medium (IMDM) and Dulbecco's Modified Eagle Medium (DMEM) were obtained from Sigma Chemical Co. (St. Louis, MO, USA). Chloroform and methanol were high purity solvents (HPLC grade). Fetal calf serum was purchased from Invitrogen (Paisley, UK). TLC silica gel 60 plates with concentrating zone (2.5x20cm) and triethylamine were obtained from Merck (Darmstadt, Germany) and boric acid was from DHB chemicals. Absolute ethanol was from Panreac. The phospholipid standards for TLC were purchased from the Avanti Lipids (USA).

2. Methods

2.1 Cell Culture

In this work were used two types of cell lines, which both mimic kinds of skin cells and and play an important role in the development of ACD: the mouse fetal skin-derived dendritic cell line (FSDC) and the human keratinocyte cell line HaCat.

The FSDC is a skin dendritic cell precursor with antigen-presenting capacity (10). Previously, this cell line was characterized by a surface phenotype consistent with a Langerhans cell progenitor (H-2d.b$^+$, IAd. b$^+$, CD54$^+$, MHCII$^+$, MHCI$^+$, CD11c$^+$, CD11b$^+$, B7.2$^+$, CD44$^+$, B220$^-$, CD3$^-$); this phenotype was confirmed in our lab for the most important of these surface markers (data not shown). Cells were cultured in IMDM endotoxin-free, supplemented with 1% (w/v) glutamine, 10% (v/v) fetal bovine serum, 3,02 g/l sodium bicarbonate, 100 µg/ml streptomycin and 100 U/ml penicillin, in a humidified incubator with 5% CO_2/95% air, at 37 ◦C. The FSDC have a doubling time of about 48 h, and these cells did not require exogenous growth factors for their continued proliferation when cultured in serum-containing medium. The cells were used after reaching 70–80% confluence. After 45 passages the cells were discarded.

HaCat cells are spontaneously transformed immortalized human epithelial cells from adult skin that maintain full epidermal differentiation capacity (11). HaCaT cells were grown for 48 h in DMEM-high glucose, 4,5 g/l) supplemented with 2 mM L-glutamine and 10% heat-inactivated fetal calf serum, 100 U/ml penicillin (Gibco) and 100 µg/ml streptomycin (Gibco) at 95% relative humidity, 5% CO_2, and 37°C. The cells were used after reaching 70–80% confluence. After 45 passages the cells were discarded.

2.2 Lipid Extraction

FSDC (15×10^6) were cultured in 150cm^2 flasks and upon reaching 70–80% confluence they were stimulated with 1 µg/ml LPS, 1 µg/ml allergen DNFB and 0,72 µg/ml irritant BC, or left untreated (control) during 24 h, at 37ºC. The HaCat cells were also cultured in 150cm^2 flasks and stimulated, during 24 h, at 37ºC, with 1 µg/ml LPS, 1,86 µg/ml DNFB and 1,44 µg/ml BC or untreated (control). Since it has been shown that cytotoxicity may play a relevant role in DC activation (86), we considered as optimal chemicals test concentrations those that induced up to 10-15% cytotoxicity. After this time of stimulation (24 h), the treated and untreated cells were washed with ice-cold PBS twice, scraped in 5 ml of ice-cold PBS and cell pellet was separated by centrifugation at 200 xg for 4 min. The final pellet was ressuspended in mili-QH_2O (Millipore) making 1 ml of cell homogenate. Three or more different cultures for each cell type were analyzed in order to verify the reproducibility of the results.

Total lipids were extracted through the Bligh and Dyer method (60). We used HPLC solvents (chloroform and methanol) and milli-Q purified water. For each 1ml of cell homogenate ready of each sample, it was added chloroform/methanol 1:2 (v/v), vortexed well, and incubated on ice for 30 min. Then, an additional volume of 1,25 ml chloroform was added and finally 1,25 ml mili-QH_2O. In all steps the mixtures were strongly vortexed, thereafter, the samples were centrifuged at 1000 rpm for 5 min at room temperature to obtain a two-phase system: an aqueous top phase and an organic bottom phase with chloroform from which lipids were obtained. Therefore, the total lipid extracts recovered from organic phase (bottom phase) were separated

into a new tube and dried in a nitrogen flow. In next, the total lipid extracts were resuspended in 300 µl of chloroform and stored at -4ºC, making our extracts ready for the following analysis.

2.3 Lipid Separation

The PLs and SPLs classes from total lipid extract were separated by Thin Layer Chromatography (TLC) (87). The samples (total lipid extract) were applied in TLC plates, silica gel plates with concentrating zone 2.5x20cm (Merck, Darmstadt, Germany). Prior to separation, plates washed in a methanol: chloroform mixture (1:1, v/v) and left in the safety hood for 15 min, then plates were sprayed with 2.3% (m/v) boric acid (DHB chemicals) and dried in an oven at 100ºC during 15 min. It was applied in the TLC plates 20 µl of lipid solution in chloroform (with a concentration of 150 µg of phosphorous (P) per 100 µl). The plates were dried in a nitrogen flow and developed in solvent mixture chloroform/ethanol/water/triethylamine (30:35:7:35, v/v/v/v). When the elution was completed, the plates were left in the safety hood until the eluent was completely dried. Lipids spots on the silica plate were observed by spraying the plate with primuline solution of 50µg/100ml dissolved in a mixture of acetone (Sigma-Aldrich) and mili-QH2O (acetone:water; 80:20(v/v)), and visualized with a UV lamp (λ=254nm).

Identification of the different classes of PLs and SLs was carried out with the use of patterns (SM, PC, PI, PS, PE, CL and Cer) from Avanti Polar Lipids, which run side by side in the TLC plate. Then, 5 spots from each class were scraped off the plates to glass tubes: one scraped spot was used by quantification of phosphorus with a phosphorus assay to calculate the percentage of each PL class in the total amount of PL in the sample (Step 2.5), and the remaining four scraped spots from each class were used for silica extraction and for subsequent identification by MS (Step 2.4).

2.4 Silica Extraction

The extraction of lipid classes from silica to further MS analysis was carried out with a mixture of chloroform/methanol. First, the samples were solubilized in 450 µl of chloroform, vortexed well and left to stand for 5min, in order to be able to extract the lipids separated from the silica. Second, the samples were filtered by vacuum and 450 µl of chloroform/methanol (2:1, v/v) were added to the glass tubes, vortexed well and also filtered. Finally, the total extracted was passed in a syringe (GASTIGHT 1ml, Sigma-Aldrich) with a filter (Syring Driver Filter Unit 0,22 µm, Millipore-Millex), in order to obtain a complete free-silica extract. The filtered samples were dried under nitrogen stream and were resuspended in 100 µl of chloroform to store at -4°C for further analysis.

For MS analysis in both positive and negative modes, samples were diluted in methanol.

2.5 Determination of phospholipid content

To quantify the total PL extract in order to determine the concentration of sample for application on TLC plate and in order to evaluate the phospholipid content of each class after separation by TLC, phosphorus assay was performed according to Bartlett and Lewis (88).

For quantification of total PL extract, 15 µl of sample was used, and dried with a nitrogen flow, and to quantify the different classes separated by TLC, the each spot was scraped off from the plates directly to the quantification tubes. Next, for both procedures, 6,5 ml of perchloric acid (70%) (Panreac) was added to phosphate standards and samples (total lipid extracts or TLC spots). Then only the samples were incubated in a heating block (Stuart) for 45 min at 180°C, followed by cooling to room temperature. After cooling, 3,3 ml of mili-QH2O, 0,5 ml of 2,5% ammonium molybdate (Riedel – de Haën) and 0,5 ml of 10% ascorbic acid (VWR BDH Prolabo) were added to all samples and standards, vortexing always after addition each solution added, followed by incubation for 5 min at 100°C in a water bath. Finally the absorbance of

standards and samples solutions, after cooling, was measured at 800nm (Multiskan 90, Thermoscientific). The standards were initially prepared from a phosphate standard solution of dihydrogenphosphate dihydrated ($NaH_2PO_4.2H_2O$) (Riedel – de Haën) with 100 µg/ml of P, using from 0,1 to 2 µg of phosphorous (P).

In the case of TLC separated lipid classes, prior to spectrophotometric determination, samples were centrifuged 5 min at 4000 rpm to separate lipids from silica. The phospholipid content of each TLC separated lipid class was assessed by relating the PL content in each spot to the total PL content in the sample, i.e. the PL content of all TLC separated spots were summed up and considered as 100% of phospholipid content, as a result the data are presented in terms of relative amount of each PL class.

2.6 Determination of ceramide content

Ceramides were extracted from cultured and treated cells the same way that for the extraction of total lipids (Step 2.1 and Step 2.2). However, for ceramide quantification from cell homogenate of each sample the sphingolipids were extracted according to the method described in Bielawski, J. et al. (89). The efficient amount of cell homogenate for MS analysis is established through the protein concentration measurement. After determination of protein content (step 2.7), cell homogenate correspondent to 100 µg of protein was fortified with 10 µl (0,05 µg) of C12 Cer (used as an internal standard), added 2ml of extraction mixture (2-propanol: H2O:EthylAcetate 30:10:60 (v/v/v)), vortexed, sonicated 3x periodically for 30 s, and centrifuged for 10 min at 4000rpm. The supernatant was transferred to new vial, and sample was re-extracted the same way after addition of extraction mixture.

The supernatants of extraction and re-extraction were combined and these organic extracts were evaporated to dryness under N_2 gas. Subsequently, these extracts of sphingolipids (Ceramides) were analyzed by Ultra Performance Liquid Chromatography (UPLC) and Tandem mass spectrometry (MS/MS) (UPLC-MS/MS). The separations were obtained with an ACQUITY UPLC BEH C18 column. All analyses were performed using a Waters ACQUITY UPLC™ System with a Quattro Premier™ XE Triple

Quadrupole equipped with an Electrospray Ionization (ESI) probe (Walters, Manchester, UK). 10 µl of the reconstituted ceramides extracts were injected onto a reverse phase C18 column and eluted using a linear gradient of 30% methanol to 100% methanol solution. The quantification of individual species (C14, C16, C18, C18:1, C20, C20:1, C24, C24:1) was achieved by multiple reaction monitoring (MRM).

2.7 Determination of protein content

The protein content was estimated based on bicinchoninic acid protocol according to manufacturer instruction (BCA™ Protein Assay Kit, Pierce, Rockford, IL, USA). Briefly, 1 ml of working solution (mixture of 50 parts of BCA™ Reagent A (solution of sodium carbonate, sodium bicarbonate, bicinchonic acid and sodium tartrate in 0.1 m sodium hydroxide) and one part of BCA™ Reagent B (4% cupric sulphate) was added into each 50 µl sample, vortexed and incubated for 30 min at 60°C. Next, the absorbance of each sample was measured at the wavelength λ=562 nm and protein content was calculated with the reference to standards of bovine serum albumin that were provided in the kit.

2.8 Conditions of Electrospray Mass Spectrometry

Lipid analysis was carried out by mass spectrometry using ESI ionization and three distinct mass spectrometers: Q-TOF2 (Micromass, Manchester, UK), linear ion trap (ThermoFinnigan, San Jose, CA, USA), and a triple quadrupole instruments (QqQ, Waters, Manchester, UK).

In the electrospray Q-TOF2 instrument, operating in positive ionization mode, the samples were introduced into the electrospray source at a flow rate of 10 $\mu L.min^{-1}$. The cone voltage was set at 30 V and capillary voltage at 3 kV. The temperature of the source was at 80ºC and the desolvation temperature was 150ºC. In the Q-TOF2 instrument, operating in negative mode, capillary voltage that was set at -2,6kV, cone voltage was set at 30 V, source temperature was at 80ºC and desolvation temperature at 150ºC. The resolution was set to about 9,000 (FWHM). Tandem mass spectra

(MS/MS) were acquired by collision-induced decomposition (CID), using argon as the collision gas (measured pressure in the penning gauge ~ $6x10^{-5}$ mBar). The collision energy used was between 25 to 30 eV. Data acquisition was carried out with a Mass Lynx data system (V4.0).

In electrospray linear ion trap instrument the samples were introduced using a flow rate of 8μL.min^{-1}. Electrospray ionization conditions are as follow: voltage was 4.7 kV in negative mode and 5 kV in positive mode; capillary temperature was 275ºC and the sheath gas flow was 25 U. An isolation width of 0.5 Da was used with a 30 ms activation time for MS/MS experiments. Full scan MS spectra and MS/MS spectra were acquired with a 50 ms and 200 ms maximum ionization time, respectively. Normalized collision energy TM (CE) was varied between 17 and 20 (arbitrary units) for MS/MS. Data acquisition of this mass spectrometer was carried out with an Xcalibur data system (V2.0).

In the electrospray triple quadruple instrument, the electrospray voltage was set at 3.5 kV in positive mode. The capillary temperature was 300ºC and the sheath gas flow was 32 U. An isolation width of 0.5 Da was used with a 30 ms activation time for MS/MS experiments. Full scan MS spectra and neutral loss and parent scan spectra were acquired with a 50 ms and 200 ms maximum ionization time, respectively. Normalized collision energy TM (CE) was varied between 20 and 30 for MS/MS. Data acquisition was also carried out with a MassLynx data system (V4.0).

2.9 Statistics

The results are presented as means ± SD values from at least three independent experiments, and statistical analyses were performed by t-test (LPS relatively to control) and One-way ANOVA test with a Bonferroni post-test to compare all conditions. The statistical significance of differences was set at $P<0.05$.

CHAPTER III

Results and Discussion

I. Changes in lipidomic profile triggered during dendritic cells maturation

Profiling changes triggered during dendritic cells maturation: a lipidomic approach

Deolinda R. Santinha[1], Diane R. Marques[2], Elisabete A. Maciel[2], Cláudia S. O. Simões[2], Susana Rosa[1], Bruno M. Neves[1], Bárbara Macedo [3], Pedro Domingues[2], M Teresa Cruz [1] and M Rosário M. Domingues[2]*.

1-Faculty of Pharmacy and Center for Neuroscience and Cell Biology (CNC), University of Coimbra, 3000-548 Coimbra, Portugal
2- Mass Spectrometry Centre, Chemistry Department, University of Aveiro, 3810-193 Aveiro, Portugal
3- Metabolomics Core Service, IBMC - Institute for Molecular and Cell Biology, Porto, Portugal

Paper submitted for publication in Journal of Lipid Research **(Annexed)**

Abstract

Lipids play an important role in several biological processes by acting as signaling and regulating molecules, or locally as membrane components that modulate protein function. This work describes thoroughly the lipid composition of dendritic cells (DCs), a cell type that plays critical roles in the inflammatory and immune responses. After activation by antigens, DCs undergo drastic phenotypical and functional transformations, in a process known as maturation. In order to better characterize this process, changes on lipid profile were evaluated through a lipidomic approach. As an experimental model of DCs, we used a fetal skin-derived dendritic cell line (FSDC) induced to mature by treatment with lipopolysaccharide (LPS). The results showed that LPS increased the ceramides (Cer) and phosphatidylcholine (PC) levels and decreased the sphingomyelin (SM) and phosphatidylinositol (PI) content. Mass spectrometry analysis from total lipid extract and from each class of lipids revealed that maturation promoted clear changes in ceramides profile, with an enhance of Cer at *m/z* value 536.6 identified as Cer(d18:1/16:0), at *m/z* 646.7 Cer(d18:1/24:1) and at *m/z* 648.7 Cer(d18:1/24:0). The pattern of change of these lipids give an extremely rich source of data for evaluating modulation of specific lipid species triggered during DC maturation.

II. Changes in lipidomic profile induced by skin sensitizer in dendritic cells

Recent advances have been made in our understanding concerning the role played by DCs in the induction of contact allergy. A number of associated changes in DCs phenotype and function required for effective skin sensitization are providing the foundations for the development of cellular assays (using DC and DC-like cells) for skin sensitization hazard identification. Using these DC cell models, several studies analyzed potential markers for the sensitization capacity, as the activation of endocytosis, the increase in phosphotyrosine levels, the upregulation of cell surface markers and the increase in cytokine and chemokine production (90-92). Thus, recent studies demonstrated that the sensitizers DNFB and $NiSO_4$ increased the expression of the membrane-associated proteins CD40 and IL-12 receptor, whereas the non-skin sensitizer DCNB was without effect on the expression of these proteins (83, 84). More recently, it was also found that the chemokine receptor CXCR4 is selectively modulated by skin sensitizers (and not by irritants) in FSDC (85). This work suggests that lipid profile evaluation could disclose potential lipid biomarkers able to be included in a future *in vitro* DC based assay. The argument subjacent to the development of *in vitro* dendritic cell (DC)-based assays is that sensitizer- induced changes in the DC phenotype can be differentiated from those induced by irritants. In this context, the work presented here was performed in a mouse skin-derived dendritic cell line, FSDC, that is a model of iDCs, with morphological, phenotypical and functional characteristics of LCs (10), and attempts to evaluate the effect of a skin sensitizer and irritant in the lipid profile of FSDC, by lipidomic analysis. The chemicals tested were the strong contact allergen DNFB that has been widely used in several models of ACD (93, 94), and the contact irritant BC.

Separation of lipid classes by TLC

Using the lipidomic approaches, total lipid extracts prepared from DC treated with DNFB and BC and untreated control cells were separated into major lipid classes (PLs

and SLs) by TLC. In TLC plate is possible to see several bands, representing the different lipid classes that constitute the lipidome of these cells. Each class of lipid was identified by comparison with lipid standards applied in the TLC plate. Separation by TLC allowed to detect important alterations in PL content between allergen DNFB and irritant BC, and both relatively to untreated cells Figure 21A. According with previous results (95), the TLC data revealed that PC and PE represented the two most abundant PL classes (Figure 21A), in all conditions (DNFB and BC) and control cells. However, other PL classes were detected on TLC plates, namely SM, PI, PS, and CL, although in lower amount. To evaluate whether DNFB or/and BC promotes effectively changes in lipid content, lipid content of each phospholipid class was quantified by the phosphorus assay. Furthermore, to complete these results and support the correct identification of each lipid class, the different lipid spots were analysed by ESI-MS and MS/MS, as it will be explained below. Once the ESI-MS and ESI-MS/MS methods allow to assess and characterize the molecular diversity of the different species within each class of PLs and SPLs.

Phosphorus assay of major phospholipid classes

In analysis of PL content by phosphorus assay, the PL content of all spots were summed up and considered as 100% of phospholipid content. The relative content of PLs classes was calculated by normalizing the PL content of corresponding spots to the total PL content of all spots. The results obtained are represented in Figure 21B.

Through the phosphorus assay it was possible to confirm that PC is most abundant PL classes in DCs, followed by PE. In addition, it was possible to observe that these fractions did not change after allergen and irritant stimuli (Figure 21B).

Although the statistical analysis did not allow assigning significance, there are significant changes in PL content either between the allergen (DNFB) and irritant (BC), and between them and control (CTL). Interestingly, we can see that in the majority of the PL classes the irritant promotes an opposite effect to the allergen or less significant changes in PL levels. In cells treated with two stimuli (DNFB and BC) it is possible to observe a significant decrease in SM and PI percentage, however this effect is

more evident with skin sensitizer, DNFB stimulus. In two most abundant PL classes there are also important alterations, the PC and PE content is slightly increased after DNFB treatment, in contrast with BC treatment that promotes a decrease in PC and PE contents. In others PL classes, PS and CL, there are no significant changes, although the CL amount has been slight reduced in cells treated with the skin sensitizer (DNFB) and slight augmented in cells treated with irritant (BC).

Although these results are not statistically significant, they are the first hint that it is possible to find lipid biomarkers able to discriminate a sensitizer from a non-sensitizer in an *in vitro* DC based assay.

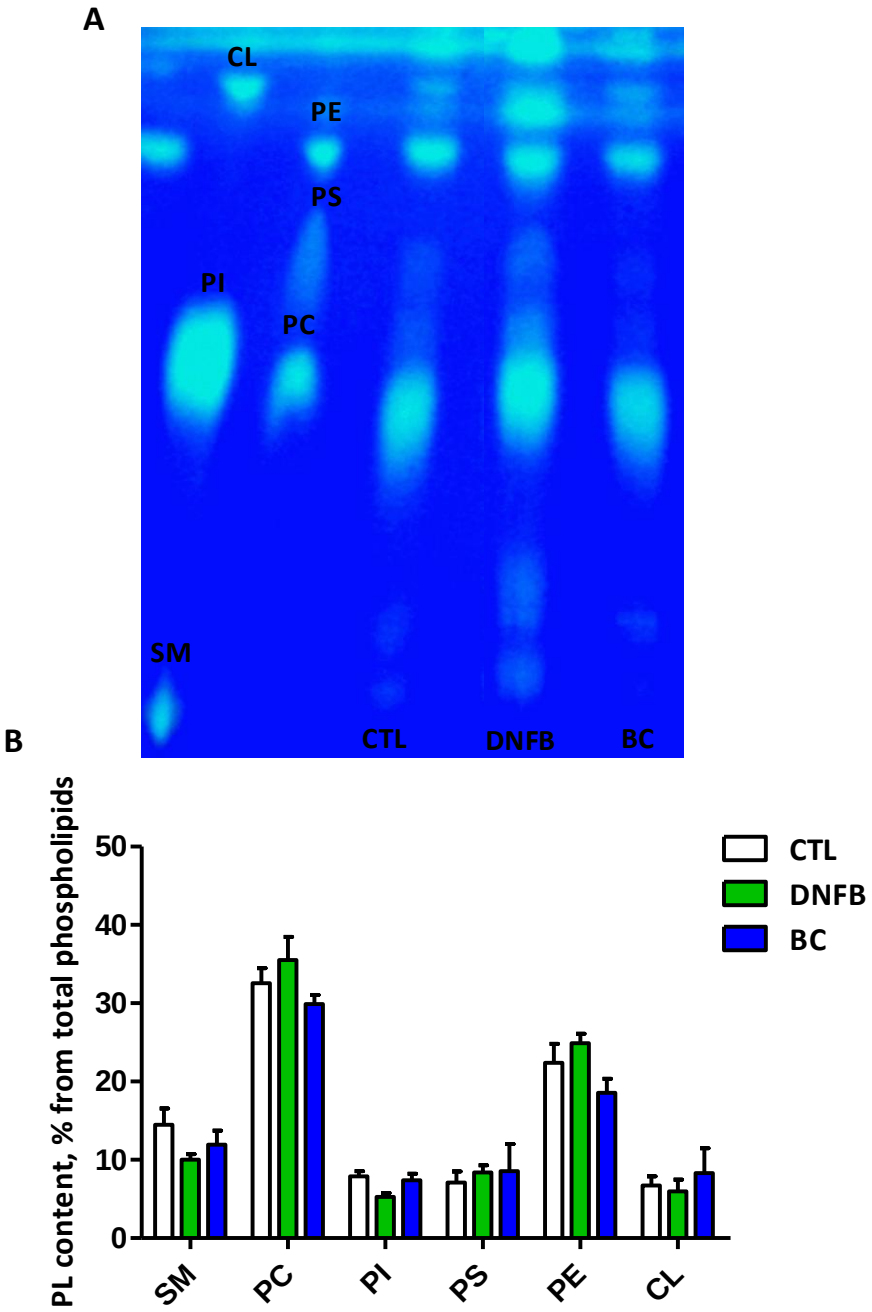

Figure 21. Effect of skin sensitizer and irritant on the phospholipid content in dendritic cells. **(A)** Typical TLC of total lipids extracted from DCs before and after treatment of cells by DNFB (skin sensitizer) and BC (irritant); **(B)** PL content, % from total lipids refers to the relative percentage of phospholipid phosphorus recovered from the respective spot in TLC.

Analysis of lipid classes by mass spectrometry

To further understand the changes in composition in molecular species within each lipid class identified by TLC, lipids were extracted from their TLC spots and subsequently analysed by ESI-MS and MS/MS experiments, as we describe below. ESI-MS and ESI-MS/MS analysis from different lipid class was performed in positive mode for PC and SM while in negative mode for PI, PS, PE and Cer. Samples were obtained from TLC spots of FSDC treated with DNFB and BC and from non treated FSDC.

As described in the previous study on the DCs maturation, PC and SM were analyzed by ESI-MS in positive mode, forming both $[MH]^+$ and $[MNa]^+$ ions. In order to identify exclusively the $[MH]^+$ ions, precursor ion scan of the ion at *m/z* 184.1 were obtained in the triple quadrupole, as typical approach for choline lipids and described previously in dendritic cell maturation study. This approach permitted to obtain the spectra shown in Figure 21, which revealed the $[MH]^+$ ions of all PC and SM molecular species present in respective TLC spot obtained after TLC separation.

Although the quantification of phospholipids showed that there are significant alterations in PC and SM levels in cells after different stimuli (Figure 21 B), which prove that the membrane composition is altered by these stimuli. However, through MS analysis it seems that the SM and PC profile of DCs in different studied conditions remain similar, with the same molecular species. In Figure 22, it is shown the typical ESI-MS spectrum obtained for SM and PC class in different conditions. Spectra obtained from DCs treated with DNFB and BC and non treated cells were very similar, for that reason it is shown only one MS spectra of each class in order to illustrate the typical pattern of DC in what concern it PC and SM composition. The identification of each molecular species and the composition in fatty acids were identified by analysis of the MS/MS spectra obtained for each ion observed in the MS spectra, according to that described in chapter I and the information is resumed in Table 2 and 3.

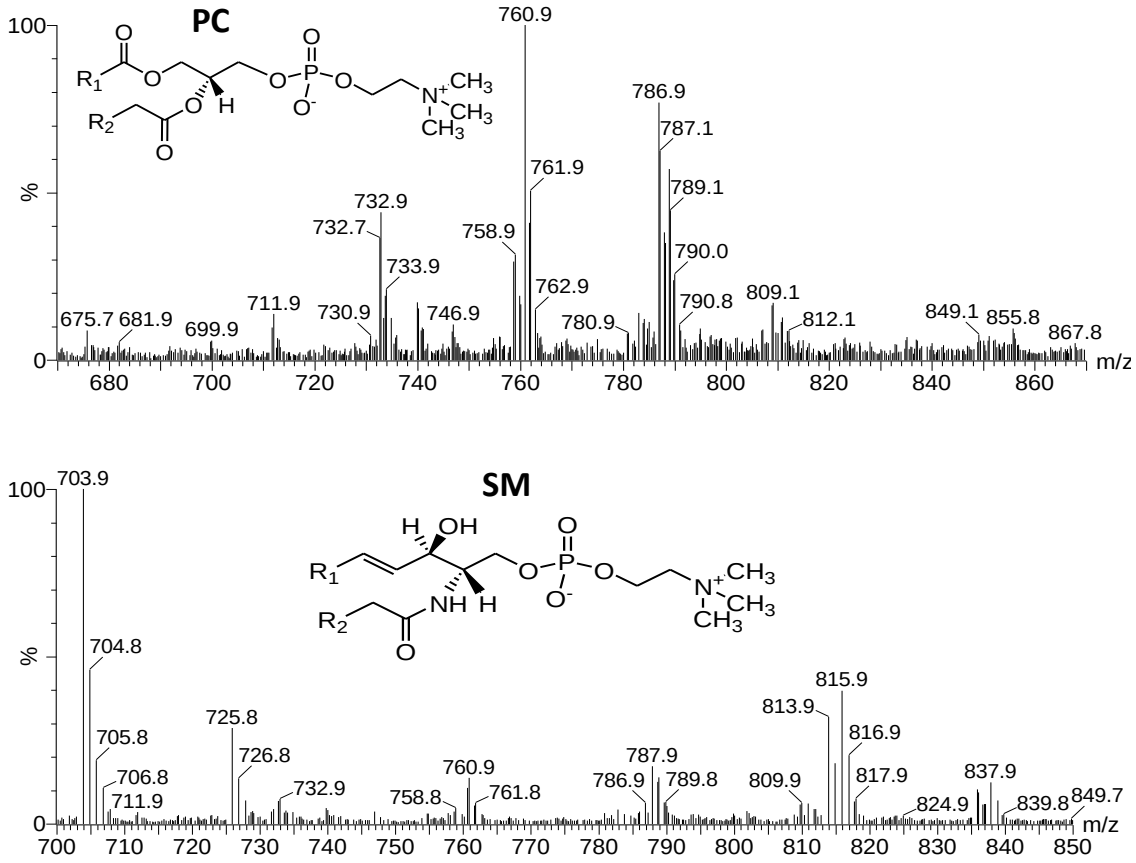

Figure 22. Phosphatidylcholine (PC) and Sphingomyelin (SM) MS spectra. MS spectra obtained by ESI-MS analysis in positive mode of PC and SM extracted from the correspondent spots separated by TLC and their correspondent diacyl structure. Molecular species, observed in the MS spectra as $[MH]^+$ ions of PCs and SMs were selectively detected by precursor ion scan MS/MS experiment of the product ion at *m/z* 184 in the positive mode, using an electrospray triple quadrupole.

Table 2. Identification of $[M+H]^+$ ions observed in the MS spectra of PC. The attribution of the fatty acyl composition of each PL molecular species was done accordingly to the interpretation of the correspondent MS/MS spectra. C: number of carbons in the fatty acid chain and N: number of double bonds; fatty acids (#:#): the first value indicates the number of carbons in the fatty acid chain and the second value, the number of double bonds in this chain.

Phosphatidylcholine (PC)		
Diacyl species		
$[MH]^+$ *m/z*	**Molecular species (C:N)**	**Fatty acid chains**
732.6	32:1	16:0/16:1; 14:0/18:1
734.6	32:0	16:0/16:0
756.6	34:3	16:1/18:2
758.6	34:2	16:1/18:1
760.6	34:1	16:0/18:1
762.6	34:0	16:0/18:0
782.6	36:4	18:2/18:2
784.6	36:3	18:1/18:2
786.6	36:2	18:1/18:1
788.6	36:1	18:0/18:1
790.6	36:0	18:0/18:0
808.6	38:5	20:4/18:1
810.6	38:4	20:4/18:0
812.6	38:3	20:1/18:2
814.6	38:2	20:1/18:1
816.6	38:1	22:0/16:1
842.6	40:2	22:1/18:1
Alkyl-Acyl species		
692.6	30:0	O-14:0/16:0
718.6	32:1	O-14:0/18:1
744.6	34:2	O-16:0/18:2
746.6	34:1	O-16:0/18:1
748.6	34:0	O-16:0/18:0
772.6	36:2	O-16:0/20:2

Table 3. Identification of $[M+H]^+$ ions observed in the MS spectra of SM. The attribution of the fatty acyl composition of each PL molecular species was done accordingly to the interpretation of the correspondent MS/MS spectra. C: number of carbons in the fatty acid chain and N: number of double bonds; fatty acids (#:#): the first value indicates the number of carbons in the fatty acid chain and the second value, the number of double bonds in this chain.

Sphingomyelin (SM) **Sphingoid base/Acyl**		
$[MH]^+$ *m/z*	**Molecular species (C:N)**	**Fatty acid chains**
703.6	34:1	d18:1/16:0
705.6	34:0	d18:0/16:0
725.6	38:4	d18:0/20:4
785.6	40:2	d18:1/22:1
787.6	40:1	d18:0/22:1
789.6	40:0	d18:0/22:0
809.6	42:4	d18:0/24:4
813.6	42:2	d18:1/24:1
815.6	42:1	d18:1/24:0
817.6	42:0	d18:0/24:0

In negative mode we analysed PI, PS, PE and Cer classes of lipids. In a similar way to the lipid classes previously described, both allergen DNFB and irritant BC appear to cause changes in the percentage of individual PI, PS and more significantly in PE classes (based on data of phosphorous content) however, MS analysis revealed that the composition of molecular species within each class does not change. In fact MS and MS/MS analysis the PI, PS and PE profile is similar in the two conditions studied (DNFB and BC), and the spectra obtained from PI, PS and PE class present the same molecular species, as summarized in the Table 4**.** In Figure 23 it is shown the typical ESI-MS spectrum obtained for PI, PS and PE class in that order.

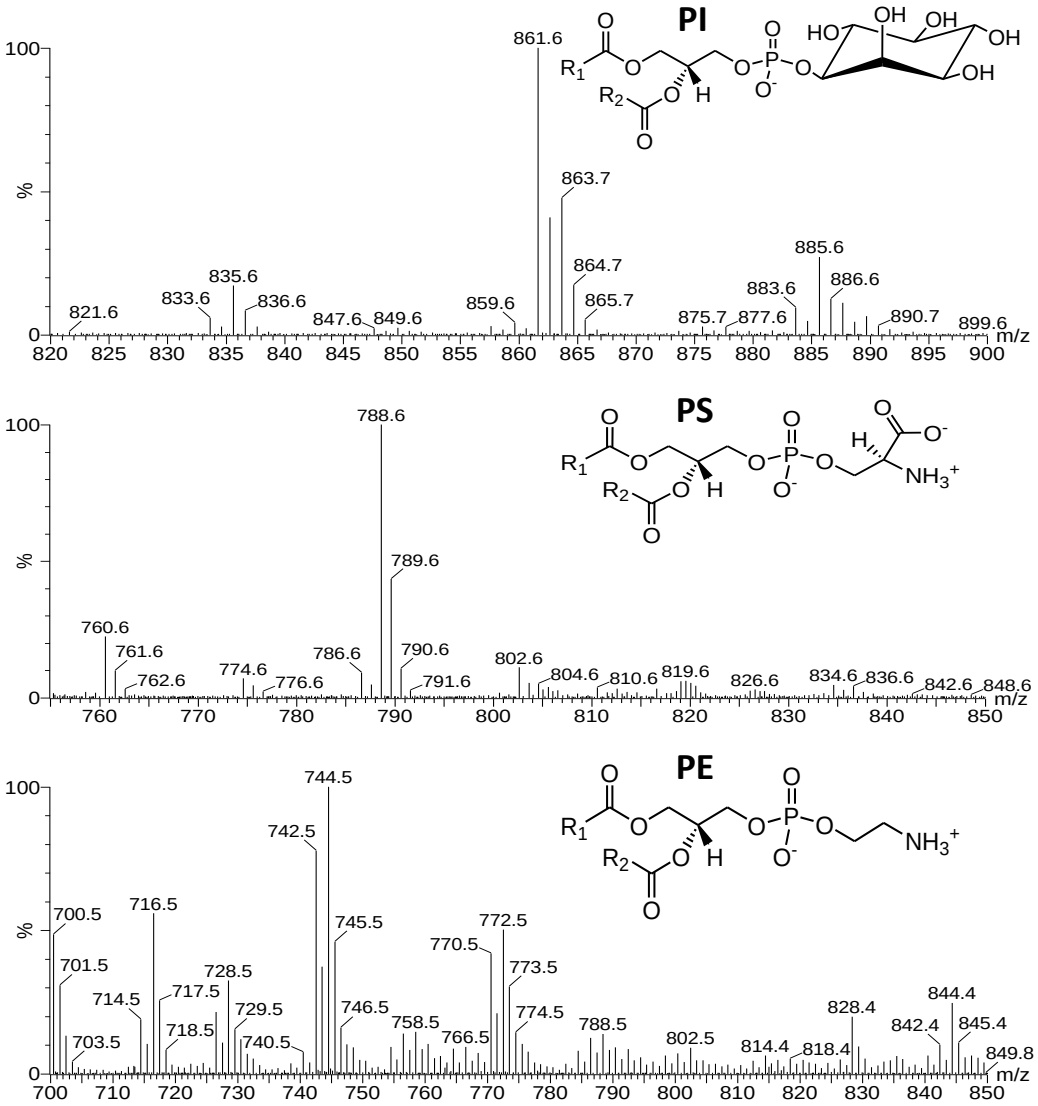

Figure 23. Phosphatidylinositol (PI), Phosphatidylserine (PS) and Phosphatidylethanolamine (PE) MS spectra. MS spectra obtained by ESI-MS analysis in negative mode, with formation of $[M-H]^-$ ions of PI, PS and PE extracted from the correspondent spots separated by TLC and their correspondent diacyl structure. For these classes of PLs no differences were observed in the MS spectra of DCs before and after treatment with DNFB and BC.

According to the data presented in previous section, it is quite noticeable that the lipid profile of ceramides triggered by DC maturation process suffers notorious changes. The same happens when DCs was stimulated by skin sensitizer (allergen) and no-sensitizer (irritant) that promotes significant changes in ceramide profile. Cer spot extracted from the TLC plaque was analysed by ESI-MS, showing the several changes triggered by allergen and irritant, as observed in spectra shown in Figure 24. Observing

these results it was possible found that the main changes are a significant increase of chlorine adducts (75) $[M\text{-}Cl]^-$ at *m/z* 572.6, 682.6 and 684.6, that was identified as to C16, C24:1 and C24:0, respectively, by MS/MS fragmentation as described in chapter I.

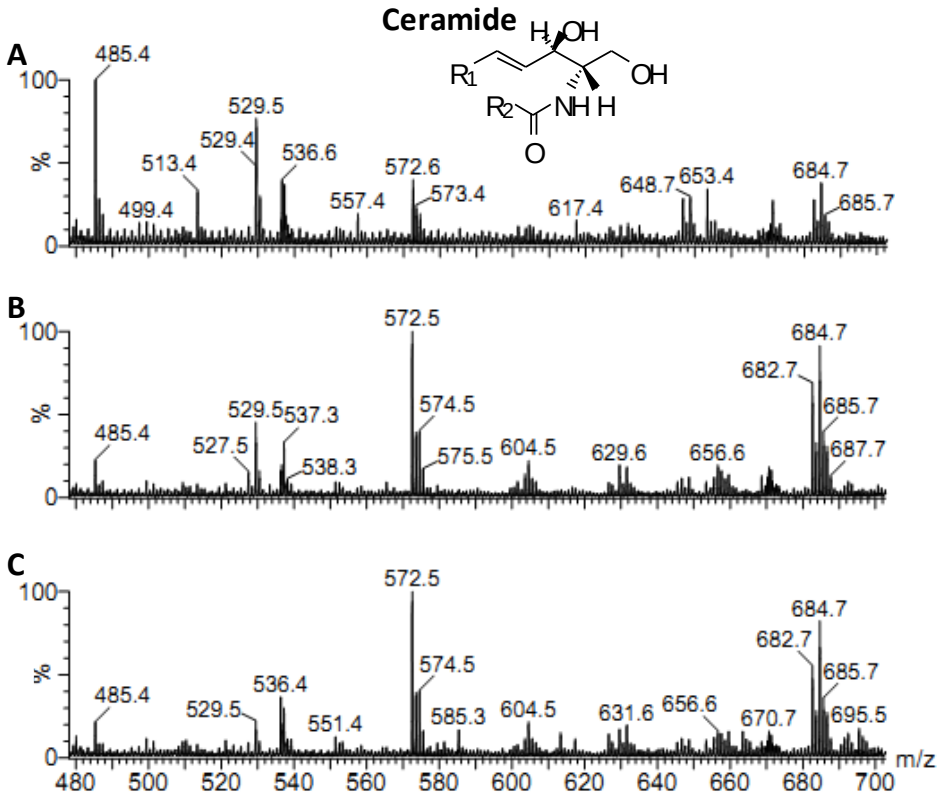

Figure 24. Ceramide MS spectra. MS spectra obtained by ESI-MS analysis in negative mode of Ceramides extracted from the correspondent spots separated by TLC and their correspondent general structure. The profiles of DC without treatment (A) and those with DNFB (B) and BC (C) treatment are aligned in the same scale of y-axis. x-axis, m/z; y-axis, percent relative abundance.

Intracellular ceramide interacts with several signaling pathways playing crucial roles in the regulation of autophagy, cell differentiation, survival, and inflammatory responses (38). Nevertheless, little is known about the implication of ceramide in DC biology, except for the positive impact on DC maturation as assessed by the decrease of phagocytic activity (96). This finding is consistent with our previous results, that allowed to identify important changes in ceramide profile after stimulation of DCs with LPS, a strong DC maturation inducer. In addition, the maturation process of DC is

triggered by TNF-α via activation of its p55 receptor (97), which in many cell types induces sphingomyelin breakdown with resulting accumulation of the lipid messenger ceramide (98, 99), corroborating with our data that after treatment with allergen and irritant was verified an increase of C16, C24:1 and C24:0 Ceramides.

Table 4. Identification of $[M-H]^-$ ions observed in the MS spectra of PE, PI, PS and Cer. The attribution of the fatty acyl composition of each PL molecular species was done accordingly to the interpretation of the correspondent MS/MS spectra. C: number of carbons in the fatty acid chain and N: number of double bonds; fatty acids (#:#): the first value indicates the number of carbons in the fatty acid chain and the second value, the number of double bonds in this chain.

Phosphatidylethanolamine (PS) **Diacyl species**		
$[M-H]^-$ *m/z*	**Molecular species**	**Fatty acid chains**
714.5	34:3	16:1/18:2
716.5	34:2	16:0/18:2
718.5	34:1	16:0/18:1;16:1/18:0
742.5	36:3	18:1/18:2
744.5	36:2	18:1/18:1; 18:0/18:2
746.5	36:1	18:0/18:1
748.5	36:0	18:0/18:0
764.5	38:6	18:2/20:4
766.5	38:5	18:1/20:4
768.5	38:4	18:0/20:4; 18:1/20:3
770.5	38:3	18:0/20:3
772.5	38:2	18:1/20:1
792.5	40:6	18:0/22:6
824.5	42:4	22:1/20:3
826.5	42:2	24:0/18:2
Alkyl-acyl species		
702.5	34:2	O-16:1/18:1
704.5	34:1	O-16:0/18:1
726.5	36:4	O-18:2/18:2
728.5	36:3	O-18:2/18:1
730.5	36:2	O-18:1/18:1

732.5	36:1	O-18:0/18:1
750.5	38:6	O-18:2/20:4;O-16:1/22:5
752.5	38:5	O-16:1/22:4;O-18:1/20:4
776.5	40:7	O-18:2/22:5
778.5	40:6	O-18:1/22:5
Phosphatidylinositol (PI) **Diacyl species**		
833.6	34:2	16:0/18:2; 16:1/18:1
835.6	34:1	16:0/18:1;16:1/18:0
837.6	34:0	16:0/18:0
857.6	36:4	16:0/20:4
859.6	36:3	16:0/20:3; 16:1/20:2
861.6	36:2	18:1/18:1; 18:0/18:2
863.6	36:1	18:0/18:1
865.6	36:0	18:0/18:0
883.6	38:5	18:1/20:4
885.6	38:4	18:0/20:4
887.6	38:3	18:0/20:3
889.6	38:2	18:0/20:2
Phosphatidylserine (PS) **Diacyl species**		
760.6	34:1	16:1/18:0; 16:0/18:1
774.6	35:1	18:0/17:1
786.6	36:2	18:1/18:1; 18:0/18:2
788.6	36:1	18:0/18:1
790.6	36:0	18:0/18:0
808.6	38:5	18:1/20:4
810.6	38:4	18:0/20:4
812.6	38:3	18:0/20:3
814.6	38:2	18:0/20:2
834.6	40:6	18:0/22:6
836.6	40:5	18:0/22:5
842.6	40:2	18:0/22:2
844.6	40:1	18:0/22:1
Ceramides (Cer)		
536.6	34:1	d18:1/16:0
630.6	41:3	d18:1/23:2
634.6	41:1	d18:1/23:0
646.6	42:2	d18:1/24:1
648.6	42:1	d18:1/ 24:0

III. Changes in lipidomic profile triggered by LPS and contact sensitizer in keratinocytes

The role of particular molecular components of the innate immune system in the epidermis is a new and exciting topic in cutaneous immunology. Song et al (2002) shown that normal human keratinocytes (KCs) are capable of expressing functional CD14 and Toll-like receptor 4 (TLR4) and to express constitutively CD14 and TLR4 mRNA that is augmented by exposure to LPS (100). Thus, LPS binding to KCs CD14 and TLR4 resulted in a rapid intracellular calcium response, nuclear factor-kB nuclear translocation, and the secretion of proinflammatory cytokines and chemokines. This in turn results in the activation of immune cells in skin that induce and perpetuate an inflammatory response. To further understand the role of this important skin cells in inflammatory response and specially, in ACD, we studied the changes in the lipid profile of HaCat cell line after LPS and skin sensitizer (DNFB) treatment. Furthermore, in order to differentiate responses between skin sensitizers and irritants we also studied changes observed in HaCat cell line after exposure to the non-sensitizer (irritant BC). This study was conducted in order to asses possible distinct effects in KC when in the presence of either an irritant or a sensitizer.

Separation of lipid classes by TLC

Analysis of lipid profile was initially evaluated using TLC, in order to separate and detect all major lipid classes in total lipid extracts from KCs treated with LPS, DNFB and BC and untreated cells (control). In TLC plate, the several bands represented the different lipid classes that constitute the lipidome of these cells, which was identified by comparison with lipid standards. In this study, TLC did not reveal marked alterations of the lipid composition after cells treatment with the three stimuli. However, after HaCaT cells stimulation with LPS and BC it is possible to detect a slight increase of PC class of PLs (Figure 25A). To evaluate whether LPS, DNFB and BC promotes effectively changes in lipid content, each TLC spot that corresponding to different phospholipid classes was analyzed by the phosphorus assay. Furthermore, to complete these results

and support the correct identification of each lipid class, the different lipid spots were also analysed by ESI-MS and MS/MS, as it will be explained below. The ESI-MS and ESI-MS/MS methods allow to assess and characterize the molecular diversity of the different species of PLs and SPLs.

Phosphorus assay of major phospholipid classes

In the analysis of PL content by phosphorus assay, the PL content of all spots were summed up and considered as 100% of phospholipid content. The relative content of PLs classes was calculated by normalizing the PL content of corresponding spots to the total PL content of all spots. The results obtained are represented in Figure 25B.

PC is most abundant PL classes in KCs, followed by PE (Figure 25B). Comparing the PL content in KCs before and after treatment with LPS, DNFB and BC it is possible to detect significant alterations. Although the statistical analysis did not allow assigning significance, the main change in PL content was observed in PS content, which significantly reduces in KCs exposure to LPS, DNFB and BC stimuli. Despite changes in PL content have been less significant in other classes of PLs, there was still a low increase in CL class content in KCs stimulated by the three stimuli applied. However, in PC there is a particular differential effect between skin sensitizer (DNFB) and non-sensitizer (BC), since the irritant BC stimulus promotes an obvious increase in PC content, in contrast with the allergen stimulus and this effect was not observed in other PL classes analysed. In the remaining PL classes analyzed, SM and PE classes, it was verified that sensitizer and non-sensitizer have the same effect and opposite effect to LPS (Figure 25B).

In summary, the stimulation of KCs by LPS, skin sensitizer and non-sensitizer appears to be characterized by changes in PLs content, mainly in PS content.

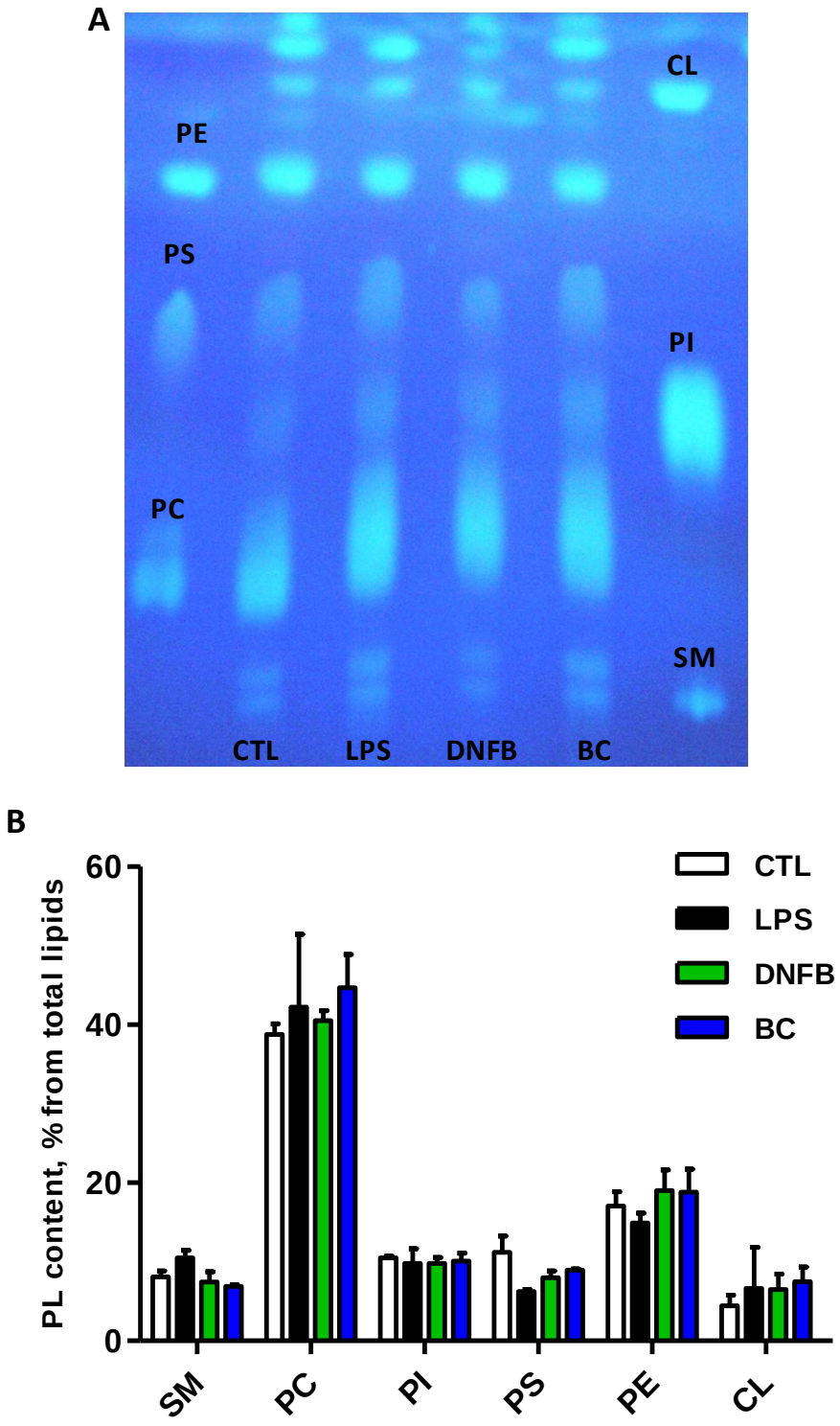

Figure 25. Effect of LPS, DNFB and BC on the phospholipid content in keratinocytes. (A) Typical TLC of total lipids extracted from KCs before and after treatment of cells by LPS, DNFB and BC; **(B)** PL content, % from total lipids refers to the relative percentage of phospholipid phosphorus recovered from the respective spot in TLC.

Analysis of lipid classes by mass spectrometry

To further understand the changes triggered by LPS and skin sensitizer in molecular species composition of each class of lipids, lipids were extracted from TLC spot and after were analysed by MS and MS/MS. ESI-MS and ESI-MS/MS analysis from different lipid class was performed in positive mode for PC, SM and PE while in negative mode for PI, PS, CL and Cer.

PC and SM lipid classes were analyzed by ESI-MS in positive mode since phosphate anion can be protonated during the electrospray process, forming readily abundant $[MH]^+$ protonated ions. However, during electrospray process the both classes can be form sodium adducts i.e. $[MNa]^+$ ions. In order to identify exclusively the $[MH]^+$ ions, precursor ion scan of the ion at *m/z* 184.1 were obtained in a triple quadrupole mass spectrometer, a typical approach for choline phospholipids which was also used in dendritic cell analysis (68). This approach permitted to obtain the spectra shown in Figure 26 and Figure 27, which respectively revealed the $[MH]^+$ ions of all PCs and SMs present in the extract from the spots obtained after TLC separation. In addition, the identification of both diacyl and alkylacyl PCs as well as their fatty acyl chains composition along the glycerol backbone was achieved by ESI-MS and interpretation of ESI-MS/MS spectra of each ion identified in the MS spectra, as resumed in Table 5**.**

Alkyl-acyl and diacyl-species of phospholipids have the same fatty acid compositions but are characterized by a mass difference of 14, due to their attachment to the glycerol backbone of phospholipid by vinyl ether or ester bond (101).

All spectra obtained from MS analysis of the lipids obtained from PCs spots exhibit two major molecular species identified by tandem mass spectrometry: PC(16:0/18:1) corresponding to $[MH]^+$ at *m/z* 760.8 and PC(18:1/18:1) that corresponds to $[MH]^+$ at *m/z* 786.8, followed by descending order of relative abundance: the diacyl PCs with $[MH]^+$ at *m/z* 758.6 and 784.6 corresponding respectively to PC(16:1/18:1) and PC(18:1/18:2), and the alkylacyl PCs, as PC(O-16:0/18:1) and PC(O-14:0/18:0) corresponding respectively to $[MH]^+$ at *m/z* 746.8 and 720.8.

Previously, it was observed a slight increase in the levels of PC through phosphorous quantification analysis (Figure 25B), and MS study allowed to detected substantial differences between stimulated cells and untreated cells (Figure 26). After LPS treatment there are a significant increase in the relative abundance of PC with *m/z* 786.6 that corresponds a PC(18:1/18:1), which is still more significant in HaCat cells treated by irritant BC. Cells treated with LPS and BC stimuli also present a slight increase in the relative abundance of alkylacyl PC(O-16:0/18:1) (*m/z* 746.8), while in allergen (DNFB) treated cells this increase seems less significant. Thus, it was possible to observe that allergen does not promote visible changes in relative abundance of PCs, which corroborates with quantification data (Figure 25B). As DCs, the molecular species of both diacyl-PC and alkyl-acyl-PC contained as major abundant fatty acyl residues those with chain length with C18 and C16, as confirmed by MS/MS analysis (Table 5).

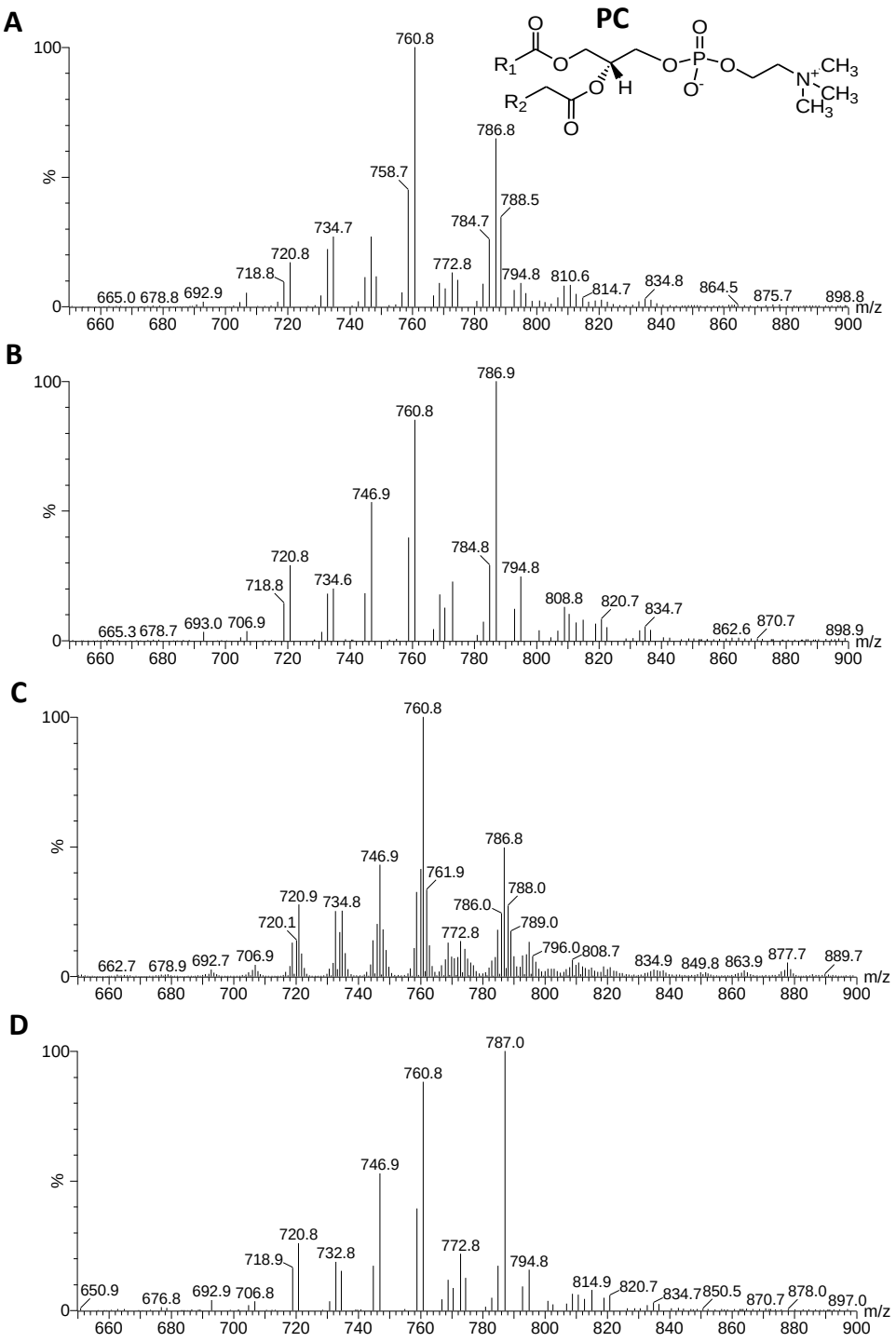

Figure 26. Phosphatidylcholine (PC) spectra. MS spectra obtained by ESI-MS analysis in positive mode with formation of $[MH]^+$ ions of PC extracted from the correspondent spots separated by TLC and their correspondent diacyl structure. Molecular species of PCs were selectively detected by precursor ion scan MS/MS experiment of the product ion at *m/z* 184 in the positive mode, using an electrospray triple quadrupole. The profiles of KCs without treatment (A) and those with LPS (B), DNFB (C) and BC (D) treatment are aligned in the same scale of y-axis. x-axis, m/z; y-axis, percent relative abundance.

SM spectra presents in Figure 27 shows that SMs ions with higher relative abundance are SM(18:1/16:0), SM(18:0/16:0), SM(18:1/22:1) and SM(18:0/22:1), corresponding to $[MH]^+$ at *m/z* 703, 705, 813 and 815 respectively followed by SM(18:0/20:1) corresponding to $[MH]^+$ at *m/z* 787. Because SM elutes close to PC class and given that in total lipid extract PCs are present in high amount, it was possible to identify, in these spectra, some PCs ion species as ions with $[MH]^+$ at *m/z* 760 and 746. However, PCs and SMs are easily to differentiate, since SM species form ions with odd value of *m/z*. Through MS and MS/MS analysis of these spectra, it appears that only LPS and DNFB stimuli promote some changes in lipid profile of SM. In SM profile of KCs treated by LPS and allergen, the relative abundance of SM(18:1/22:1) and SM(18:0/20:1) was increased. However, there are no changes in SM lipid profile after the stimulation with irritant.

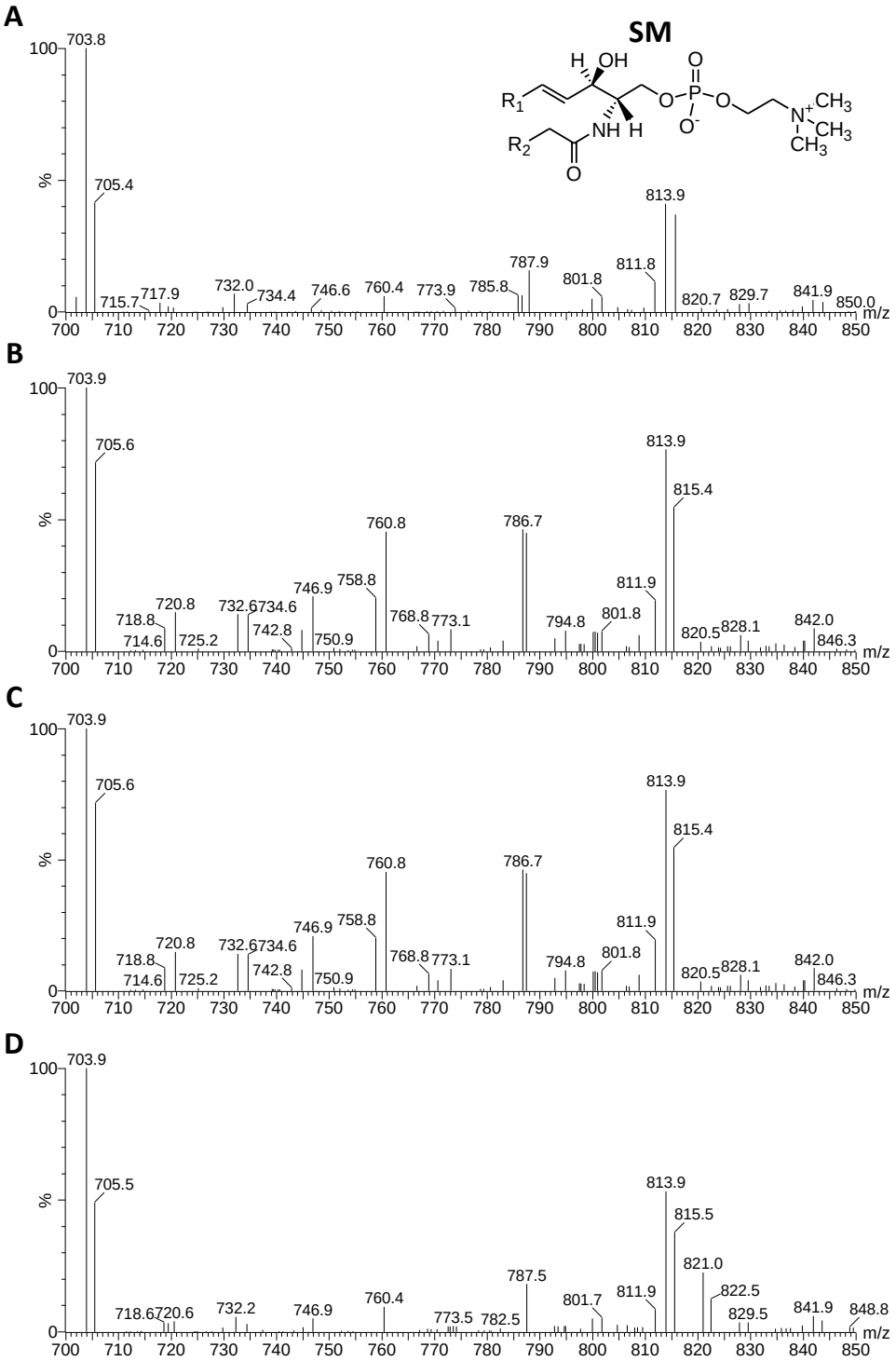

Figure 27. Sphingomyelin (SM) spectra. MS spectra obtained by ESI-MS analysis in positive mode with formation of $[MH]^+$ ions of SM extracted from the correspondent spots separated by TLC and their correspondent structure. Molecular species of SMs were selectively detected by precursor ion scan MS/MS experiment of the product ion at *m/z* 184 in the positive mode, using an electrospray triple quadrupole. The profiles of KCs without treatment (A) and those with LPS (B), DNFB (C) and BC (D) treatment are aligned in the same scale of y-axis. x-axis, m/z; y-axis, percent relative abundance.

PE was also analyzed in the triple quadrupole by ESI-MS in positive mode, formatting $[M+H]^+$ ions, the identification of this phospholipid class in MS spectrum was confirmed by neutral loss scan experiment (neutral loss of polar head, -141 Da), a typical approach for PEs (42, 69). This approach permitted to obtain the spectra in the Figure 28, which revealed the $[M+H]^+$ ions of PEs present in the TLC spot. Direct interpretation of MS/MS spectra of each ion present in the MS spectra allowed the identification of diacyl and alkylacyl PEs molecular species and both their fatty acyl chains composition along the glycerol backbone, as described previously and resumed in Table 5.

The most abundant PEs under the different conditions used were PE(18:1/18:1 and 18:0/18:2) and PE(18:0/18:1) corresponding respectively to the ion $[M+H]^+$ at *m/z* of 744.8 and 746.8 by followed PE(20:4/18:0 and 20:3/18:1) with *m/z* 768.8. In cells treated with LPS and untreated, molecular specie of PE identified as PE(18:0/18:1) were more abundant than PE(18:1/18:1 and 18:0/18:2), however, after DNFB and BC treatment this relationship is reversed, i.e., these stimuli appear to promote increasing relative abundance of this molecular specie PE(18:1/18:1 and 18:0/18:2)(*m/z* 744.8). This was the most significant change in PE spectra, since the different stimuli applied in HaCat cells do not appear to significantly alter the lipid profile of the remaining PE molecular species identified.

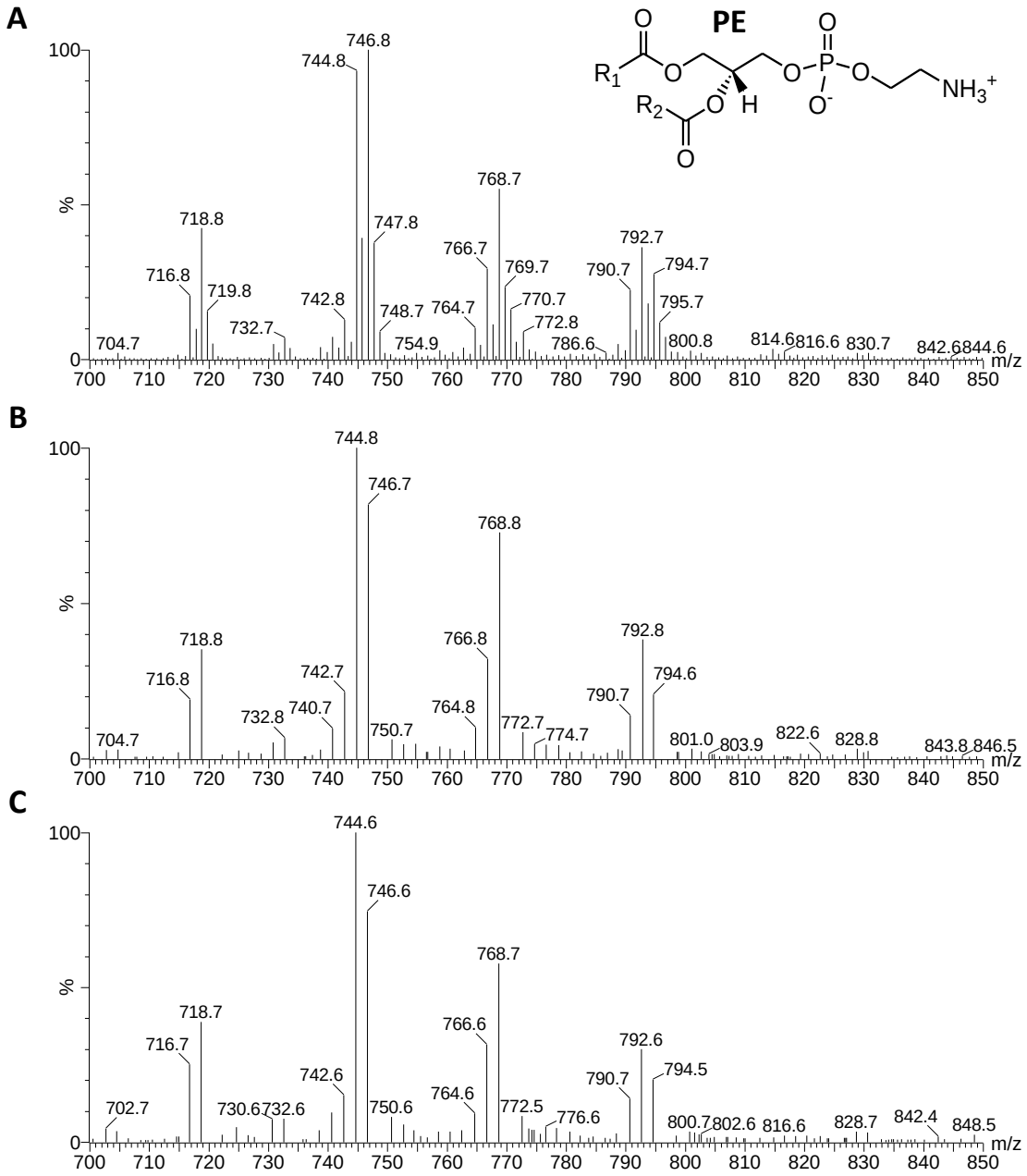

Figure 28. Phosphatidylethanolamine (PE) spectra. MS spectra obtained by ESI-MS analysis in positive mode with formation of $[MH]^+$ ions analysis of PE extracted from the correspondent spots in TLC and their correspondent structure. Using an electrospray triple quadrupole in the positive mode, molecular species of PEs were selectively detected by neutral loss MS/MS experiment of the PE polar head, which corresponds to product ion at *m/z* 141. The profiles of KCs without treatment (A) and those with LPS (A), DNFB (B) and BC (C) treatment are aligned in the same scale of y-axis. x-axis, m/z; y-axis, percent relative abundance.

Table 5. Identification of $[M+H]^+$ ions observed in the MS spectra of PC, SM and PE. The attribution of the fatty acyl composition of each PL molecular species was done accordingly to the interpretation of the correspondent MS/MS spectra. C: number of carbons in the fatty acid chain and N: number of double bonds; fatty acids (#:#): the first value indicates the number of carbons in the fatty acid chain and the second value, the number of double bonds in this chain.

Phosphatidylcholine (PC)		
Diacyl species		
$[MH]^+$ *m/z*	**Molecular species**	**Fatty acid chains**
704.6	30:1	14:0/16:1
706.6	30:0	14:0/16:0
732.6	32:1	16:0/16:1; 14:0/18:1
734.6	32:0	16:0/16:0
756.6	34:3	16:1/18:2
758.6	34:2	16:1/18:1
760.6	34:1	16:0/18:1
762.6	34:0	16:0/18:0
782.6	36:4	18:2/18:2
784.6	36:3	18:1/18:2
786.6	36:2	18:1/18:1
788.6	36:1	18:0/18:1
790.6	36:0	18:0/18:0
808.6	38:5	20:4/18:1
810.6	38:4	20:4/18:0
812.6	38:3	20:1/18:2
814.6	38:2	20:1/18:1
816.6	38:1	22:0/16:1
842.6	40:2	22:1/18:1
Alkyl-Acyl species		
692.6	30:0	O-14:0/16:0
718.6	32:1	O-14:0/18:1
744.6	34:2	O-16:0/18:2
746.6	34:1	O-16:0/18:1
748.6	34:0	O-16:0/18:0
772.6	36:2	O-16:0/20:2

Sphingomyelin (SM) Sphingoid base/Acyl		
703.6	34:1	d18:1/16:0
705.6	34:0	d18:0/16:0
725.6	38:4	d18:0/20:4
785.6	40:2	d18:1/22:1
787.6	40:1	d18:0/22:1
789.6	40:0	d18:0/22:0
809.6	42:4	d18:0/24:4
813.6	42:2	d18:1/24:1
815.6	42:1	d18:1/24:0
Phosphatidylethanolamine (PE) **Diacyl species**		
714.5	34:3	16:1/18:2
716.5	34:2	16:0/18:2
718.5	34:1	16:0/18:1;16:1/18:0
742.5	36:3	18:1/18:2
744.5	36:2	18:1/18:1; 18:0/18:2
746.5	36:1	18:0/18:1
748.5	36:0	18:0/18:0
764.5	38:6	18:2/20:4
766.5	38:5	18:1/20:4
768.5	38:4	18:0/20:4; 18:1/20:3
770.5	38:3	18:0/20:3
772.5	38:2	18:1/20:1
792.5	40:6	18:0/22:6
824.5	42:4	22:1/20:3
826.5	42:2	24:0/18:2
Alkyl-acyl species		
702.5	34:2	O-16:1/18:1
704.5	34:1	O-16:0/18:1
726.5	36:4	O-18:2/18:2
728.5	36:3	O-18:2/18:1
730.5	36:2	O-18:1/18:1
732.5	36:1	O-18:0/18:1
750.5	38:6	O-18:2/20:4;O-16:1/22:5

752.5	38:5	O-16:1/22:4;O-18:1/20:4
776.5	40:7	O-18:2/22:5
778.5	40:6	O-18:1/22:5

Either as membrane constituents or as participants in essential metabolic processes, PIs are an important class of lipids in cells. PIs extracted from their corresponding TLC spots were analyzed by ESI-MS in negative mode, with formation of $[M-H]^-$. This approach permitted to obtain the spectra shown in Figure 29, which revealed the all PI $[M-H]^-$ ions. Analysis of PIs showed three predominant $[M-H]^-$ ions observed in descending order at *m/z* 885.5, 863.5 and 835.5, identified as PI(20:4/18:0), PI(18:0/18:1) and PI(16:0/18:1 and 18:0/16:1) respectively, as demonstrated in Figure 29. The other PIs present in minor relative abundance were identified as resumed in Table 6. All these ions were analysed by MS/MS as described in chapter I, for to confirm the composition in fatty acids.

Except for slight relative increase in the PI(18:0/18:2 or 18:1/18:1) and PI (18:1/16:1 or 18:2/16:0) that correspond to at *m/z* 861.5 and 833.5 respectively, after only LPS treatment, the PI spectra revealed no change in lipid profile of PIs triggered by different stimuli, as we can see in Figure 29.

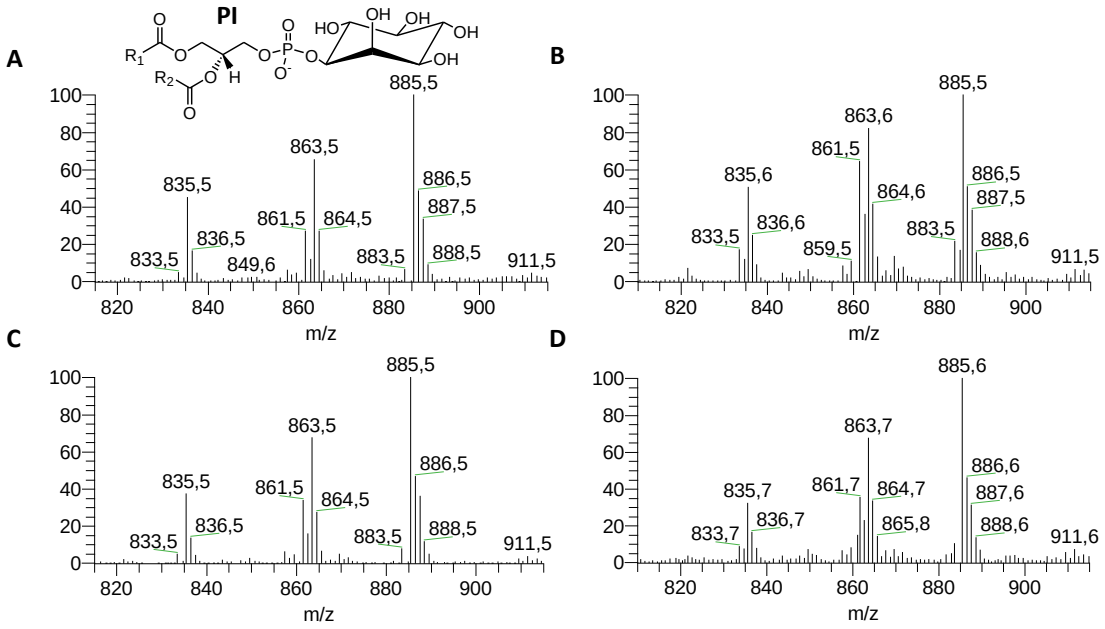

Figure 29. Phosphatidylinositol (PI) spectra. MS spectra obtained by ESI-MS analysis in negative mode with formation of $[M-H]^-$ ions of PI extracted from the correspondent spots in TLC and their correspondent structure. Molecular species of PIs were detected by electrospray ion trap in the negative mode. The profiles of KCs without treatment (A) and those with LPS (B), DNFB (C) and BC (D) treatment are aligned in the same scale of y-axis. x-axis, m/z; y-axis, percent relative abundance.

PSs are a class of PLs with the unique characteristic of being predominantly found on the inner leaflet of normal cells (78, 102). This normal distribution is altered in many biological events, including platelet aggregation, cell adhesion, and during cellular apoptosis (103). Stimulation of KCs with the different stimuli appears to modulate notably the proportion and composition of PLs this class. Figure 30 represent to ESI-MS spectra of PS, revealing two major $[M-H]^-$ ions at *m/z* 788.6 identified as PS(18:0/18:1) and at *m/z* 760.4 that correspond to PS(16:0/18:1 or 16:1/18:0). All PS molecular species (Table 6) were characterized by MS/MS analysis of all $[M-H]^-$ ions found in MS spectra, revelling the formation of typical product ions that correspond to the loss of serine with formation of the ion $[M-H-87]^-$, as demonstrated in chapter I (68). In Table 6 the remaining identified PSs are summarized.

The $[M-H]^-$ ion with *m/z* value 806.3, despite its presence in MS spectra with high abundance, analysis by tandem mass spectrometry found that it does not correspond to a PS molecular specie (Figure 30B,C). The presence of this ion in the MS spectra, although modifying the relative abundance of other ions, also revealed the occurrence of very important changes in lipid profile of this PL class. The most important change occurs after LPS, allergen and irritant stimulation, that promotes a drastic reduction in one of the most abundant PS presents in KCs, PS(16:0/18:1 or 16:1/18:0) at *m/z* 760.4. Comparing with KCs treated by LPS and DNFB, the stimulation of KCs with the irritant BC also demonstrated some changes, such as the absence of PS molecular specie identified as PS(18:0/22:2) at *m/z* 842.4. These MS data are consistent with data from the quantification previously described, which also showed a significant decrease in the amount of PS in the cell, mainly in cell membrane.

In addition to a structural function, PS is also involved in signaling pathways such as protein kinase C pathway (104) and in localization of intracellular proteins to the cytosolic membrane leaflets (105). The presence of PS on the outer leaflet of lipid bilayer initiates many biological events, including platelet aggregation, cell adhesion, and is an indicator of cellular apoptosis. In accordance to several *in vitro* studies previously performed (106-108) demonstrating that skin inflammation triggered during contact hypersensitivity induces keratinocyte apoptosis, we hypothesize that alteration on PS profile detected in HaCat cells may be associated with apoptosis induced by contact sensitizer and LPS.

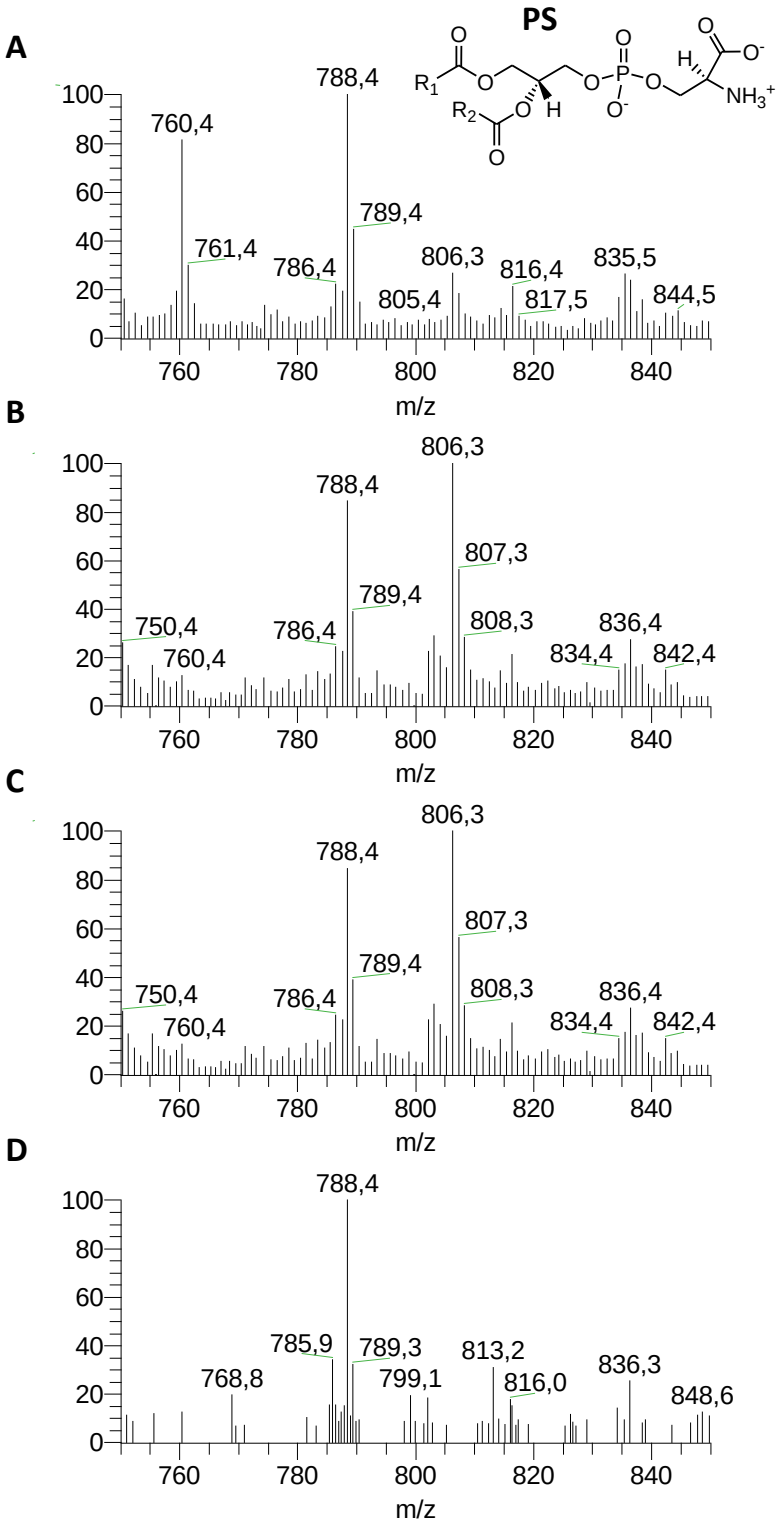

Figure 30. Phosphatidylserine (PS) spectra. MS spectra obtained by ESI-MS analysis in negative mode with formation of $[M-H]^-$ ions of PS extracted from the correspondent spots in TLC and their correspondent structure. Molecular species of PSs were using a electrospray ion trap mass spectrometer. The profiles of KCs without treatment (A) and those with LPS (B), DNFB (C) and BC (D) treatment are aligned in the same scale of y-axis. x-axis, m/z; y-axis, percent relative abundance.

CL is found almost exclusively on the inner membrane of the mitochondria within cells, however, their exact role in cellular biochemistry is not been fully explained but it is clear that CL is necessary for cytochrome C placing into the mitochondrial membrane, and that it is involved in mitochondrial stability and function (109). CL is one of the most complex phospholipid present in eukaryotic cells, because this PL consists of two phosphatidic acids with a glycerol bond.

CLs obtained from KCs stimulated by three stimuli (LPS, DNFB and BC) and untreated KCs were analyzed by ESI-MS in negative mode, with formation of both singly charged $[M-H]^-$ ions and doubly charged $[M-2H]^2$ ions, because they have two phosphodiester groups in its structure. The figure 31 represent the MS spectra of the $[M-H]^-$ ions present in the TLC spots correspondent to the CL class.

Analysis of CLs species allowed to identify diacyl CLs, as resumed in Table 6. This analysis was achieved by direct interpretation of MS/MS spectra of each ion identified in the MS spectra, both $[M-H]^-$ and $[M-2H]^{2-}$ (110).

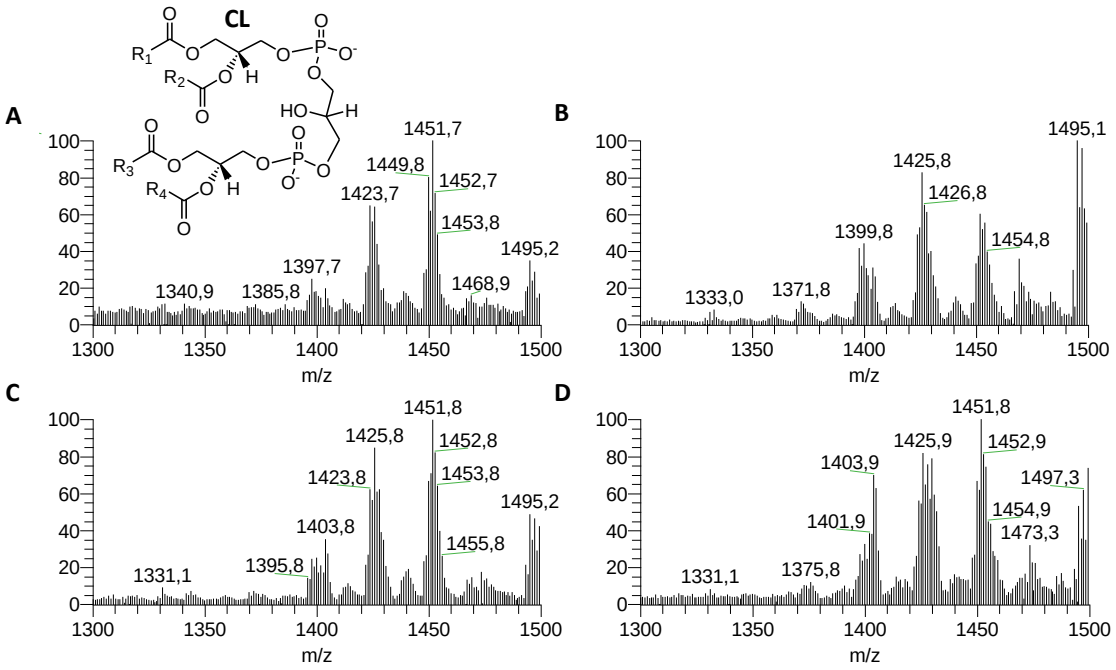

Figure 31. Cardiolipin (CL) spectra. MS spectra obtained by ESI-MS analysis in negative mode with formation of $[M-H]^-$ ions of CL extracted from the correspondent spots in TLC and their correspondent structure. Molecular species of CLs were detected by electrospray ion trap mass spectrometer. The profiles of KCs without treatment (A) and those with LPS (B), DNFB (C) and BC (D) treatment are aligned in the same scale of y-axis. x-axis, m/z; y-axis, percent relative abundance.

The most abundant CLs were CL(18:1/18:1/18:2/18:2) and CL(16:1/18:1/18:1/18:2) and CL (16:1/18:1/18:2/18:2) corresponding to the ion $[M-H]^-$ at *m/z* 1451.7, 1425.7 and 1423.7 of respectively, followed by CL(16:0/16:0/18:1/18:1) and CL(16:0/16:1/18:1/18:2) corresponding to the ion $[M-H]^-$ at *m/z* of 1403.7 and 1399.7 and 1475.7, respectively.

It is interesting to notice that in addition to changes in CL content dependent on the cell stimuli inferred by the results obtained in phospholipid quantification, Figure 31, analysis of CL MS spectra showed that all stimuli applied in KCs promoted some remarkable changes in the profile of molecular species of CL. Thus, KCs stimulated with LPS, allergen and irritant show a higher relative abundance for CL(16:1/18:1/18:1/18:2) Table 6. However there are some specific alterations that allow to differentiate between different stimuli, seeing that the LPS stimuli fostered a significant decrease of

the most abundant CL, CL(18:1/18:1/18:2/18:2), increasing the relative abundance of second most abundant CL, CL(16:1/18:1/18:1/18:2) and CL(16:0/16:1/18:1/18:2) corresponding to the ion $[M-H]^-$ at *m/z* of 1425.7 and 1399.7, respectively. After DNFB stimulation there seems to be an increase in the relative abundance of CL(16:0/16:0/18:1/18:1)(*m/z*1403.7) and the irritant BC appears to further promote this change, as demonstrated in Figures 31C, 31D, comparing with the non treated cell.

In mammalian cells, CL is found almost exclusively in the inner mitochondrial membrane where it is essential for the optimal function of numerous enzymes that are involved in mitochondrial energy metabolism. After oxidation, CL is transferred from the inner to the outer membrane, and then helps in the release of cyt c, one of the fundamental steps of apoptosis (111). Alterations in the content and/or structure of CL have been reported in several tissues in a variety of pathological conditions.

Finally, ceramides, present in the last spot of TLC plate (which corresponds to the spot with highest RF) were analyzed by ESI-MS and MS/MS in negative mode. Thus, Cer obtained from untreated KCs and KCs stimulated with LPS, allergen and irritant show in the ESI-MS the with formation of negatively charged $[M-H]^-$ ions, as the Figure 32 represents.

Keratinocytes contain abundant ceramides compared to other cells. However, studies on these cells have mainly focused on the barrier function of ceramide, while their other roles, have not been well addressed. Cer is the central core of SPL metabolism and has also been involved in the regulation of signal transduction processes. The different Cer may localize into distinct cell compartments and may be involved in the regulation of different cell functions, namely cell cycle arrest and apoptosis (55, 112). Furthermore, Cer play important roles in the regulation of autophagy, cell differentiation, survival, and inflammatory responses (113).

Evaluation of ESI-MS spectra of Cer spot presents in Figure 32, allowed the observation that Cer(d18:1/16:0) identified, as chlorine adducts $[M-Cl]^-$ at *m/z* 572.5, is present in all conditions studied. This Ceramide after LPS treatment of HaCat cells

show a lower relative abundance in MS spectra. However, the LPS stimuli appears promoted the formation of Ceramide-1-phosphate (C1P) identified by the ion $[M-H]^-$ at *m/z* 576.8, and confirmed by MS/MS, since in addition the typical product ions corresponding to the Cer fragmentation process, it was also observed neutral loss of 98Da that correspond the loss of the phosphate group under fragmentation conditions. The others Cer were identified, as we can see in Table 6.

In recent study was examined the effects of different Cer on apoptosis in HaCaT keratinocytes, and it was found that these epidermal cells exhibit selective responses according to the carbon length of the fatty acids of Cer (114). Thus, the further studies are necessary to explore the changes in profile of Cer in these cells that may be related with Cer-induced apoptosis.

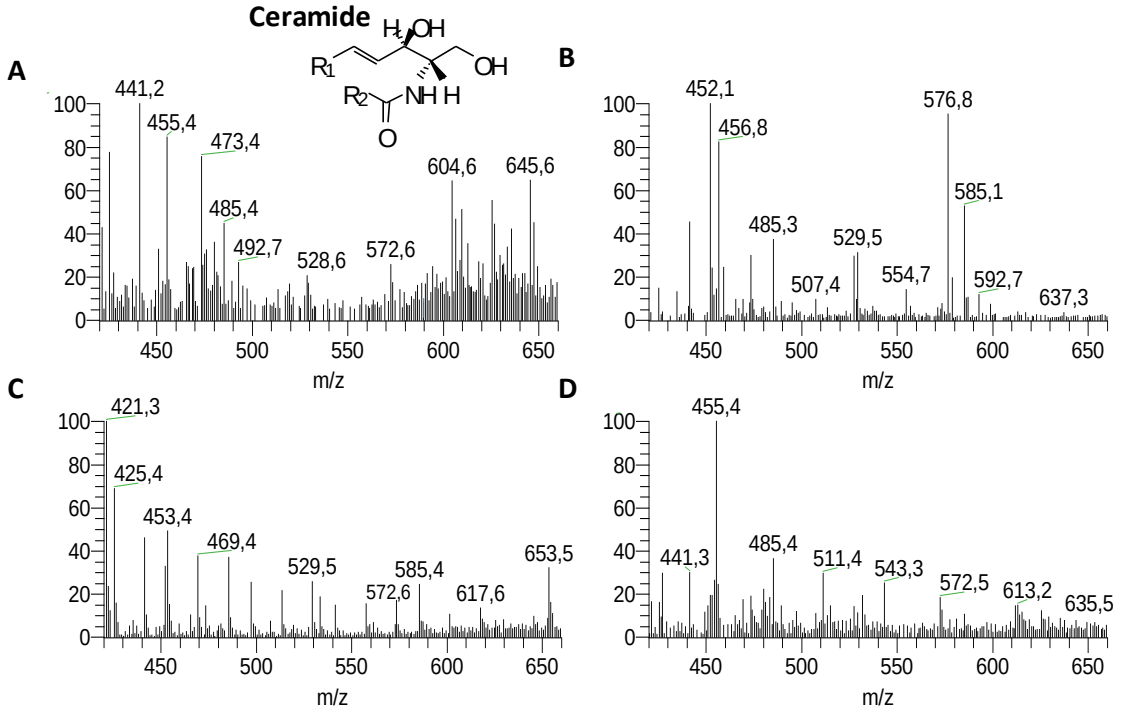

Figure 32. Ceramide (Cer) spectra. MS spectra obtained by ESI-MS analysis in positive mode with formation of $[M-H]^-$ ions of Cer extracted from the correspondent spots in TLC and their correspondent structure. Molecular species of Cer were detected by electrospray ion trap mass spectrometer. The profiles of KCs without treatment (A) and those with LPS (B), DNFB (C) and BC (D) treatment are aligned in the same scale of y-axis. x-axis, m/z; y-axis, percent relative abundance.

Table 6. Identification of $[M-H]^-$ ions observed in the MS spectra of PI, PS, CL and Cer. The attribution of the fatty acyl composition of each PL molecular species was done accordingly to the interpretation of the correspondent MS/MS spectra. C: number of carbons in the fatty acid chain and N: number of double bonds; fatty acids (#:#): the first value indicates the number of carbons in the fatty acid chain and the second value, the number of double bonds in this chain.

Phosphatidylinositol (PI) **Diacyl species**		
833.6	34:2	16:0/18:2; 16:1/18:1
835.6	34:1	16:0/18:1;16:1/18:0
837.6	34:0	16:0/18:0
857.6	36:4	16:0/20:4
859.6	36:3	16:0/20:3; 16:1/20:2
861.6	36:2	18:1/18:1; 18:0/18:2
863.6	36:1	18:0/18:1
865.6	36:0	18:0/18:0
883.6	38:5	18:1/20:4
885.6	38:4	18:0/20:4
887.6	38:3	18:0/20:3
889.6	38:2	18:0/20:2
909.6	40:6	18:0/22:6
911.6	40:5	18:0/22:5
913.6	40:4	18:0/22:4
Phosphatidylserine (PS) **Diacyl species**		
760.6	34:1	16:1/18:0; 16:0/18:1
786.6	36:2	18:1/18:1; 18:0/18:2
788.6	36:1	18:0/18:1
790.6	36:0	18:0/18:0
808.6	38:5	18:1/20:4
810.6	38:4	18:0/20:4
812.6	38:3	18:0/20:3
814.6	38:2	18:0/20:2
834.6	40:6	18:0/22:6
836.6	40:5	18:0/22:5
842.6	40:2	18:0/22:2
844.6	40:1	18:0/22:1
Cardiolipin (CL)		
1377.5	66:1	16:0/16:0/16:0/18:1
1399.5	68:4	16:0/16:1/18:1/18:2

1403.5	68:2	16:0/16:0/18:1/18:1
1423.5	70:6	16:1/18:1/18:2/18:2
1425.5	70:5	16:1/18:1/18:1/18:2
1427.5	70:4	16:1/18:1/18:1/18:1
1429.5	70:3	16:0/18:1/18:1/18:1
1447.5	72:8	18:2/18:2/18:2/18:2
1449.5	72:7	18:1/18:2/18:2/18:2
1451.5	72:6	18:1/18:1/18:2/18:2
1453.5	72:5	18:1/18:1/18:1/18:2
1455.5	72:4	18:1/18:1/18:1/18:1
1475.5	74:8	18:1/18:2/18:2/20:3 18:2/18:2/18:2/20:2
1477.5	74:7	18:1/18:1/18:2/20:3 18:1/18:2/18:2/20:2
Ceramide (Cer)		
536.6	34:1	d18:1/16:0
630.6	41:3	d18:1/23:2
634.6	41:1	d18:1/23:0
646.6	42:2	d18:1/24:1
648.6	42:1	d18:1/ 24:0

CHAPTER IV

Conclusion

IV. Conclusion

Allergic contact dermatitis, a clinical condition caused by skin exposure to a large subset of chemicals, is one of the commonest occupational diseases in developed countries. Nowadays, the sensitizing potential of chemicals is commonly assessed in animals; however existing and forthcoming European legislation imposes the adoption of new alternative approaches. The modifications induced by chemicals in skin cell models form the basis for the most favourable predictive strategies. All of these modifications, both at the genomic, proteomic and lipidomic levels, are the consequence of a coordinated orchestration of different intracellular signalling pathways that are specifically triggered by strong skin sensitizers and not by irritants. Here and through lipidomic approach we provide evidence of significant changes on phospholipids and sphingolipids, in skin dendritic cells and keratinocytes, triggered by allergens and irritants.

DC maturation triggered by LPS induced some significant changes in the cellular levels of both signalling and structural lipids, mainly an increase in PC and Cer levels and a decrease in SM and PI content. Furthermore, this work provided precise information about changes in phospholipids and sphingolipids composition during DC maturation, allowing the identification of significant lipidic changes in the profile of Cer. Curiously, the skin sensitizer induced the same changes in the lipid profile of DCs, including decreased of PI content and increased of C16, C24:1 and C24:0 Ceramides. Thus, our data suggest that skin sensitizer and LPS likely triggered similar intracellular signalling pathways, which modulated the ceramide profile. This data indicate that lipidomics is a promising area of research deserving to be explored, in order to study in more depth the consequences of changes in these specific lipid classes.

Skin sensitizer and LPS promoted similar modifications in the lipid profile of KCs, specially triggering a drastic reduction of the content one of the most abundant PS presents in KCs, PS(16:0/18:1 or 16:1/18:0). Interesting, the stimulation of KCs with the irritant BC does not trigger the same profile, particularly, promoted a significant decrease of PS molecular specie identified as PS(18:0/22:2) at *m/z* 842.4. These findings suggest that skin sensitizer and LPS affect the phospholipid and sphingolipids

profile in a similar way, which can be related with an apoptotic process triggered in these cells, since PS are inductor factor of apoptosis. Therefore, additional work is required to understand, in detail, the transduction pathways triggered by chemical sensitizers and also to clarify the role of each phospholipid or sphingolipid, here identified, in DC maturation events and in KC activation, and consequently, their involvement in the development of ACD.

The results obtained in this work strongly suggest the screening of lipid changes elicited by allergens and irritants in skin cells in order to disclose good biomarkers for further use in an integrative test strategy towards the reduction of animals use for skin sensitization prediction.

PAPER

Changes in lipidomic profile triggered during dendritic cells maturation

Profiling changes triggered during dendritic cells maturation: a lipidomic approach

Deolinda R. Santinha[1], Diane R. Marques[2], Elisabete A. Maciel[2], Cláudia S. O. Simões[2], Susana Rosa[1], Bruno M. Neves[1], Bárbara Macedo [3], Pedro Domingues[2], M Teresa Cruz [1] and M Rosário M. Domingues[2].

1-Faculty of Pharmacy and Center for Neuroscience and Cell Biology (CNC), University of Coimbra, 3000-548 Coimbra, Portugal

2- Mass Spectrometry Centre, Chemistry Department, University of Aveiro, 3810-193 Aveiro, Portugal

3- Metabolomics Core Service, IBMC - Institute for Molecular and Cell Biology, Porto, Portugal

* Author to whom correspondence should be addressed:

M.Rosário M. Domingues

e-mail: mrd@ua.pt

Phone:+351 234 370 698

Fax:+ 351 234 370 084

ABSTRACT

Lipids play an important role in several biological processes by acting as signaling and regulating molecules, or locally as membrane components that modulate protein function. This work describes the pattern of lipid composition of dendritic cells (DCs), a cell type that plays critical roles in the inflammatory and immune responses. After activation by antigens, DCs undergo drastic phenotypical and functional transformations, in a process known as maturation. In order to better characterize this process, changes on lipid profile were evaluated through a lipidomic approach. As an experimental model of DCs, we used a fetal skin-derived dendritic cell line (FSDC) induced to mature by treatment with lipopolysaccharide (LPS). The results showed that LPS increased the ceramides (Cer) and phosphatidylcholine (PC) levels and decreased the sphingomyelin (SM) and phosphatidylinositol (PI) content. Mass spectrometry analysis from total lipid extract and from each class of lipids revealed that maturation promoted clear changes in ceramides profile, and quantification analysis allow to identify an increase of total amount of ceramide content and an enhance of Cer at *m/z* value 546.7 identified as Cer(d18:1/24:1) and at *m/z* 648.7 identified as Cer(d18:1/24:0). The pattern of change of these lipids give an extremely rich source of data for evaluating modulation of specific lipid species triggered during DC maturation.

Key-words: Lipidomic, Phospholipids, Sphingolipids, Dendritic Cells, Lipopolysaccharide, Mass Spectrometry, Electrospray Ionization

Abbreviations: DCs, dendritic Cells; iDCs, immature dendritic cells; mDCs, mature dendritic cells; LPS, lipopolysaccharide; PLs, phospholipids; SPLs, Sphingolipids; SM, sphingomyelin; PC, phosphatidylcholine; PE, phosphatidylethanolamine; PS, phosphatidylserine; PI, phosphatidylinositol; PG, phosphatidylglycerol; Cer, Ceramide;

1. INTRODUCTION

Lipids are essential cellular constituents that have multiple important roles in cell functions, regulating several biological processes. The majority of cellular lipids composed the membrane bilayer, whose integrity and physical characteristics are fundamental in biological systems. Lipids can also promote appropriate hydrophobic medium for the functional implementation of membrane proteins and their interactions. The chemical and physical properties of membranes are largely dependent on the lipid composition (1,2). Thus, as major structural elements of cellular membranes, the membrane fluidity depends on the lipids type and proteins content, as well as their mutual interactions. Consequently, membrane fluidity controls, at least in part, the cellular events that occur at the cell membrane interphase, such as ligand–receptor interactions, endocytosis and antigen presentation (3,4). In addition, membrane lipids metabolism is regulated by distinct types of extracellular receptor-regulated pathways in a variety of ways, including modifications associated with membrane fusion, secretion, trafficking, and plasma membrane shape changes, and to date, vaguely described, changes in bilayer structure seems to be regulate the activities of enzymes, channels, and transport proteins. Furthermore, a variety of lipids play a very important role in the regulation of various cellular functions by acting as signaling molecules (PI and Cer), or as precursors for second messengers (e.g. inositol trisphosphates (IP3)/DAG) (5,6). Specifically, studies on phospholipids (PLs) and sphingolipids (SPLs) metabolism and function have revealed that these metabolites are involved in the regulation of signal transduction pathways, cell proliferation, inflammation, immunity, apoptosis, angiogenesis, among others (7-9).

In mammalian cells there are numerous different species of lipids, including PLs, glycerol based phospholipids (such as phosphatidylcholine (PC), phosphatidylserine (PS), phosphatidylinositol (PI), etc.) consist in approximately 60 mol% of total lipids, SPLs, ceramide-based sphingolipids (such as sphingomyelin (SM) and Ceramide (Cer), account for approximately 10 mol% and non-polar lipids (including TAG and cholesterol) range from 0.1 to 40 mol% depending on cell type and subcellular compartment. Metabolites (such as lysolipids, DAG, Cer, acyl carnitines, acyl CoA) typically represent less than 5 mol% of total cellular lipids (4). Each lipid class has specific roles, participating in distinct metabolic and signaling events, and thus it is important to assess variation of specific lipidic specie under each particular metabolic

process. In this sense, lipidomics, the systematic study of lipids and their function in biological systems, has emerged as an active area of interest ((10). The growth of lipidomics is primarily a result of technological advances in mass spectrometry. Electrospray Ionization (ESI)-mass spectrometry (MS) has become a powerful qualitative tool in analysis of biomolecules (11) . It requires no derivatization, possesses high sensitivity, and has moderate experimental complexity, which affords highly reproducible results (12). This important tool has been used greatly for proteomic studies describing the differentiation and maturation process of dendritic cells (DCs) at the protein level (13, 14), however, there is scarce information about lipids modulation triggered during DCs maturation (15). This cell type represents an important interface between innate and adaptive immunity. DCs are specialized in the uptake, processing, and presentation of antigens, conferring them a unique capacity to induce adaptive immune responses, as well as to generate and maintain tolerance. In the epidermis they represent 1–3% of the cells and dynamically influence the induction and regulation of innate and adaptive immunity (16). Thus, in the peripheral tissues, immature DCs (iDC) capture and process antigens, such as allergens and microorganism antigens, and then they migrate towards T-cell-rich areas of the secondary lymphoid organs where they present antigens to naïve T cells. During migration, DCs lose their capacity to internalize further antigens and acquire the capacity to present antigens to naïve T cells, in a well coordinated succession of events referred to as maturation (16-19). In spite of the importance these cell types and their role in immune responses, the knowledge of the lipid role and even lipid changes that occur in the maturation process is scanty. Thus, in the current study and using a lipidomic approach we performed the characterisation of the molecular diversity of major classes of PLs and SPLs in dendritic cells, through thin layer chromatography (TLC) and ESI-MS plus MS/MS. Furthermore, we also evaluated changes on the lipid composition occurred during lipopolysaccharide (LPS)-triggered DCs maturation. We found that LPS induced significant changes on the lipidic profile of DC, mainly in PC, SM, PI and Cer classes.

2. EXPERIMENTAL PROCEDURES

2.1 Materials

Lipopolysaccharide (LPS) from *Escherichia coli* (serotype 026:B6), trypsin, chloroform, methanol and IMDM were obtained from Sigma Chemical Co. (St. Louis, MO, USA). Fetal calf serum was purchased from Invitrogen (Paisley, UK). TLC silica gel 60 plates with concentrating zone (2.5x20cm) were obtained from Merck (Darmstadt, Germany) and boric acid was from DHB chemicals. Absolute ethanol was from Panreac, triethylamine from Acros Organics and primuline was from Sigma. The phospholipid standards for TLC were purchased from the Avanti Lipids (USA).

2.2 Cell Culture

The mouse fetal skin-derived dendritic cell line (FSDC) is a skin dendritic cell precursor with antigen-presenting capacity (20). Previously, this cell line was characterized by a surface phenotype consistent with a Langerhans cell progenitor (H-2d.b$^+$, IAd. b$^+$, CD54$^+$, MHCII$^+$, MHCI$^+$, CD11c$^+$, CD11b$^+$, B7.2$^+$, CD44$^+$, B220$^-$, CD3$^-$); this phenotype was confirmed in our lab for the most important of these surface markers (data not shown). Cells were cultured in Iscove's Modified Dulbecco's Medium (IMDM) endotoxin-free, supplemented with 1% (w/v) glutamine, 10% (v/v) fetal bovine serum, 3.02 g/l sodium bicarbonate, 100 µg/ml streptomycin and 100 U/ml penicillin, in a humidified incubator with 5% CO_2/95% air, at 37 ◦C. The FSDC have a doubling time of about 48 h, and these cells did not require exogenous growth factors for their continued proliferation when cultured in serum-containing medium. The cells were used after reaching 70–80% confluence. After 45 passages the cells were discarded.

2.3 Lipid Extraction

FSDC (15×10^6) were cultured in 150cm^2 flasks and stimulated with 1µg/ml LPS, or left untreated (control) during 24 h, at 37ºC. The cells were washed with ice-cold PBS twice, scraped in 5ml of ice-cold PBS and cell pellet was separated by centrifugation at 200xg for 4 min. Total lipids were extracted through the Bligh and Dyer method (21). Briefly, for each 1ml of sample it was added chloroform/methanol 1:2 (v/v), then chloroform and finally ultra-pure water. In all steps the mixtures were vortexed and centrifuged at 100xg for 5 min at room temperature, to give a two-phase

system: an aqueous top phase and an organic bottom phase. The total lipid extracts, recovered from the bottom phase, were dried under N_2 gas and stored at -5°C.

2.4 Lipid Separation

The total lipid extracts were separated in different classes by TLC (22). The samples were applied in TLC plates with concentrating zone 2.5x20cm (Merck, Darmstadt, Germany**)**. Prior to separation, plates were sprayed with 2.3% boric acid in ethanol. The plates were developed in solvent mixture chloroform/ethanol/water/ triethylamine (30:35:7:35, v/v/v/v). Lipids spots on the silica plates were observed by spraying the plates with primuline and identified by comparison with authentic lipidic standards. After this, the spots were scraped from the silica plates, and lipids were extracted by chloroform/methanol (2:1, v/v) for MS analysis and other spots were used for phosphorus assay.

2.5 Phospholipids Quantification

In order to evaluate the phospholipid content of each class separated by TLC, phosphorus assay was performed according to previous described methodology (23). Briefly, perchloric acid (70%) was added to phosphate standards and samples. The samples were incubated for 1h at 180°C, followed by cooling to room temperature. After that, water, ammonium molybdate and ascorbic acid were added to standards and samples, and were than incubated for 10 min at 100°C in a water bath. In the case of the samples were centrifuged 5 min at 4000 rpm to separate PLs from silica. Finally the standards and samples solutions were measured at 800nm.

The relative abundance of each PL class was calculated by relating the amount of PL in each spot to the total amount of PL in the sample.

2.6 Mass spectrometry

Lipidic analysis was carried out in positive and negative modes on Q-TOF2 instrument (Waters, Manchester, UK) and a triple quadruple instrument with ESI source (Walters, Manchester, UK). In the Q-TOF2 instrument, in positive ionization mode the samples were introduced into the electrospray source at a flow rate of 10 $\mu L.min^{-1}$. The cone voltage was set at 30 V and capillary voltage at 3 kV. Source temperature was at 80ºC and desolvation temperature at 150ºC. In negative mode, capillary voltage that was change by -2,6kV, cone voltage was set at 30 V, source temperature was at 80ºC

and desolvation temperature at 150ºC. The resolution was set to about 9,000 (FWHM). Tandem mass spectra (MS/MS) were acquired by collision-induced decomposition (CID), using argon as the collision gas (measured pressure in the penning gauge ~ $6x10^{-5}$ mBar). The collision energy used was between 25 to 30 eV.

In the triple quadruple instrument the electrospray voltage was 3.5 kV in positive mode. The capillary temperature was 300ºC and the sheath gas flow was 32 U. An isolation width of 0.5 Da was used with a 30 ms activation time for MS/MS experiments. Full scan MS spectra and MS/MS spectra were acquired with a 50 ms and 200 ms maximum ionization time, respectively. Normalized collision energy TM (CE) was varied between 20 and 30 for MS/MS.

For these two instruments, data acquisition was carried out with a MassLynx 4.0 data system.

2.7 Ceramide Quantification

Ceramides were extracted from cultured cells the same way that for the extraction of total lipids (Step 2.3). For ceramide quantification cell pellet was fortify with 10µl (0,05µg) of C12 Cer (used as an internal standard) and proceeded the ceramide extraction according to Bielawski J. (24). Ceramide extracts were analyzed by Ultra Performance Liquid Chromatography (UPLC) and Tandem mass spectrometry (MS/MS) (UPLC-MS/MS). The separations were obtained with an ACQUITY UPLC BEH C18 column. All analyses were performed using a Waters ACQUITY UPLC™ System with a Quattro Premier™ XE Triple Quadrupole equipped with an Electrospray Ionization (ESI) probe (Walters, Manchester, UK). 10µl of the reconstituted ceramides extracts were injected onto a reverse phase C18 column and eluted using a linear gradient of 30% methanol to 100% methanol solution. The quantification of individual species (C14, C16, C18, C18:1, C20, C20:1, C24, C24:1) was achieved by multiple reaction monitoring (MRM).

2.8 Statistics

The results are presented as means ± SD values from at least three independent experiments, and statistical analyses were performed by one-way ANOVA. The statistical significance of differences was set at $P< 0.05$.

3. RESULTS AND DISCUSSION

The immature DCs show active endocytosis and antigen-processing properties, but weak antigen presenting functions. Upon stimuli, such as LPS, DC experience several morphologic, phenotypic and functional changes in a process referred to as maturation. This process is crucial to the biological functions of DC since their maturation status confer them the ability to polarize distinct T-cell subsets and consequently the type of the immune response (25). Although the changes that occurred in the protein profile of DCs during maturation are already partially established (26), very limited and scarce information exists concerning its lipid profile modulation. So, in this study, we analyzed the lipid profile of a mouse skin-derived dendritic cell line, FSDC, that is a model of immature DC, in the absence and in the presence of the potent DC maturation stimulus LPS. Changes in cell morphology may be correlated with changes in phospholipids, as it was previously reported for erythrocytes (27).

The study of DCs was performed in two steps: first, direct analysis of total lipid extract was performed through ESI-MS and ESI-MS/MS; second, after separation by TLC of major PLs and SPLs classes, namely PC, SM, PE, PI, PS, PG and Cer, each class of lipids was analysed by ESI-MS and ESI-MS/MS in order to assess and characterize the molecular diversity of the different species of PLs and SPLs. Furthermore, for each PL class it was still evaluated changes in PLs content by the phosphorus assay. The concentration of Total and individuals Cer was quantified by UPLC-MS and MRM, respectively.

3.1 Phosphorus assay of major phospholipid classes

A representative TLC profile obtained after lipid classes separation of the total lipid extract from immature and mature DCs is shown in Figure 1A, demonstrating the most abundant lipid classes. In both cases, and after comparison with standards applied in the TLC plate, it was possible to detect different lipid spots, which were later confirmed by ESI-MS and ESI-MS/MS, as it will be explained below. In order to assess the contents of each PLs class we performed the phosphorus assay. The results obtained are represented in Figure 1B.

PC and PE in iDCs and mDCs represented the two most abundant PL classes (Figure 1B). However, other PLs were detected on TLC plates, namely SM, PI, PS, and PG, which is in accordance with previous results addressing the relative abundance of

PLs in cells (28). After DCs exposure to LPS it was possible to observe a statistically significant increase in the PC class content and a decrease in SM class content. Furthermore, the content of PI class in mDC was decreased in comparison with iDCs, although the statistical analysis did not allow assigning significance. The other classes of PLs did not show significant changes. Therefore, the process of maturation appears to be characterized by changes in PLs content. To complete these results and support the correct identification of each PL class, analysis of the different PL spots was further conducted by ESI-MS and MS/MS. MS/MS data is a source of relevant structural characterization providing information about phospholipid head groups and allowing the identification and positional localization of individual acyl chains at *sn*-1 and *sn*-2 (29, 30).

3.2 Analysis of total lipid extract by mass spectrometry

ESI-MS spectra from total lipid extract of iDCs (Control) and mDCS (LPS), using positive and negative ionization modes, are shown in Figure 2A and Figure 2B, respectively. Total lipid extract analysis by ESI-MS in positive mode allow detecting some molecular species of PC, PE and SM., according with MS/MS analysis (Figure 2A). Comparison of both spectra obtained in positive mode revealed no significant changes in their profile.. Indeed, comparing the two spectra of Figure 2A we concluded that the most abundant molecular ions, $[MH]^+$ at *m/z* 760.6, 788.6, and 732.6 correspond the PC(18:1/16:0), PC(18:0/18:1) and PC(16:0/16:1), respectively. In these spectra we also identified ions from the class of PEs, namely, $[MH]^+$ at *m/z* 764.6 and *m/z* 766.6, identified as PE(18:2/20:4) and PE(18:1/20:4). Although, with lower relative abundance, in these spectra we also identified ions from the class of SM, for example, $[MH]^+$ at *m/z* 703.6 identified as SM(d18:1/16:0) and SM(d18:0/24:4) with ion $[MH]^+$ at *m/z* 809.6 (Table 1).

Total lipid extracted was also analyzed by ESI-MS in negative mode (Figure 2B). In this mode we identified as major lipids components ions from the PG, PI PS and Cer classes. The most abundant ions in iDCs and mDCs were at $[M-H]^-$ at *m/z* 773.6 and 747.6, identified as PG(18:1/18:1) and PG(18:1/16:0), respectively. Other ions identified from other PL classes were PI (18:1/18:1) with $[M-H]^-$ at *m/z* 861.6. In the mass region of mass spectra in m/z 700 and 900 there is no significant changes in PL profile (Figure 2B). Curiously, the ESI-MS spectrum of mDCs showed some ions between *m/z* 500 at 700 (Figure 2B), that were absent, or present very low relative

abundance in the ESI-MS spectrum of iDCs. These ions were $[M-H]^-$ at *m/z* 536.6 (Cer d18:1/16:0), at *m/z* 646.7 (Cer d18:1/24:1), at *m/z* 648.7 (Cer d18:1/24:0), and $[M-Cl]^-$ at m/z 572.7 and 684.7 that correspond to Cer(d18:1/16:0) and Cer(18:1/24:0) as confirmed by ESI-MS/MS analysis performed on each ion (31). Considering that ions attributed to ceramides were observed in MS spectrum of mature DC with higher relative abundance, in comparison of the most abundant ion in spectrum, *m/z* 773.6 identified as PG(18:1/18:1) and since PG content is similar in iDC and mDC, we can infer that ceramides are increased in mDC. Therefore, from direct analysis of the total lipid extract it is possible to conclude that there are changes in the lipid profile of DC during maturation, namely in Cer lipid class.

3.3 Analysis of lipid classes by mass spectrometry

To further understand the changes in molecular species composition of each class of lipids, lipids extracted from TLC spot were analysed by MS and MS/MS, after lipid classes separation by TLC, as we describe below. ESI-MS and ESI-MS/MS analysis from different lipid class separated by TLC, was performed in positive mode for PC and SM while in negative mode for PE, PI, PS, PG and Cer.

PCs are some of the most abundant species of neutral phospholipids in eukaryotic cells, and are characterized by the presence of a quaternary nitrogen atom which positive charge is neutralized by the negative charge of the phosphate group. The quaternary nitrogen atom readily forms abundant $[MH]^+$ protonated ions by ESI because the phosphate anion can be protonated during the electrospray process. SM behaves similarly in consequence of the presence of the choline polar head moiety. However, under ESI-MS conditions, every so often PC and SM can ionize as protonated ions $[MH]^+$ and sodium adducts $[MNa]^+$. In order to avoid misinterpretation, PC and SM classes were analyzed by precursor ion scanning of the typical product ion at *m/z* 184.1 obtained in a triple quadruple mass spectrometer, yielding an ESI-MS spectrum exclusively with the $[MH]^+$ ions (32). The molecular species of PC identified using this methodology included two groups: diacyl-PC (*m/z* 760.6, 786.6, 758.6, 732.6) and alkenyl-acyl-PC (*m/z* 746.6, 748.6, 772.6) as resumed in Table 1 (33, 34). Alkenyl-acyl and diacyl-species of phospholipids were detectable in ESI-MS and ESI-MS/MS spectra which have the same fatty acid compositions but are characterized by a mass difference of 14, due to their attachment to the glycerol backbone of phospholipid by vinyl ether or ester bond (34).

Although we previously observed an increase in the levels of PC through phosphorous quantification analysis (Figure 1B), apparently we did not found substantial differences between the two spectra presents in Figure 3A, that correspond to the PC from iDC and mDC. One exception is a slight increased of diacyl-PC with *m/z* 786.6 that corresponds a PC(18:1/18:1), which showed an higher relative abundance in mDCs. Molecular species of both diacyl-PC and alkenyl-acyl-PC contained as major abundant fatty acyl residues those with chain length with C18 and C16, as confirmed by MS/MS analysis (Table 1). For this identification, tandem mass spectrometry of the $[MH]^+$ ions identified was performed for all ions of PC class and the MS/MS spectra obtained showed an abundant PC ion at *m/z* 184.1, which is typical of all PC-containing lipids, and revealed that most abundant ion corresponded to the loss of the fatty-acyl substituent from the *sn-1* position, $R_1C=C=O > R_2C=C=O$, allowing the identification of fatty acyl pattern substitution (35).

The plasma membrane of cells is highly enriched in sphingomyelin (SM), a SPL largely found in the exoplasmic leaflet of the cell membrane. However, there are some evidences demonstrating the existence of a SM pool in the inner leaflet of the membrane. The function of SM remained unclear until recently, but it has become increasingly evident that they have a crucial role in signal transduction (7). As previously describe in our results, we observed a decrease in the percentage of this PL levels in cells treated with LPS (Figure 1B), which prove that the membrane composition is altered during DC maturation. However, through MS analysis it seems that the SM profile of DC in both studied conditions remain similar, with the same molecular species, as summarized in the Table 1 and in Figure 3B it is shown the typical ESI-MS spectrum obtained for SM class. Ionization of SM is closely related with PC, since, the presence of the quaternary nitrogen atom dominates the behavior of this molecule, so, the fragmentation of the SM cations yields a major ion at *m/z* 184.1. SM identification was obtained by parent ion scanning of the ion *m/z* 184.1 in a similar procedure to that performed for PC, but they can be easily discriminated, since PC appear at even *m/z* values, whereas protonated molecules of SM exhibit odd *m/z* values, due to the presence of an additional nitrogen atom. ESI-MS spectrum of SM demonstrated the presence of protonated ions $[MH]^+$ with dominant peak at *m/z* 703.6 corresponding to the sphingosine long-chain base (LCB) d18:1 and palmitic acid C16:0 (Figure 3B and Table 1). With low relative abundance, we identified the SM(d18:1/24:0) corresponding to the *m/z* 815.6. The most common SM was LCB d18:1

that corresponds to the sphingosine. We still found LCB d18:0 that corresponds to the sphingasine.

Beyond of PCs, PEs are also one of the major classes of lipids that are present in cell membranes. ESI–MS analysis of PE spot was performed in negative mode and revealed that major diacyl-PE species correspond to $[M-H]^-$ with *m/z* 716.5, 744.5 and 772.5 identified correspond to the PE(16:0/18:2), PE(18:1/18:1) or PE(18:0/18:2) and PE(18:1/20:1), respectively. We also identified abundant alkenyl-acyl-PE species at *m/z* 700.5 and 728.5, correspondent to PE(O-16:1/18:1) and PE(O-18:2/18:1), as present in Table 2 (33, 34, 36, 37). All these components were confirmed by the study of fragmentation pathways observed in the MS/MS spectra that allowed the identification of the composition of fatty acyl residues of both diacyl-PE and alkenyl-PE and the most probable localization along the glycerol backbone (33). Diacyl-PE specie with $[M-H]^-$ *m/z* 744.5, the most prevalent PE, was taken as an example, thus, their study by MS/MS revealed two abundant $RCOO^-$ ions at *m/z* 281 and *m/z* 283, that correspond to oleic (C18:1) and stearic (C18:0) fatty acids respectively. Since MS/MS spectrum of PE, when using standards and the same experimental conditions in negative mode, showed $R_1COO^- > R_2COO^-$ and *m/z* 281 was more abundant than *m/z* 283, we concluded that Oleic acid (C18:1) is present in *sn-1* glycerol position and Stearic acid (C18:0) in *sn-2*. On the other hand, the MS/MS spectra of the alkenyl-acyl showed only the R_2COO^-, and considering the molecular weight, it was possible to identify the composition of alkenyl chain. This approach was applied to all PE species allowing the confirmation of the fatty acid composition. Relatively to identification of PEs, we detected a variety of components of this class, as is shown in Figure 4A and Table 2,that indicate the most probable identification of each PE, but we did not found substantial variations in the composition of PEs triggered during DCs maturation. As can be seen in Table 2, both immature and mature DCs have a predominance of saturated fatty acyl chains, namely palmitic acid (C16:0) and stearic acid (C18:0).

Phospholipid classes PI, PS and PG, were also analysed by ESI-MS and MS/MS in negative mode. Comparison of these classes in immature and mature DCs revealed that there are no significant changes in each PL class composition. Using this approach it was possible to structurally characterize the DCs PL composition among each class as it will be explain in detail follow.

PIs are an important class of lipids, both as key membrane constituents and as participants in essential metabolic processes, both directly and indirectly, via its

different metabolites. Analysis of PIs showed two predominant $[M-H]^-$ ions at *m/z* 861.6 and 863.7, identified as PI(18:1/18:1) and PI(18:1/20:4), respectively, as demonstrated in Figure 4B. The other PIs present in minor relative abundance were identified as resumed in Table 2. Characterization of PI molecular species were performed by MS/MS that typically showed the carboxylate anions $R_1COO^- > R_2COO^-$ allowing the identification of the fatty acyl composition and its location. In PI MS/MS spectra it was also detectable a prominent and characteristic ion at *m/z* 241 (inositol phosphate-H_2O) (32, 38). The major fragmentation pathways for PI arise from neutral loss of free fatty acid substitution and neutral loss of ketenes ($R_2C=C=O$), followed by consecutive loss of the inositol head group (-162 Da) (1). In both cell types it was evident that fatty acid composition was mostly composed by saturated palmitic acid (C16:0), stearic acid (C18:0) and insaturated oleic acid (C18:1).

The PSs are a class of PLs with the unique characteristic of being predominantly found on the inner leaflet of normal cells (39, 40). This normal distribution is altered in many biological events, including platelet aggregation, cell adhesion, and during cellular apoptosis. Maturation of DCs appears to not modulate the proportion and composition of this PLs class. Figure 4C represent to ESI-MS spectrum of PS in iDCs and mDCs and revealed one major $[M-H]^-$ ion at *m/z* 788.6 identified as PS(18:0/18:1). All PS molecular species (Table 2) were characterized by MS/MS analysis of all ions $[M-H]^-$ and showed the formation of typical product ions that correspond to the loss of serine with formation of the ion $[M-H-87]^-$ (32). In Table 2 the remaining identified PSs are summarized.

The PG class is a constituent of cell membranes, present at 1-2% in most animal tissues, and is less abundant than the other PL species. However, it is an important precursor of more complex PLs, including the cardiolipins found in mitochondria. In iDCs and mDCs this PL class is also one of the less abundant and we observed no significant changes in its composition during the maturation process. ESI-MS spectrum shown in Figure 4D and representing the PG profile of these cells, allowing the identification of several molecular species with very low relative abundance, besides the predominant one, with $[M-H]^-$ ion at *m/z* 773.6 and identified as PG(18:1/18:1). The sorting of PG was performed by ESI-MS/MS in order to identify the fatty-acyl constituent esterified to the glycerol backbone. Furthermore, the decomposition induced by ESI-MS/MS of $[M-H]^-$ led to formation of the ion attributed to glycerol-phosphate dehydrated and glycerol-phosphate hydrated, that corresponds to *m/z* 153 and 171,

respectively (41). Regardless of very low relative abundance we found other PG, as shown in Table 2, and we observed that the major fatty acid was the oleic acid (C18:1).

Finally, in negative mode we identified the Cer, in the last spot of TLC plate, correspondent to the spot with highest RF. Cer is the central core of SPL metabolism, but has also been involved in the regulation of signal transduction processes. Cer can be generated by two major mechanisms, by the *de novo* synthesis, which is an anabolic pathway with several reactions of condensation, reduction and acylation, catalyzed by different enzymes that generate distinct ceramide species. The second major mechanism for ceramide generation is a catabolic pathway involving sphingomyelinase (SMase) activation to form ceramide directly. In turn, Cer can be acted upon by different biosynthetic enzymes to form cerebrosides and gangliosides, or can incorporate a phosphocholine head group from PC to form SM through the action of SM synthases (9). The different Cer may localize into distinct cell compartments and may be involved in the regulation of different cell functions, namely cell cycle arrest and apoptosis (7, 42). Furthermore, Cer play important roles in the regulation of autophagy, cell differentiation, survival, and inflammatory responses (43). ESI-MS spectra of Cer spot, allows the confirmation of the differences previously observe in the direct analysis of the total lipid extract. Interestingly, the analysis of both spectra (Figure 5B) allowed the observation of significant changes in the relative abundance of several ion species that have an increased relative abundance in the spectrum of mature cells, mainly $[M-H]^-$ at *m/z* 536.6 identified as Cer (d18:1/16:0), m/z 646.7 Cer (d18:1/24:1) and m/z 648.7 Cer(d18:1/24:0). In addition, the analysis of the mDCs spectrum (Figure 5B) allowed also the identification of ions with higher relative abundance that correspond to the chlorine adducts $[M-Cl]^-$ at m/z 572.6, 682.7 and 684.7, of Cer previously described, respectively. Thus, a marked change in the profile of Cer during maturation was clearly detected, corroborating the data obtained with ESI-MS from the total lipid extract. The composition of the Cer species is resumed in Table 2 and was confirmed by analysis of fragmentation process. Their ESI-MS/MS fragmentation was characterized by typical loss of -30 Da that corresponds to loss of $H_2C=O$ and the combined loss of $H_2C=O$ and H_2O, -48Da, and neutral losses of - 240 Da and - 256 Da (44).

The results obtained both from the spectra of total lipid extract and ESI-MS spectra from of the Cer spot of immature and mature cells, indicate that there was an increase in the relative abundance of ceramides during dendritic cell maturation. Thus, despite we did not detect changes in the PL profile within SM class, we observed a

decrease in the amount of SM content in mature DCs and an increase in the relative abundance of Cer, also in mature DCs, which corroborates with the data of Cer concentration, as it will be demonstrated following.

Ceramides are emerging as intramembrane messengers involved in a variety of cellular adaptive and differentiate responses. In fact, Sallusto, et al (45) shown that ceramides are implicated in maturation process of DCs, promoting its accumulation and shown that endogenous production of ceramide modulated antigen presentation. Here, we also provide evidence that ceramides have an important function in DCs maturation process and considering that Cer are metabolically generated from SM through the action of sphingomyelinase (46), our data shown that a DC maturation stimulus is able to trigger sphingomyelin hydrolysis, in order to regulate professional antigen-presenting cell function.

In Figure 6 it is demonstrated the scheme of catabolic pathway from SM involving sphingomyelinase action to form ceramide directly, taking for example the SM d18:1/16:0 and ceramide d18:1/16:0, that we found in mature DCs.

3.4 Evaluation of Ceramides content

Due to the absence of the phosphate group, ceramides cannot be quantified by phosphorus assay, however, the quantification of ceramides was performed by UPLC-MS and MRM analysis as described in experimental section. We analyzed the level of ceramides in iDCs and DC after LPS treatment (mDCs) and data demonstrated that total ceramide content increased significantly in mature DC (Figure 7). Besides, the results obtained in the quantification of individual ceramides species indicate that C24 and C24:1 ceramides were the ones that showed a major increase its content.C16 Ceramide is the most abundant ceramide within this class of lipids, but show only a slight variation. The C14, C18, C18:1, C20, C20:1 Cer were also quantified but they are present in small amounts and does not change during DC maturation. These results are in agreement with the higher relative abundance observed in the MS spectra of ceramide spot and total ion extract analysis by MS in negative mode.

4. CONCLUSION

On this first characterization of the DCs lipidome, we determined and quantified the relative changes on the major lipid species during DCs maturation, at a level not previously reported. This process is accompanied by significant changes in the cellular

levels of both signalling and structural lipids, mainly an increase in PC and Cer levels and a decrease in SM and PI content. Furthermore, this work provided precise information about changes in lipid composition during DC maturation, allowing present as major lipidic change the profile of Cer. However, the changes in SM content and Cer profile that occur during the differentiation of these cells appear to be correlated and likely have a key role in the immunomodulatory properties of dendritic cells, namely in the activation of T lymphocytes and, consequently, in the orchestration of the acquired immune response. Further studies are necessary to explore the functional relevance of these lipidic changes occurring during DCs maturation.

Acknowledgments

This work was supported by Fundação para a Ciência e Tecnologia (FCT), Fundo Comunitário Europeu (FEDER) and Programa Operacional Temático Factores de Competitividade (COMPETE) to (Grant number PTDC/SAUOSM/099762/2008 and Bruno Neves fellowship number SFRH/BD/30563/2006). The authors thank the financial support provided to QOPNA (project PEst-C/QUI/UI0062/2011) and RNEM (REDE/1504/REM/2005 -that concerns the Portuguese Mass Spectrometry Network) by FCT.

5. REFERENCES

1. Ivanova, P. T. 2001. Electrospray ionization mass spectrometry analysis of changes in phospholipids in RBL-2H3 mastocytoma cells during degranulation. *Proceedings of the National Academy of Sciences* 98: 7152-7157.
2. Leidl, K., G. Liebisch, D. Richter, and G. Schmitz. 2008. Mass spectrometric analysis of lipid species of human circulating blood cells. *Biochim Biophys Acta* 1781: 655-664.
3. Escriba, P. V., J. M. Gonzalez-Ros, F. M. Goni, P. K. Kinnunen, L. Vigh, L. Sanchez-Magraner, A. M. Fernandez, X. Busquets, I. Horvath, and G. Barcelo-Coblijn. 2008. Membranes: a meeting point for lipids, proteins and therapies. *J Cell Mol Med* 12: 829-875.
4. Han, X., and R. W. Gross. 2005. Shotgun lipidomics: electrospray ionization mass spectrometric analysis and quantitation of cellular lipidomes directly from crude extracts of biological samples. *Mass Spectrom Rev* 24: 367-412.
5. Yeung, T., and S. Grinstein. 2007. Lipid signaling and the modulation of surface charge during phagocytosis. *Immunol Rev* 219: 17-36.
6. Shaikh, S. R., and M. Edidin. 2006. Polyunsaturated fatty acids, membrane organization, T cells, and antigen presentation. *Am J Clin Nutr* 84: 1277-1289.
7. Hannun, Y. A., and L. M. Obeid. 2008. Principles of bioactive lipid signalling: lessons from sphingolipids. *Nat Rev Mol Cell Biol* 9: 139-150.

8. Ledeen, R. W., and G. Wu. 2008. Nuclear sphingolipids: metabolism and signaling. *J Lipid Res* 49: 1176-1186.
9. Gangoiti, P., L. Camacho, L. Arana, A. Ouro, M. H. Granado, L. Brizuela, J. Casas, G. Fabrias, J. L. Abad, A. Delgado, and A. Gomez-Munoz. 2010. Control of metabolism and signaling of simple bioactive sphingolipids: Implications in disease. *Prog Lipid Res* 49: 316-334.
10. Hu, C., R. van der Heijden, M. Wang, J. van der Greef, T. Hankemeier, and G. Xu. 2009. Analytical strategies in lipidomics and applications in disease biomarker discovery☆. *Journal of Chromatography B* 877: 2836-2846.
11. Forrester, J. S., S. B. Milne, P. T. Ivanova, and H. A. Brown. 2004. Computational lipidomics: a multiplexed analysis of dynamic changes in membrane lipid composition during signal transduction. *Mol Pharmacol* 65: 813-821.
12. Hsu, F. F., and J. Turk. 2009. Electrospray ionization with low-energy collisionally activated dissociation tandem mass spectrometry of glycerophospholipids: mechanisms of fragmentation and structural characterization. *J Chromatogr B Analyt Technol Biomed Life Sci* 877: 2673-2695.
13. Gundacker, N. C., V. J. Haudek, H. Wimmer, A. Slany, J. Griss, V. Bochkov, C. Zielinski, O. Wagner, J. Stockl, and C. Gerner. 2009. Cytoplasmic proteome and secretome profiles of differently stimulated human dendritic cells. *J Proteome Res* 8: 2799-2811.
14. Richards, J., F. Le Naour, S. Hanash, and L. Beretta. 2002. Integrated genomic and proteomic analysis of signaling pathways in dendritic cell differentiation and maturation. *Ann N Y Acad Sci* 975: 91-100.
15. Thurnher, M. 2007. Lipids in dendritic cell biology: messengers, effectors, and antigens. *J Leukoc Biol* 81: 154-160.
16. Toebak, M. J., S. Gibbs, D. P. Bruynzeel, R. J. Scheper, and T. Rustemeyer. 2009. Dendritic cells: biology of the skin. *Contact Dermatitis* 60: 2-20.
17. Nestle, F. O., P. Di Meglio, J.-Z. Qin, and B. J. Nickoloff. 2009. Skin immune sentinels in health and disease. *Nature Reviews Immunology*.
18. Aiba, S. 2007. Dendritic cells: importance in allergy. *Allergol Int* 56: 201-208.
19. Banchereau, J., F. Briere, C. Caux, J. Davoust, S. Lebecque, Y. J. Liu, B. Pulendran, and K. Palucka. 2000. Immunobiology of dendritic cells. *Annu Rev Immunol* 18: 767-811.
20. Girolomoni, G., M. B. Lutz, S. Pastore, C. U. Assmann, A. Cavani, and P. Ricciardi-Castagnoli. 1995. Establishment of a cell line with features of early dendritic cell precursors from fetal mouse skin. *Eur J Immunol* 25: 2163-2169.
21. Bligh, E. G., and W. J. Dyer. 1959. A rapid method of total lipid extraction and purification. *Can J Biochem Physiol* 37: 911-917.
22. Fuchs, B., R. Suss, K. Teuber, M. Eibisch, and J. Schiller. 2010. Lipid analysis by thin-layer chromatography-A review of the current state. *J Chromatogr A*.
23. Bartlett, E. M., and D. H. Lewis. 1970. Spectrophotometric determination of phosphate esters in the presence and absence of orthophosphate. *Anal Biochem* 36: 159-167.
24. Bielawski, J., Z. M. Szulc, Y. A. Hannun, and A. Bielawska. 2006. Simultaneous quantitative analysis of bioactive sphingolipids by high-performance liquid chromatography-tandem mass spectrometry. *Methods* 39: 82-91.
25. Neves, B. M., M. T. Cruz, V. Francisco, C. Garcia-Rodriguez, R. Silvestre, A. Cordeiro-da-Silva, A. M. Dinis, M. T. Batista, C. B. Duarte, and M. C. Lopes. 2009. Differential roles of PI3-Kinase, MAPKs and NF-κB on the manipulation of dendritic cell Th1/Th2 cytokine/chemokine polarizing profile. *Molecular Immunology* 46: 2481-2492.

26. Pereira, S. R., V. M. Faca, G. G. Gomes, R. Chammas, A. M. Fontes, D. T. Covas, and L. J. Greene. 2005. Changes in the proteomic profile during differentiation and maturation of human monocyte-derived dendritic cells stimulated with granulocyte macrophage colony stimulating factor/interleukin-4 and lipopolysaccharide. *Proteomics* 5: 1186-1198.
27. Daleke, D. L., and W. H. Huestis. 1989. Erythrocyte morphology reflects the transbilayer distribution of incorporated phospholipids. *J Cell Biol* 108: 1375-1385.
28. Reis, A., P. Domingues, A. J. Ferrer-Correia, and M. R. Domingues. 2004. Tandem mass spectrometry of intact oxidation products of diacylphosphatidylcholines: evidence for the occurrence of the oxidation of the phosphocholine head and differentiation of isomers. *J Mass Spectrom* 39: 1513-1522.
29. Manicke, N. E., J. M. Wiseman, D. R. Ifa, and R. G. Cooks. 2008. Desorption electrospray ionization (DESI) mass spectrometry and tandem mass spectrometry (MS/MS) of phospholipids and sphingolipids: ionization, adduct formation, and fragmentation. *J Am Soc Mass Spectrom* 19: 531-543.
30. Tyurin, V. A., Y. Y. Tyurina, W. Feng, A. Mnuskin, J. Jiang, M. Tang, X. Zhang, Q. Zhao, P. M. Kochanek, R. S. B. Clark, H. Bayır, and V. E. Kagan. 2008. Mass-spectrometric characterization of phospholipids and their primary peroxidation products in rat cortical neurons during staurosporine-induced apoptosis. *Journal of Neurochemistry* 107: 1614-1633.
31. Haynes, C. A., J. C. Allegood, H. Park, and M. C. Sullards. 2009. Sphingolipidomics: Methods for the comprehensive analysis of sphingolipids☆. *Journal of Chromatography B* 877: 2696-2708.
32. Pulfer, M., and R. C. Murphy. 2003. Electrospray mass spectrometry of phospholipids. *Mass Spectrom Rev* 22: 332-364.
33. Hsu, F. F., and J. Turk. 2007. Differentiation of 1-O-alk-1'-enyl-2-acyl and 1-O-alkyl-2-acyl glycerophospholipids by multiple-stage linear ion-trap mass spectrometry with electrospray ionization. *J Am Soc Mass Spectrom* 18: 2065-2073.
34. Taguchi, R., J. Hayakawa, Y. Takeuchi, and M. Ishida. 2000. Two-dimensional analysis of phospholipids by capillary liquid chromatography/electrospray ionization mass spectrometry. *J Mass Spectrom* 35: 953-966.
35. Ho, Y. P., and P. C. Huang. 2002. A novel structural analysis of glycerophosphocholines as TFA/K(+) adducts by electrospray ionization ion trap tandem mass spectrometry. *Rapid Commun Mass Spectrom* 16: 1582-1589.
36. Kim, H., H. K. Min, G. Kong, and M. H. Moon. 2009. Quantitative analysis of phosphatidylcholines and phosphatidylethanolamines in urine of patients with breast cancer by nanoflow liquid chromatography/tandem mass spectrometry. *Anal Bioanal Chem* 393: 1649-1656.
37. Simoes, C., V. Simoes, A. Reis, P. Domingues, and M. R. Domingues. 2008. Determination of the fatty acyl profiles of phosphatidylethanolamines by tandem mass spectrometry of sodium adducts. *Rapid Commun Mass Spectrom* 22: 3238-3244.
38. Hsu, F. F., and J. Turk. 2000. Characterization of phosphatidylinositol, phosphatidylinositol-4-phosphate, and phosphatidylinositol-4,5-bisphosphate by electrospray ionization tandem mass spectrometry: a mechanistic study. *J Am Soc Mass Spectrom* 11: 986-999.
39. Fadok, V. A., A. de Cathelineau, D. L. Daleke, P. M. Henson, and D. L. Bratton. 2001. Loss of phospholipid asymmetry and surface exposure of phosphatidylserine is required for phagocytosis of apoptotic cells by macrophages and fibroblasts. *J Biol Chem* 276: 1071-1077.

40. Leventis, P. A., and S. Grinstein. 2010. The distribution and function of phosphatidylserine in cellular membranes. *Annu Rev Biophys* 39: 407-427.
41. Hein, E. M., L. M. Blank, J. Heyland, J. I. Baumbach, A. Schmid, and H. Hayen. 2009. Glycerophospholipid profiling by high-performance liquid chromatography/mass spectrometry using exact mass measurements and multi-stage mass spectrometric fragmentation experiments in parallel. *Rapid Commun Mass Spectrom* 23: 1636-1646.
42. Zheng, W., J. Kollmeyer, H. Symolon, A. Momin, E. Munter, E. Wang, S. Kelly, J. C. Allegood, Y. Liu, Q. Peng, H. Ramaraju, M. C. Sullards, M. Cabot, and A. H. Merrill, Jr. 2006. Ceramides and other bioactive sphingolipid backbones in health and disease: lipidomic analysis, metabolism and roles in membrane structure, dynamics, signaling and autophagy. *Biochim Biophys Acta* 1758: 1864-1884.
43. Arana, L., P. Gangoiti, A. Ouro, M. Trueba, and A. Gómez-Muñoz. 2010. Ceramide and ceramide 1-phosphate in health and disease. *Lipids in Health and Disease* 9: 15.
44. Han, X. 2002. Characterization and direct quantitation of ceramide molecular species from lipid extracts of biological samples by electrospray ionization tandem mass spectrometry. *Anal Biochem* 302: 199-212.
45. Sallusto, F., C. Nicolo, R. De Maria, S. Corinti, and R. Testi. 1996. Ceramide inhibits antigen uptake and presentation by dendritic cells. *J Exp Med* 184: 2411-2416.
46. Kolesnick, R. 2002. The therapeutic potential of modulating the ceramide/sphingomyelin pathway. *J Clin Invest* 110: 3-8.

FIGURE LEGENDS:

Figure 1 - Effect of LPS on the phospholipid content in dendritic cells before (immature DCs) and after (mature DCs) treatment. (A) Typical TLC of total lipids extracted from dendritic cells before (Control) and after treatment of cells by LPS; **(B)** PL content, % from total refers to the relative percentage of phospholipid phosphorus recovered from the respective spot in TLC. Sphingomyelin(SM), phosphatidylcholine (PC), phosphatidylinositol(PI), phosphatidylserine(PS), phosphatidylethanolamine(PE), and phosphatidylglycerol (PG). *$p<0.05$ versus control, n=3 independent experiments.

Figure 2 - Total lipid MS spectra. ESI-MS spectra of total lipid extract obtained from immature (Control) and mature (LPS) dendritic cells, in positive (A) and negative modes (B).

Figure 3 - Phosphatidylcholine (PC) and Sphingomyelin (SM) MS spectra. Positive ion ESI-MS spectra of the lipid extract obtained from the TLC spots, allowing to

indentify the ions corresponding to the molecular species of **(A)** PC and **(B)** SM classes from immature (control) and mature dendritic cells (LPS).

Figure 4 - Phosphatidylethanolamine (PE), Phosphatidylinositol (PI), Phosphatidylserine (PS) and Phosphatidylglycerol (PI) MS spectra. Negative ion ESI-MS spectra of the lipid extract obtained from the TLC spots, allowing to indentify the ions corresponding to the molecular species of **(A)** PE, **(B)** PI, **(C)** PS, **(D)** PG classes from mature (control) and immature dendritic cells (LPS). For these classes of PLs no differences were observed in the MS spectra of dendritic cells before and after treatment.

Figure 5 - Ceramide MS spectra. Negative ion ESI-MS spectra of the lipid extract obtained from the TLC spots, allowing to indentify the ions corresponding to the molecular species of Cer classes from immature (**A**) and mature dendritic cells (**B)**.

Figure 6 – Scheme of sphingomyelinase action. Catabolic pathway involving sphingomyelinase activation that lead to the formation of ceramides.

Figure 7 – Ceramide Content. Total ceramide concentration (A) and individual ceramide content measured by UPLC-MS/MS-MRM in dendritic cells before (iDCs) and after (mDCs) treatment by LPS.

Table 1 - Major lipid molecular species from DCs in mode positive

Table 2 - Major lipid molecular species from DCs in mode negative

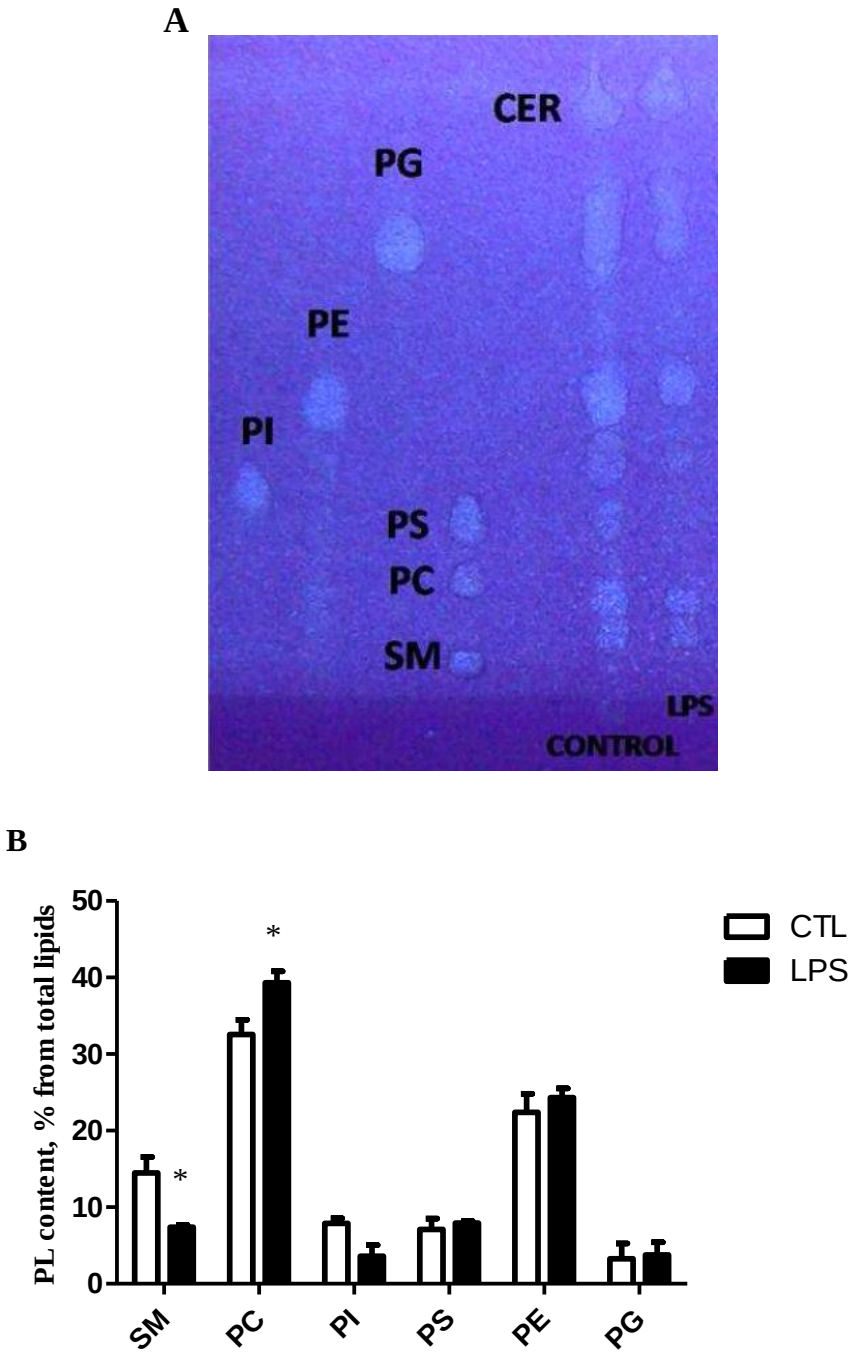

Figure 1 - Effect of LPS on the phospholipid content in dendritic cells before (immature DCs) and after (mature DCs) treatment. (A) Typical TLC of total lipids extracted from dendritic cells before (Control) and after treatment of cells by LPS; **(B)** PL content, % from total refers to the relative percentage of phospholipid phosphorus recovered from the respective spot in TLC. Sphingomyelin(SM), phosphatidylcholine (PC), phosphatidylinositol(PI), phosphatidylserine(PS), phosphatidylethanolamine(PE), and phosphatidylglycerol (PG). *$p<0.05$ versus control, n=3 independent experiments.

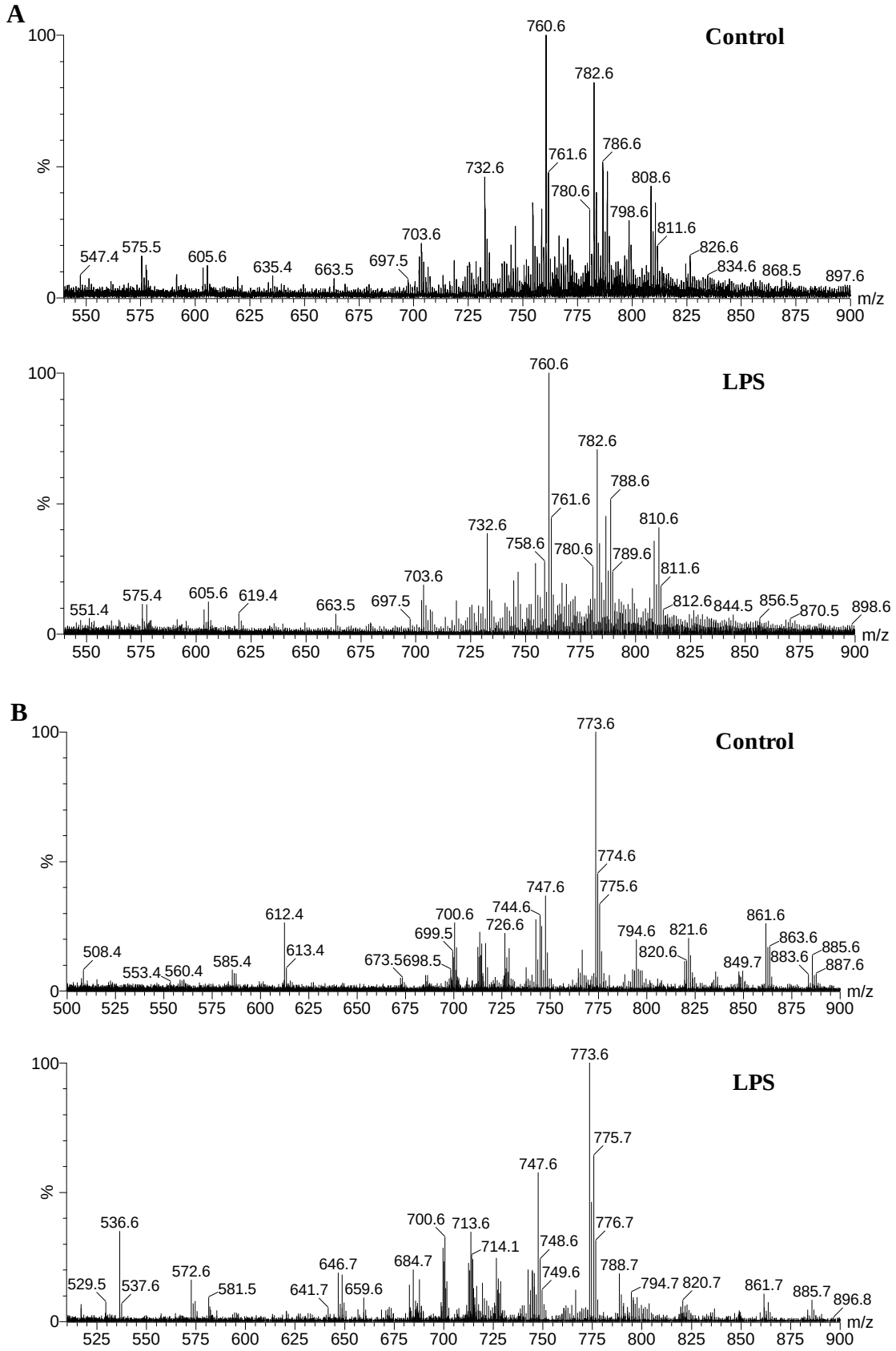

Figure 2 - Total lipid MS spectra. ESI-MS spectra of total lipid extract obtained from immature (Control) and mature (LPS) dendritic cells, in positive **(A)** and negative modes **(B)**.

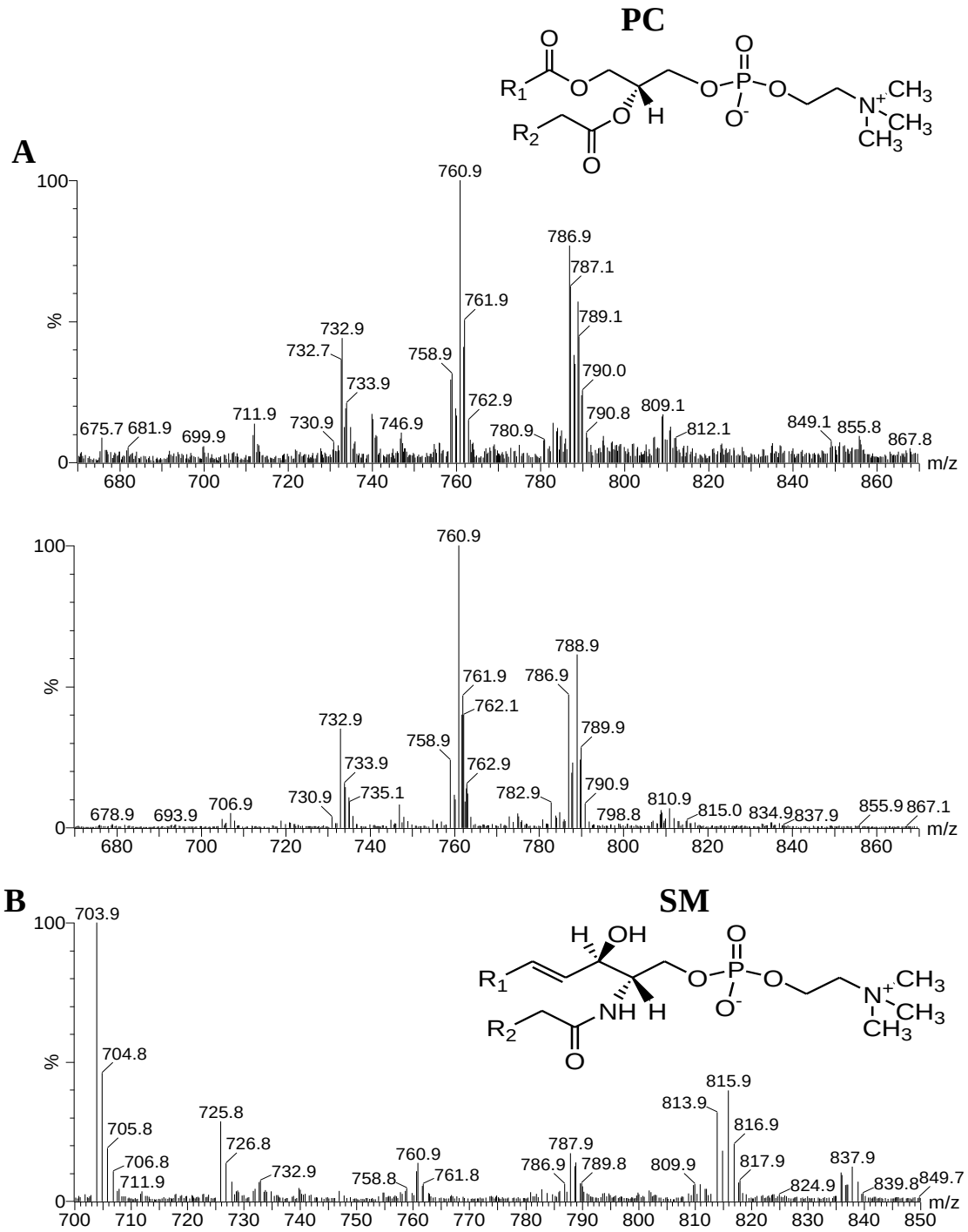

Figure 3 - Phosphatidylcholine (PC) and Sphingomyelin (SM) MS spectra. Positive ion ESI-MS spectra of the lipid extract obtained from the TLC spots, allowing to indentify the ions corresponding to the molecular species of **(A)** PC and **(B)** SM classes from immature (control) and mature dendritic cells (LPS).

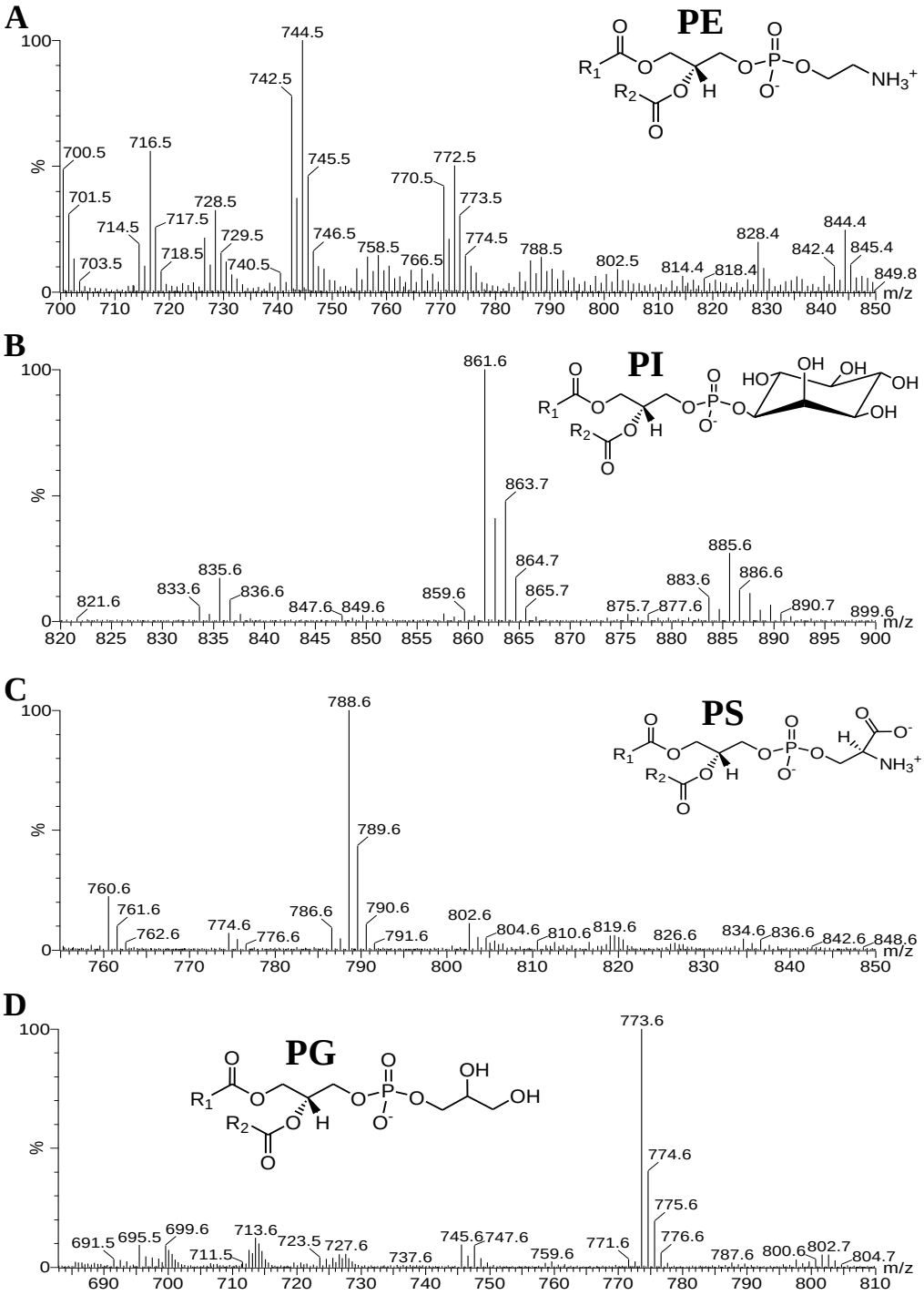

Figure 4 - Phosphatidylethanolamine (PE), Phosphatidylinositol (PI), Phosphatidylserine (PS) and Phosphatidylglycerol (PI) MS spectra. Negative ion ESI-MS spectra of the lipid extract obtained from the TLC spots, allowing to indentify the ions corresponding to the molecular species of (**A)** PE, (**B)** PI, (**C)** PS, (**D)** PG classes from mature (control) and immature dendritic cells (LPS). For these classes of PLs no differences were observed in the MS spectra of dendritic cells before and after treatment.

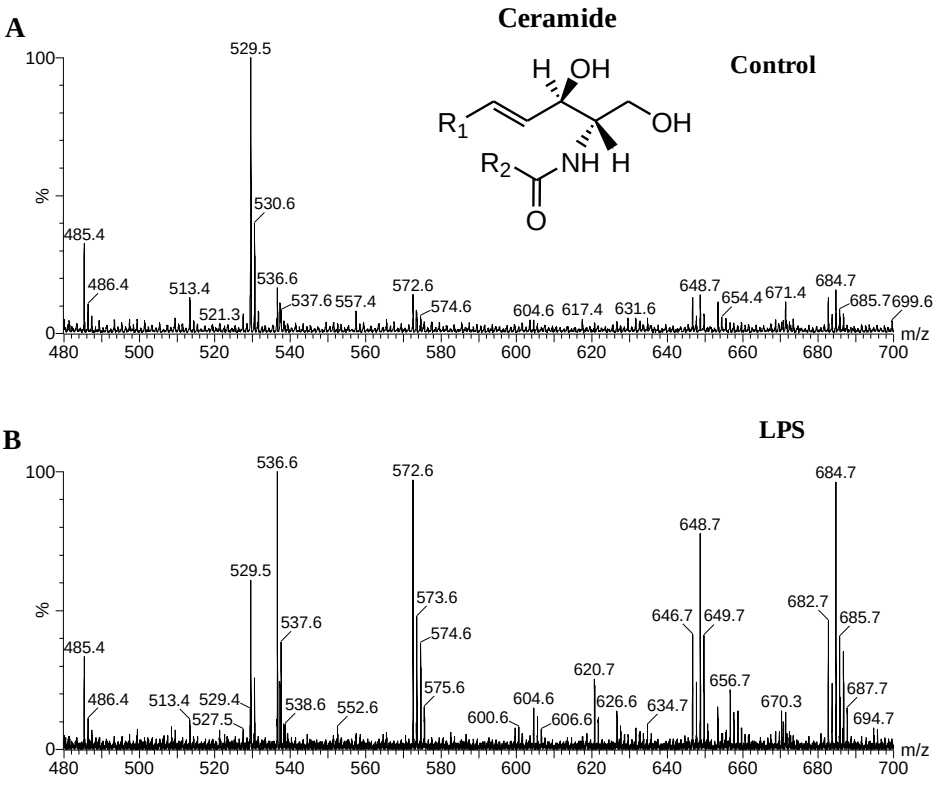

Figure 5 –Ceramide MS spectra. Negative ion ESI-MS spectra of the lipid extract obtained from the TLC spots, allowing to indentify the ions corresponding to the molecular species of Cer classes from immature (**A**) and mature dendritic cells (**B)**.

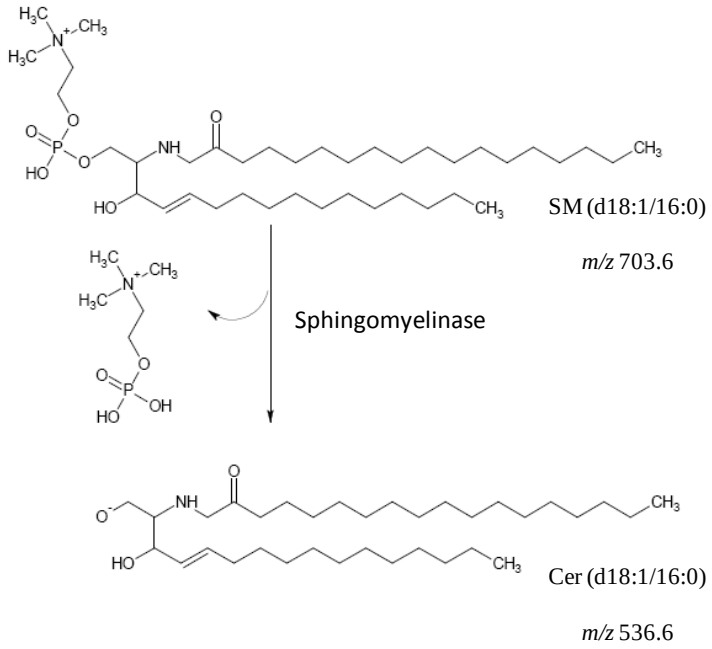

Figure 6 – Scheme of sphingomyelinase action. Catabolic pathway involving sphingomyelinase activation that lead to the formation of ceramides.

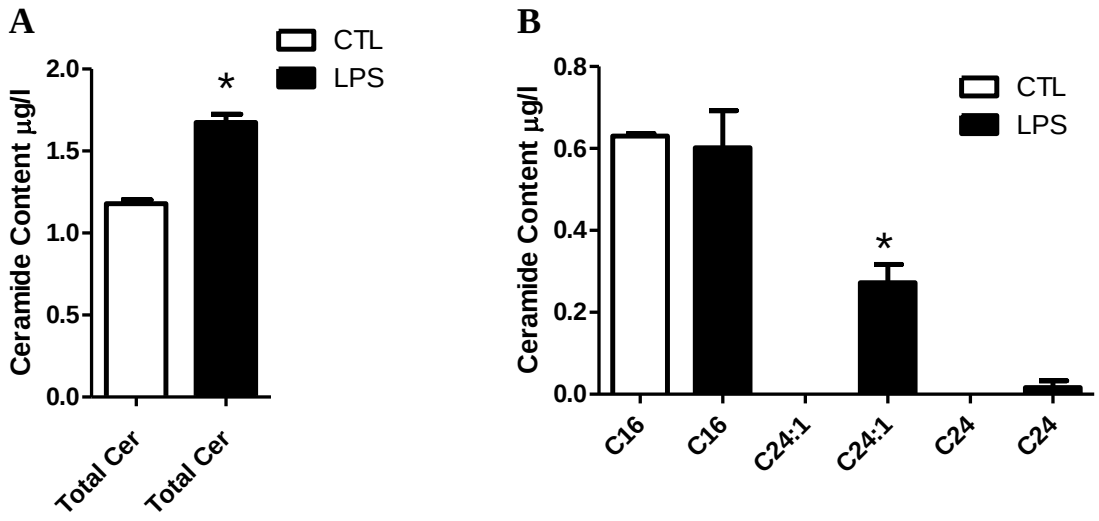

Figure 7 – Ceramide Content. Total ceramide concentration (A) and individual ceramide content measured by UPLC-MS/MS-MRM in dendritic cells before (iDCs) and after (mDCs) treatment by LPS.

Table 1 - Major lipid molecular species from DCs in mode positive

Molecular species	$[M+H]^+$ *m/z*	Identified acyl chains
Phosphatidylcholine		
Diacyl species		
28:1	**676.6**	12:0/16:1
28:0	**678.6**	14:0/14:0
30:1	**704.6**	14:0/16:0
30:0	**706.6**	14:0/16:0
32:1	**732.6**	16:0/16:1
32:0	**734.6**	16:0/16:0
34:3	**756.6**	16:1/18:2
34:2	**758.6**	16:1/18:1
34:1	**760.6**	18:1/16:0
36:6	**778.6**	16:2/20:4
36:3	**784.6**	18:1/18:2
36:2	**786.6**	18:1/18:1
36:1	**788.6**	18:0/18:1
38:5	**808.6**	20:4/18:1
38:4	**810.6**	20:4/18:0
38:3	**812.6**	20:1/18:2

38:2	**814.6**	20:1/18:1
38:1	**816.6**	22:0/16:1
Alkenyl-acyl species		
34:1	**746.6**	O-16:0/18:1
34:0	**748.6**	O-16:0/18:0
36:2	**772.6**	O-16:0/20:2
Sphingomyelin		
Sphingoid base/Acyl		
34:1	**703.6**	d18:1/16:0
38:4	**725.6**	d18:0/20:4
40:0	**789.6**	d18:0/22:0
42:4	**809.6**	d18:0/24:4
42:2	**813.6**	d18:1/24:1
42:1	**815.6**	d18:1/24:0

Table 2 - Major lipid molecular species from DCs in mode negative

Molecular species	**$[M-H]^-$ *m/z***	**Identified acyl chains**
Phosphatidylethanolamine		
Diacyl species		
34:3	**714.5**	16:1/18:2
34:2	**716.5**	16:0/18:2
34:1	**718.5**	16:0/18:1;16:1/18:0
36:3	**742.5**	18:1/18:2
36:2	**744.5**	18:1/18:1; 18:0/18:2
36:1	**746.5**	18:0/18:1
36:0	**748.5**	18:0/18:0
38:6	**764.5**	18:2/20:4
38:5	**766.5**	18:1/20:4
38:4	**768.5**	18:0/20:4; 18:1/20:3
38:3	**770.5**	18:0/20:3
38:2	**772.5**	18:1/20:1
40:6	**792.5**	18:0/22:6
Alkenyl-acyl species		
34:2	**700.5**	O-16:1/18:1
36:4	**722.5**	O-16:0/20:4
36:4	**726.5**	O-18:2/18:2;O-16:0/20:4

36:3	**728.5**	O-18:2/18:1
36:1	**732.5**	O-18:0/18:1
38:6	**750.5**	O-16:1/22:5;O-18:2/20:4
38:5	**752.5**	O-16:1/22:4;O-18:1/20:4
40:7	**776.5**	O-18:2/22:5
40:6	**778.5**	O-18:0/22:6; O-18:1/22:5
Phosphatidylinositol		
Diacyl species		
34:2	**833.6**	16:0/18:2; 16:1/18:1
34:1	**835.6**	16:0/18:1
36:4	**857.6**	16:0/20:4
36:3	**859.6**	16:0/20:3; 16:1/20:2
36:2	**861.6**	18:1/18:1; 18:0/18:2; 16:0/20:2
36:1	**863.7**	18:0/18:1
38:5	**883.6**	18:1/20:4
38:4	**885.7**	18:0/20:4
38:3	**887.7**	18:0/20:3
38:2	**889.7**	18:0/20:2
40:5	**891.7**	18:0/22:5
Phosphatidylserine		
Diacyl species		
34:1	**760.6**	18:0/16:1; 16:0/18:1
35:1	**774.6**	18:0/17:1
36:2	**786.6**	18:1/18:1; 18:0/18:2
36:1	**788.6**	18:0/18:1
38:5	**808.6**	18:1/20:4
38:4	**810.6**	18:0/20:4
40:6	**834.6**	18:0/22:6
40:5	**836.6**	18:0/22:5
Phosphatidylglycerol		
Diacyl species		
34:3	**743.6**	18:2/16:1
34:2	**745.6**	18:1/16:1
34:1	**747.6**	18:1/16:0
36:4	**769.6**	18:1/18:3
36:3	**771.6**	18:1/18:2
36:2	**773.6**	18:1/18:1
38:4	**797.6**	20:3/18:1
38:3	**799.6**	20:2/18:1
38:2	**801.7**	20:1/18:1

Ceramides		
34:1	**536.6**	d18:1/16:0
41:3	**630.6**	d18:1/23:2
41:1	**634.6**	d18:1/23:0
42:2	**646.6**	d18:1/24:1
42:1	**648.6**	d18:1/ 24:0

REFERENCES

References

1. Kimber, I., and R. J. Dearman. 2002. Allergic contact dermatitis: the cellular effectors. *Contact Dermatitis* **46**: 1-5.
2. Toebak, M. J., S. Gibbs, D. P. Bruynzeel, R. J. Scheper, and T. Rustemeyer. 2009. Dendritic cells: biology of the skin. *Contact Dermatitis* **60**: 2-20.
3. Thyssen, J. P., A. Linneberg, T. Menne, and J. D. Johansen. 2007. The epidemiology of contact allergy in the general population--prevalence and main findings. *Contact Dermatitis* **57**: 287-299.
4. Saint-Mezard, P., A. Rosieres, M. Krasteva, F. Berard, B. Dubois, D. Kaiserlian, and J. F. Nicolas. 2004. Allergic contact dermatitis. *Eur J Dermatol* **14**: 284-295.
5. Basketter, D. A., P. Evans, R. J. Fielder, G. F. Gerberick, R. J. Dearman, and I. Kimber. 2002. Local lymph node assay - validation, conduct and use in practice. *Food Chem Toxicol* **40**: 593-598.
6. Neves, B. M., M. Goncalo, A. Figueiredo, C. B. Duarte, M. C. Lopes, and M. T. Cruz. 2011. Signal transduction profile of chemical sensitisers in dendritic cells: an endpoint to be included in a cell-based in vitro alternative approach to hazard identification? *Toxicol Appl Pharmacol* **250**: 87-95.
7. Nestle, F. O., P. Di Meglio, J.-Z. Qin, and B. J. Nickoloff. 2009. Skin immune sentinels in health and disease. *Nature Reviews Immunology*.
8. Van Och, F. M., H. Van Loveren, J. C. Van Wolfswinkel, A. J. Machielsen, and R. J. Vandebriel. 2005. Assessment of potency of allergenic activity of low molecular weight compounds based on IL-1alpha and IL-18 production by a murine and human keratinocyte cell line. *Toxicology* **210**: 95-109.
9. Ryan, C. A., I. Kimber, D. A. Basketter, M. Pallardy, L. A. Gildea, and G. F. Gerberick. 2007. Dendritic cells and skin sensitization: biological roles and uses in hazard identification. *Toxicol Appl Pharmacol* **221**: 384-394.
10. Girolomoni, G., M. B. Lutz, S. Pastore, C. U. Assmann, A. Cavani, and P. Ricciardi-Castagnoli. 1995. Establishment of a cell line with features of early dendritic cell precursors from fetal mouse skin. *Eur J Immunol* **25**: 2163-2169.
11. Boukamp, P., R. T. Petrussevska, D. Breitkreutz, J. Hornung, A. Markham, and N. E. Fusenig. 1988. Normal keratinization in a spontaneously immortalized aneuploid human keratinocyte cell line. *J Cell Biol* **106**: 761-771.
12. Randolph, G. J. 2001. Dendritic cell migration to lymph nodes: cytokines, chemokines, and lipid mediators. *Semin Immunol* **13**: 267-274.
13. Aiba, S. 2007. Dendritic cells: importance in allergy. *Allergol Int* **56**: 201-208.
14. Banchereau, J., F. Briere, C. Caux, J. Davoust, S. Lebecque, Y. J. Liu, B. Pulendran, and K. Palucka. 2000. Immunobiology of dendritic cells. *Annu Rev Immunol* **18**: 767-811.
15. Neves, B. M., M. T. Cruz, V. Francisco, C. Garcia-Rodriguez, R. Silvestre, A. Cordeiro-da-Silva, A. M. Dinis, M. T. Batista, C. B. Duarte, and M. C. Lopes. 2009. Differential roles of PI3-Kinase, MAPKs and NF-κB on the manipulation of dendritic cell Th1/Th2 cytokine/chemokine polarizing profile. *Molecular Immunology* **46**: 2481-2492.
16. Romani, N., S. Ebner, C. H. Tripp, V. Flacher, F. Koch, and P. Stoitzner. 2006. Epidermal Langerhans cells--changing views on their function in vivo. *Immunol Lett* **106**: 119-125.

17. Schaerli, P., K. Willimann, L. M. Ebert, A. Walz, and B. Moser. 2005. Cutaneous CXCL14 targets blood precursors to epidermal niches for Langerhans cell differentiation. *Immunity* **23**: 331-342.
18. Dieu-Nosjean, M. C., C. Massacrier, B. Vanbervliet, W. H. Fridman, and C. Caux. 2001. IL-10 induces CCR6 expression during Langerhans cell development while IL-4 and IFN-gamma suppress it. *J Immunol* **167**: 5594-5602.
19. Hunger, R. E., P. A. Sieling, M. T. Ochoa, M. Sugaya, A. E. Burdick, T. H. Rea, P. J. Brennan, J. T. Belisle, A. Blauvelt, S. A. Porcelli, and R. L. Modlin. 2004. Langerhans cells utilize CD1a and langerin to efficiently present nonpeptide antigens to T cells. *J Clin Invest* **113**: 701-708.
20. Klechevsky, E., R. Morita, M. Liu, Y. Cao, S. Coquery, L. Thompson-Snipes, F. Briere, D. Chaussabel, G. Zurawski, A. K. Palucka, Y. Reiter, J. Banchereau, and H. Ueno. 2008. Functional specializations of human epidermal Langerhans cells and CD14+ dermal dendritic cells. *Immunity* **29**: 497-510.
21. Lenz, A., M. Heine, G. Schuler, and N. Romani. 1993. Human and murine dermis contain dendritic cells. Isolation by means of a novel method and phenotypical and functional characterization. *J Clin Invest* **92**: 2587-2596.
22. Kissenpfennig, A., S. Henri, B. Dubois, C. Laplace-Builhe, P. Perrin, N. Romani, C. H. Tripp, P. Douillard, L. Leserman, D. Kaiserlian, S. Saeland, J. Davoust, and B. Malissen. 2005. Dynamics and function of Langerhans cells in vivo: dermal dendritic cells colonize lymph node areas distinct from slower migrating Langerhans cells. *Immunity* **22**: 643-654.
23. Fukunaga, A., N. M. Khaskhely, C. S. Sreevidya, S. N. Byrne, and S. E. Ullrich. 2008. Dermal dendritic cells, and not Langerhans cells, play an essential role in inducing an immune response. *J Immunol* **180**: 3057-3064.
24. Cumberbatch, M., K. Clelland, R. J. Dearman, and I. Kimber. 2005. Impact of cutaneous IL-10 on resident epidermal Langerhans' cells and the development of polarized immune responses. *J Immunol* **175**: 43-50.
25. Schwarzenberger, K., and M. C. Udey. 1996. Contact allergens and epidermal proinflammatory cytokines modulate Langerhans cell E-cadherin expression in situ. *J Invest Dermatol* **106**: 553-558.
26. Mandell, K. J., B. A. Babbin, A. Nusrat, and C. A. Parkos. 2005. Junctional adhesion molecule 1 regulates epithelial cell morphology through effects on beta1 integrins and Rap1 activity. *J Biol Chem* **280**: 11665-11674.
27. Staquet, M. J., N. Piccardi, A. Piccirilli, C. Vincent, D. Schmitt, and P. Msika. 2004. Novel protein kinase C and matrix metalloproteinase inhibitors of vegetable origin as potential modulators of Langerhans cell migration following hapten-induced sensitization. *Int Arch Allergy Immunol* **133**: 348-356.
28. Cyster, J. G. 1999. Chemokines and the homing of dendritic cells to the T cell areas of lymphoid organs. *J Exp Med* **189**: 447-450.
29. Steinman, R. M., S. Turley, I. Mellman, and K. Inaba. 2000. The induction of tolerance by dendritic cells that have captured apoptotic cells. *J Exp Med* **191**: 411-416.
30. Aiba, S., A. Terunuma, H. Manome, and H. Tagami. 1997. Dendritic cells differently respond to haptens and irritants by their production of cytokines and expression of co-stimulatory molecules. *Eur J Immunol* **27**: 3031-3038.
31. Verhasselt, V., C. Buelens, F. Willems, D. De Groote, N. Haeffner-Cavaillon, and M. Goldman. 1997. Bacterial lipopolysaccharide stimulates the production of

cytokines and the expression of costimulatory molecules by human peripheral blood dendritic cells: evidence for a soluble CD14-dependent pathway. *J Immunol* **158**: 2919-2925.

32. Schnare, M., G. M. Barton, A. C. Holt, K. Takeda, S. Akira, and R. Medzhitov. 2001. Toll-like receptors control activation of adaptive immune responses. *Nat Immunol* **2**: 947-950.
33. Schoeters, E., J. M. Nuijten, R. L. Van Den Heuvel, I. Nelissen, H. Witters, G. E. Schoeters, V. F. Van Tendeloo, Z. N. Berneman, and G. R. Verheyen. 2006. Gene expression signatures in CD34+-progenitor-derived dendritic cells exposed to the chemical contact allergen nickel sulfate. *Toxicol Appl Pharmacol* **216**: 131-149.
34. Toebak, M. J., P. R. Pohlmann, S. C. Sampat-Sardjoepersad, B. M. von Blomberg, D. P. Bruynzeel, R. J. Scheper, T. Rustemeyer, and S. Gibbs. 2006. CXCL8 secretion by dendritic cells predicts contact allergens from irritants. *Toxicol In Vitro* **20**: 117-124.
35. Miller, L. S., and R. L. Modlin. 2007. Human keratinocyte Toll-like receptors promote distinct immune responses. *J Invest Dermatol* **127**: 262-263.
36. Martinon, F., A. Mayor, and J. Tschopp. 2009. The inflammasomes: guardians of the body. *Annu Rev Immunol* **27**: 229-265.
37. Watanabe, H., O. Gaide, V. Petrilli, F. Martinon, E. Contassot, S. Roques, J. A. Kummer, J. Tschopp, and L. E. French. 2007. Activation of the IL-1beta-processing inflammasome is involved in contact hypersensitivity. *J Invest Dermatol* **127**: 1956-1963.
38. Arend, W. P., G. Palmer, and C. Gabay. 2008. IL-1, IL-18, and IL-33 families of cytokines. *Immunol Rev* **223**: 20-38.
39. Ivanova, P. T. 2001. Electrospray ionization mass spectrometry analysis of changes in phospholipids in RBL-2H3 mastocytoma cells during degranulation. *Proceedings of the National Academy of Sciences* **98**: 7152-7157.
40. Leidl, K., G. Liebisch, D. Richter, and G. Schmitz. 2008. Mass spectrometric analysis of lipid species of human circulating blood cells. *Biochim Biophys Acta* **1781**: 655-664.
41. Escriba, P. V., J. M. Gonzalez-Ros, F. M. Goni, P. K. Kinnunen, L. Vigh, L. Sanchez-Magraner, A. M. Fernandez, X. Busquets, I. Horvath, and G. Barcelo-Coblijn. 2008. Membranes: a meeting point for lipids, proteins and therapies. *J Cell Mol Med* **12**: 829-875.
42. Han, X., and R. W. Gross. 2005. Shotgun lipidomics: electrospray ionization mass spectrometric analysis and quantitation of cellular lipidomes directly from crude extracts of biological samples. *Mass Spectrom Rev* **24**: 367-412.
43. Yeung, T., and S. Grinstein. 2007. Lipid signaling and the modulation of surface charge during phagocytosis. *Immunol Rev* **219**: 17-36.
44. Shaikh, S. R., and M. Edidin. 2006. Polyunsaturated fatty acids, membrane organization, T cells, and antigen presentation. *Am J Clin Nutr* **84**: 1277-1289.
45. Hu, C., R. van der Heijden, M. Wang, J. van der Greef, T. Hankemeier, and G. Xu. 2009. Analytical strategies in lipidomics and applications in disease biomarker discovery☆. *Journal of Chromatography B* **877**: 2836-2846.
46. Fahy, E., S. Subramaniam, H. A. Brown, C. K. Glass, A. H. Merrill, Jr., R. C. Murphy, C. R. Raetz, D. W. Russell, Y. Seyama, W. Shaw, T. Shimizu, F. Spener, G. van Meer, M. S. VanNieuwenhze, S. H. White, J. L. Witztum, and E. A. Dennis. 2005. A comprehensive classification system for lipids. *J Lipid Res* **46**: 839-861.

47. van Meer, G., D. R. Voelker, and G. W. Feigenson. 2008. Membrane lipids: where they are and how they behave. *Nat Rev Mol Cell Biol* **9**: 112-124.
48. Christie, W. W. 1987. High-performance liquid chromatography and Lipids: A Practical Guide. *Pergamon Press, Oxford*.
49. Wenk, M. R. 2005. The emerging field of lipidomics. *Nat Rev Drug Discov* **4**: 594-610.
50. Christie, W. W. 2003. Lipid Analysis - third edition. *The Oily Press, Bridgwater*
51. Christie, W. W. 2003. Lipid Analysis: Isolation, Separation, Identification, and Structural Analysis. *Bridgewater, England: Oily Press*.
52. Bleijerveld, O. B., M. Houweling, M. J. Thomas, and Z. Cui. 2006. Metabolipidomics: profiling metabolism of glycerophospholipid species by stable isotopic precursors and tandem mass spectrometry. *Anal Biochem* **352**: 1-14.
53. Schlame, M., D. Rua, and M. L. Greenberg. 2000. The biosynthesis and functional role of cardiolipin. *Prog Lipid Res* **39**: 257-288.
54. Bartke, N., and Y. A. Hannun. 2009. Bioactive sphingolipids: metabolism and function. *J Lipid Res* **50 Suppl**: S91-96.
55. Hannun, Y. A., and L. M. Obeid. 2008. Principles of bioactive lipid signalling: lessons from sphingolipids. *Nat Rev Mol Cell Biol* **9**: 139-150.
56. Watson, A. D. 2006. Thematic review series: systems biology approaches to metabolic and cardiovascular disorders. Lipidomics: a global approach to lipid analysis in biological systems. *J Lipid Res* **47**: 2101-2111.
57. Han, X., and R. W. Gross. 2003. Global analyses of cellular lipidomes directly from crude extracts of biological samples by ESI mass spectrometry: a bridge to lipidomics. *J Lipid Res* **44**: 1071-1079.
58. Milne, S., P. Ivanova, J. Forrester, and H. Alex Brown. 2006. Lipidomics: an analysis of cellular lipids by ESI-MS. *Methods* **39**: 92-103.
59. Folch, J., M. Lees, and G. H. Sloane Stanley. 1957. A simple method for the isolation and purification of total lipidies from animal tissues. *Journal of Biological Chemistry* **226**: 497-509.
60. Bligh, E. G., and W. J. Dyer. 1959. A rapid method of total lipid extraction and purification. *Can J Biochem Physiol* **37**: 911-917.
61. Peterson, B. L., and B. S. Cummings. 2006. A review of chromatographic methods for the assessment of phospholipids in biological samples. *Biomed Chromatogr* **20**: 227-243.
62. Fuchs, B., R. Süß, K. Teuber, M. Eibisch, and J. Schiller. 2010. Lipid analysis by thin-layer chromatography—A review of the current state. *Journal of Chromatography A*.
63. Müthing, J., and U. Distler. 2009. Advances on the compositional analysis of glycosphingolipids combining thin-layer chromatography with mass spectrometry. *Mass Spectrometry Reviews*: n/a-n/a.
64. Ryhage, R., and E. Stenhagen. 1960. Mass spectrometry in lipid research. *J Lipid Res* **1**: 361-390.
65. Whitehouse, C. M., R. N. Dreyer, M. Yamashita, and J. B. Fenn. 1985. Electrospray interface for liquid chromatographs and mass spectrometers. *Anal Chem* **57**: 675-679.
66. Hsu, F.-F., and J. Turk. 2009. Electrospray ionization with low-energy collisionally activated dissociation tandem mass spectrometry of glycerophospholipids:

Mechanisms of fragmentation and structural characterization☆. *Journal of Chromatography B* **877**: 2673-2695.
67. Zehethofer, N., and D. M. Pinto. 2008. Recent developments in tandem mass spectrometry for lipidomic analysis. *Anal Chim Acta* **627**: 62-70.
68. Pulfer, M., and R. C. Murphy. 2003. Electrospray mass spectrometry of phospholipids. *Mass Spectrom Rev* **22**: 332-364.
69. Hsu, F. F., and J. Turk. 2009. Electrospray ionization with low-energy collisionally activated dissociation tandem mass spectrometry of glycerophospholipids: mechanisms of fragmentation and structural characterization. *J Chromatogr B Analyt Technol Biomed Life Sci* **877**: 2673-2695.
70. Fenn, J. B., M. Mann, C. K. Meng, S. F. Wong, and C. M. Whitehouse. 1989. Electrospray ionization for mass spectrometry of large biomolecules. *Science* **246**: 64-71.
71. Douglas, D. J., A. J. Frank, and D. Mao. 2005. Linear ion traps in mass spectrometry. *Mass Spectrom Rev* **24**: 1-29.
72. Taguchi, R., T. Houjou, H. Nakanishi, T. Yamazaki, M. Ishida, M. Imagawa, and T. Shimizu. 2005. Focused lipidomics by tandem mass spectrometry. *J Chromatogr B Analyt Technol Biomed Life Sci* **823**: 26-36.
73. Cui, Z., and M. J. Thomas. 2009. Phospholipid profiling by tandem mass spectrometry. *J Chromatogr B Analyt Technol Biomed Life Sci* **877**: 2709-2715.
74. Hou, W., H. Zhou, F. Elisma, S. A. Bennett, and D. Figeys. 2008. Technological developments in lipidomics. *Brief Funct Genomic Proteomic* **7**: 395-409.
75. Kanto, T., P. Kalinski, O. C. Hunter, M. T. Lotze, and A. A. Amoscato. 2001. Ceramide mediates tumor-induced dendritic cell apoptosis. *J Immunol* **167**: 3773-3784.
76. Hsu, F. F., and J. Turk. 2000. Characterization of phosphatidylethanolamine as a lithiated adduct by triple quadrupole tandem mass spectrometry with electrospray ionization. *J Mass Spectrom* **35**: 595-606.
77. Domingues, M. R., A. Reis, and P. Domingues. 2008. Mass spectrometry analysis of oxidized phospholipids. *Chem Phys Lipids* **156**: 1-12.
78. Fadok, V. A., A. de Cathelineau, D. L. Daleke, P. M. Henson, and D. L. Bratton. 2001. Loss of phospholipid asymmetry and surface exposure of phosphatidylserine is required for phagocytosis of apoptotic cells by macrophages and fibroblasts. *J Biol Chem* **276**: 1071-1077.
79. Taylor, C. W. 2002. Controlling calcium entry. *Cell* **111**: 767-769.
80. Hsu, F. F., and J. Turk. 2000. Characterization of phosphatidylinositol, phosphatidylinositol-4-phosphate, and phosphatidylinositol-4,5-bisphosphate by electrospray ionization tandem mass spectrometry: a mechanistic study. *J Am Soc Mass Spectrom* **11**: 986-999.
81. Hsu, F. F., and J. Turk. 2002. Characterization of ceramides by low energy collisional-activated dissociation tandem mass spectrometry with negative-ion electrospray ionization. *J Am Soc Mass Spectrom* **13**: 558-570.
82. Han, X. 2002. Characterization and direct quantitation of ceramide molecular species from lipid extracts of biological samples by electrospray ionization tandem mass spectrometry. *Anal Biochem* **302**: 199-212.
83. Vital, A. L., M. Goncalo, M. T. Cruz, A. Figueiredo, C. B. Duarte, and M. Celeste Lopes. 2004. The sensitizers nickel sulfate and 2,4-dinitrofluorobenzene increase

CD40 and IL-12 receptor expression in a fetal skin dendritic cell line. *Biosci Rep* **24**: 191-202.

84. Matos, T. J., C. B. Duarte, M. Goncalo, and M. C. Lopes. 2005. DNFB activates MAPKs and upregulates CD40 in skin-derived dendritic cells. *J Dermatol Sci* **39**: 113-123.
85. Neves, B. M., M. T. Cruz, V. Francisco, M. Goncalo, A. Figueiredo, C. B. Duarte, and M. C. Lopes. 2008. Differential modulation of CXCR4 and CD40 protein levels by skin sensitizers and irritants in the FSDC cell line. *Toxicol Lett* **177**: 74-82.
86. Hulette, B. C., C. A. Ryan, L. A. Gildea, and G. F. Gerberick. 2005. Relationship of CD86 surface marker expression and cytotoxicity on dendritic cells exposed to chemical allergen. *Toxicol Appl Pharmacol* **209**: 159-166.
87. Fuchs, B., R. Suss, K. Teuber, M. Eibisch, and J. Schiller. 2010. Lipid analysis by thin-layer chromatography-A review of the current state. *J Chromatogr A*.
88. Bartlett, E. M., and D. H. Lewis. 1970. Spectrophotometric determination of phosphate esters in the presence and absence of orthophosphate. *Anal Biochem* **36**: 159-167.
89. Bielawski, J., Z. M. Szulc, Y. A. Hannun, and A. Bielawska. 2006. Simultaneous quantitative analysis of bioactive sphingolipids by high-performance liquid chromatography-tandem mass spectrometry. *Methods* **39**: 82-91.
90. dos Santos, G. G., J. Reinders, K. Ouwehand, T. Rustemeyer, R. J. Scheper, and S. Gibbs. 2009. Progress on the development of human in vitro dendritic cell based assays for assessment of the sensitizing potential of a compound. *Toxicol Appl Pharmacol* **236**: 372-382.
91. Ryan, C. A., G. F. Gerberick, L. A. Gildea, B. C. Hulette, C. J. Betts, M. Cumberbatch, R. J. Dearman, and I. Kimber. 2005. Interactions of contact allergens with dendritic cells: opportunities and challenges for the development of novel approaches to hazard assessment. *Toxicol Sci* **88**: 4-11.
92. Pichowski, J. S., M. Cumberbatch, R. J. Dearman, D. A. Basketter, and I. Kimber. 2001. Allergen-induced changes in interleukin 1 beta (IL-1 beta) mRNA expression by human blood-derived dendritic cells: inter-individual differences and relevance for sensitization testing. *J Appl Toxicol* **21**: 115-121.
93. Xie, Q., H. L. Yan, Y. Q. Li, J. Wang, and J. Y. Wang. 2007. [Effect of etoposide on allergic contact dermatitis induced by dinitrofluorobenzene and its action mechanism in mice]. *Yao Xue Xue Bao* **42**: 1050-1053.
94. Yuan, X. Y., W. Liu, P. Zhang, R. Y. Wang, and J. Y. Guo. 2010. Effects and mechanisms of aloperine on 2, 4-dinitrofluorobenzene-induced allergic contact dermatitis in BALB/c mice. *Eur J Pharmacol* **629**: 147-152.
95. Reis, A., P. Domingues, A. J. Ferrer-Correia, and M. R. Domingues. 2004. Tandem mass spectrometry of intact oxidation products of diacylphosphatidylcholines: evidence for the occurrence of the oxidation of the phosphocholine head and differentiation of isomers. *J Mass Spectrom* **39**: 1513-1522.
96. Sallusto, F., C. Nicolo, R. De Maria, S. Corinti, and R. Testi. 1996. Ceramide inhibits antigen uptake and presentation by dendritic cells. *J Exp Med* **184**: 2411-2416.
97. Sallusto, F., M. Cella, C. Danieli, and A. Lanzavecchia. 1995. Dendritic cells use macropinocytosis and the mannose receptor to concentrate macromolecules in the major histocompatibility complex class II compartment: downregulation by cytokines and bacterial products. *J Exp Med* **182**: 389-400.

98. Kolesnick, R. N., and M. Kronke. 1998. Regulation of ceramide production and apoptosis. *Annu Rev Physiol* **60**: 643-665.
99. Perry, D. K., and Y. A. Hannun. 1998. The role of ceramide in cell signaling. *Biochim Biophys Acta* **1436**: 233-243.
100. Song, P. I., Y. M. Park, T. Abraham, B. Harten, A. Zivony, N. Neparidze, C. A. Armstrong, and J. C. Ansel. 2002. Human keratinocytes express functional CD14 and toll-like receptor 4. *J Invest Dermatol* **119**: 424-432.
101. Taguchi, R., J. Hayakawa, Y. Takeuchi, and M. Ishida. 2000. Two-dimensional analysis of phospholipids by capillary liquid chromatography/electrospray ionization mass spectrometry. *J Mass Spectrom* **35**: 953-966.
102. Leventis, P. A., and S. Grinstein. 2010. The distribution and function of phosphatidylserine in cellular membranes. *Annu Rev Biophys* **39**: 407-427.
103. Fadok, V. A., D. L. Bratton, S. C. Frasch, M. L. Warner, and P. M. Henson. 1998. The role of phosphatidylserine in recognition of apoptotic cells by phagocytes. *Cell Death Differ* **5**: 551-562.
104. Stace, C. L., and N. T. Ktistakis. 2006. Phosphatidic acid- and phosphatidylserine-binding proteins. *Biochim Biophys Acta* **1761**: 913-926.
105. Yeung, T., G. E. Gilbert, J. Shi, J. Silvius, A. Kapus, and S. Grinstein. 2008. Membrane phosphatidylserine regulates surface charge and protein localization. *Science* **319**: 210-213.
106. Trautmann, A., M. Akdis, P. Schmid-Grendelmeier, R. Disch, E. B. Brocker, K. Blaser, and C. A. Akdis. 2001. Targeting keratinocyte apoptosis in the treatment of atopic dermatitis and allergic contact dermatitis. *J Allergy Clin Immunol* **108**: 839-846.
107. Akiba, H., J. Kehren, M. T. Ducluzeau, M. Krasteva, F. Horand, D. Kaiserlian, F. Kaneko, and J. F. Nicolas. 2002. Skin inflammation during contact hypersensitivity is mediated by early recruitment of CD8+ T cytotoxic 1 cells inducing keratinocyte apoptosis. *J Immunol* **168**: 3079-3087.
108. Reich, A., D. Schwudke, M. Meurer, B. Lehmann, and A. Shevchenko. 2010. Lipidome of narrow-band ultraviolet B irradiated keratinocytes shows apoptotic hallmarks. *Exp Dermatol* **19**: e103-110.
109. Ostrander, D. B., G. C. Sparagna, A. A. Amoscato, J. B. McMillin, and W. Dowhan. 2001. Decreased cardiolipin synthesis corresponds with cytochrome c release in palmitate-induced cardiomyocyte apoptosis. *J Biol Chem* **276**: 38061-38067.
110. Hsu, F. F., J. Turk, E. R. Rhoades, D. G. Russell, Y. Shi, and E. A. Groisman. 2005. Structural characterization of cardiolipin by tandem quadrupole and multiple-stage quadrupole ion-trap mass spectrometry with electrospray ionization. *J Am Soc Mass Spectrom* **16**: 491-504.
111. Esposti, M. D. 2002. Lipids, cardiolipin and apoptosis: a greasy licence to kill. *Cell Death Differ* **9**: 234-236.
112. Zheng, W., J. Kollmeyer, H. Symolon, A. Momin, E. Munter, E. Wang, S. Kelly, J. C. Allegood, Y. Liu, Q. Peng, H. Ramaraju, M. C. Sullards, M. Cabot, and A. H. Merrill, Jr. 2006. Ceramides and other bioactive sphingolipid backbones in health and disease: lipidomic analysis, metabolism and roles in membrane structure, dynamics, signaling and autophagy. *Biochim Biophys Acta* **1758**: 1864-1884.
113. Arana, L., P. Gangoiti, A. Ouro, M. Trueba, and A. Gómez-Muñoz. 2010. Ceramide and ceramide 1-phosphate in health and disease. *Lipids in Health and Disease* **9**: 15.

114. Takeda, S., S. Mitsutake, K. Tsuji, and Y. Igarashi. 2006. Apoptosis occurs via the ceramide recycling pathway in human HaCaT keratinocytes. *J Biochem* **139**: 255-262.